WP3 – Activity 3.2

Characterization of the marine water bodies and sediments quality of marine and tourist port areas

Deliverable 3.2.3

Report of geochemical characterization quality of sediments: information on how to manage and dredge sludge and remediation methods will be provided. Sediment seasonal sampling will be helpful provide scenarios on the evolution of coastal area of the project related to climate variation: it will be useful to estimate maintenance costs and dredging management. Maps of trace elements distribution will provide useful information for hydraulic maintenance and handling of dredged sediments. The environmental status tests of the sediments will be repeated for a seasonal cycle in Goro test site in order to verify the impact of hydrodynamics on the distribution and dissemination of pollution. Chemical analyses of sediments and water (c.a.300 in total) for each port involved in the project, will be carried out in order to assess their environment status

Project Acronym	ECOMAP
Project ID Number	10047543
Project Title	Ecosustainable management of marine and tourist ports
Priority Axis	3
Specific objective	3.3
Work Package Number	3
Work Package Title	Monitoring/research of sea environment in marinas/ports ecosystems
Activity Number	3.2
Activity Title	Characterization of the marine water bodies and sediments quality of marine and tourist port areas
Partner in Charge	PP8 – University of Ferrara
Partners involved	PP9 – CFR; PP8 – UniFe
Status	Final
Distribution	Public
Date	27/06/2022

Authors:
Carmela Vaccaro, Elena Marrocchino, Antonello Aquilano, Dino Di Renzo, Negar Eftekhari, Maria Grazia Paletta

Contents

Figure index

Introduction

This final report represents one of the three activity deliverables belonging to Work package 3, Activity 2. This report will describe the sampling activities and the analysis of sediments with the related analytical results that were performed during the ECOMAP project.

Materials and Methods

Sediments Sampling

The sediments sampling, in the different pilot sites of the project, was performed differently according to the type of sampling environment:

- Beaches: in these environments, the sediments were collected using a small shovel and immediately placed into appropriately labelled plastic bags. A volume of approximately one liter was recovered for each sample.
- Seabed: in these environments it was necessary to sample from a boat, taking the material through a Van Veen grab sampler. This tool is useful for sampling sandy and clayey sediments in an underwater environment. It is equipped with clamps held open by a pin that keeps them open until they touch the bottom. At this point, the pin yields, and the clamps close quickly. Their closure becomes complete when the grab sampler is lifted (which is lowered and raised using a rope). At this point, it is possible to pull up the grab sampler and recover the collected material. The latter was immediately introduced in labelled plastic bags. The volume of sampled material amounts to approximately 1 liter for each sample.

The samplings were repeated over time in the\ various pilot sites.

Figure 1: Images of the sampling activities carried out within the project.

Texture Analyses

The samples were subjected to texture analyses to determine the dimensional distribution of the sediments and to classify them from a textural point of view.

The samples consisting of sediments ranging from sands to clays were subjected to quartering to obtain a smaller quantity than the starting one, representative of each corresponding sample. Subsequently, those samples underwent some treatments before the analytical phase:

Oxidation: the samples were treated with hydrogen peroxide until the effervescence was completely exhausted. This allows any organic substance that acts as a cement between the sediment particles, to be degraded. This phase is fundamental as it allows to favour the separation of the particles that would otherwise be united and, in the analytical phase, would be considered as a single particle (larger than the real ones) altering the analytical results. Oxygenation is not able to degrade coarse organic material present (such as algae, vegetable frustules, etc.); the latter was manually removed in later stages.

Wet sieving: at the end of the oxygenation phase, the samples were subjected to a wet separation process to separate the sandy material from the muddy one. This was done through a 63 micron-sized sieve. The material with a sandy granulometry obtained was immediately put to dry in an oven at a temperature of 105 ° C; the muddy fraction was, on the other hand, left to settle in collection jugs. After all the muddy sediment was settled, the water contained in the jugs was taken away by siphoning to allow the recovery of the material deposited on the bottom. As for the sandy fraction, after drying, the samples were weighed on a precision balance. Subsequently, a further quartering of each of them was carried out to obtain a quantity of material of 3.0 ± 0.2 grams to be subjected to the texture analyses. These were performed using the sedimentation balance. The balance consists of a sedimentation tube filled with water, 2 meters high, which is surmounted by a lid in which the material to be analyzed is placed and on the bottom contains a plate of a balance immersed in it. The material is then dropped from above and the coarser particles will fall on the plate first; over time, smaller and smaller particles will gradually fall off. The accumulation of particles on the plate (expressed by their weight) is automatically recorded and related to the dimensions, according to the principle of Stokes' law, through a computer. The analysis is thus expressed cumulatively, in which the percentages of each single particle size fraction are obtained by difference.

Figure 2: Sedimentation balance used for the analyses.

As regards the muddy material, however, the analytical methods were different based on the quantity of mud present in the samples:

In the samples where there was a low quantity of muddy fraction, the sedimented material in the jugs was collected through filter paper (previously weighed), put to dry, and subsequently weighed. In this case, the abundance of material less than the size of the sand was expressed simply as a percentage of mud, that is the sum of the abundances of silt and clay since it was not possible to perform the analyses to quantify the abundance of these two different granulometric classes.

In the samples where there was a high amount of muddy material, this was recovered from the jugs and collected in beakers. A portion of this material was used to determine the percentage of moisture present, in order to calculate the dry weight of the sample. Another portion was instead taken for analysis through the X-ray sedigraph, to determine the abundance of silty and clayey fractions in the samples. The X-ray sedigraph is an instrument that determines the size of particles dispersed in a liquid by measuring the attenuation of a collimated X-ray beam and using Stokes' law. The X-ray beam is attenuated the more, the greater the number (and the volume) of suspended particles. Consequently, as the particles are deposited, the intensity of the X-ray beam increases, as the suspension becomes less charged with particles. The intensity of the beam is then used to calculate the quantity of particles having a given size using Stokes' law.

Figure 3: Instrumentation of the X-ray sedigraph used for the analyses.

At the end of the analytical phases, the abundances of the granulometric class differences are normalized to the total weight of each sample.

On the other hand, as regards the samples made up of mainly gravelly material, the texture analyses were carried out using the sieves method. The sieves usually consist of mesh with square holes and the analysis is done by placing a stack of sieves, starting from the coarsest at the top to the finest at the bottom. The stack is closed at the bottom by a plate for collecting the material passing through the last sieve. The pile is placed in a stirring apparatus which has the task of shaking the material so that each granule sooner or later comes into contact with a hole in the mesh according to its minimum diameter. Then, those clasts that have minimum and average diameters smaller than the mesh will pass through the sieves and those that have minimum and average diameters greater than the mesh size will be retained.
After shaking the material for about 15 minutes, the material retained by each sieve was weighed to determine the percentage abundance of each particle size class.

Loss on ignition analyses (L.O.I.)

The L.O.I. is a ponderal analysis technique for determining the content of volatile components in a rock, loose sediments, or soil. It consists of the strong heating of a sample at a given temperature to eliminate certain volatile substances. As a result of the leakage of the latter, the weight of the sample decreases, related to the quantity of volatile substances initially contained in the sample. Among the most common substances that are determined with the L.O.I. there is organic carbon (500 ° C), carbon dioxide (750 ° C), sulfur, chlorine, fluorine, and recrystallization water.
The analytical procedure was as follows:

1. The samples were first ground, to pulverize the starting material, through an electric mill with an agate jar. A certain quantity of material obtained from each sample was subsequently dried at 105 ° C in an oven.
2. Using a precision balance, the empty porcelain refractory crucible was weighed. Subsequently, the weighing was carried out after having introduced a certain quantity of the powder to be subjected to the L.O.I (approximately 0.5-0.6 g per sample).
3. The crucibles were placed in the oven and the powders were "calcined" at a temperature of 1000 C for 8 hours.
4. The crucibles were removed from the oven and left to cool in the desiccator.
5. Once cooled, the crucibles were weighed again.

At this point, it was possible to calculate the L.O.I. expressed as a percentage weight obtained as a proportion of the weight loss relative to the weight of the powder initially inserted.

Calcimetry

Calcimetry is an analytical technique used to measure the carbonate content in a rock (stone or loose material) or soil. The content of carbonate present in a sample represents a fundamental element in the study of sedimentary rocks.

The carbonate content is determined through an analysis that is based on the chemical reaction between the material under examination and hydrochloric acid. The instrument used to carry out this analysis is the calcimeter. This instrument can determine the amount of carbon dioxide that develops from the chemical reaction between a known quantity of suitably prepared samples and hydrochloric acid. The volume (expressed as a percentage) of carbon dioxide developed is equal to the percentage of carbonate present in the sample.

The instrumentation used for these analyses is composed as follows:

- Glass container with hermetic cap in which the reaction between the sample and hydrochloric acid takes place.
- A connection pipe in which the passage of carbon dioxide takes place.
- The electronic calcimeter, equipped with a pressure transducer for the developed CO2, barometer, and thermometer for the environmental conditions.

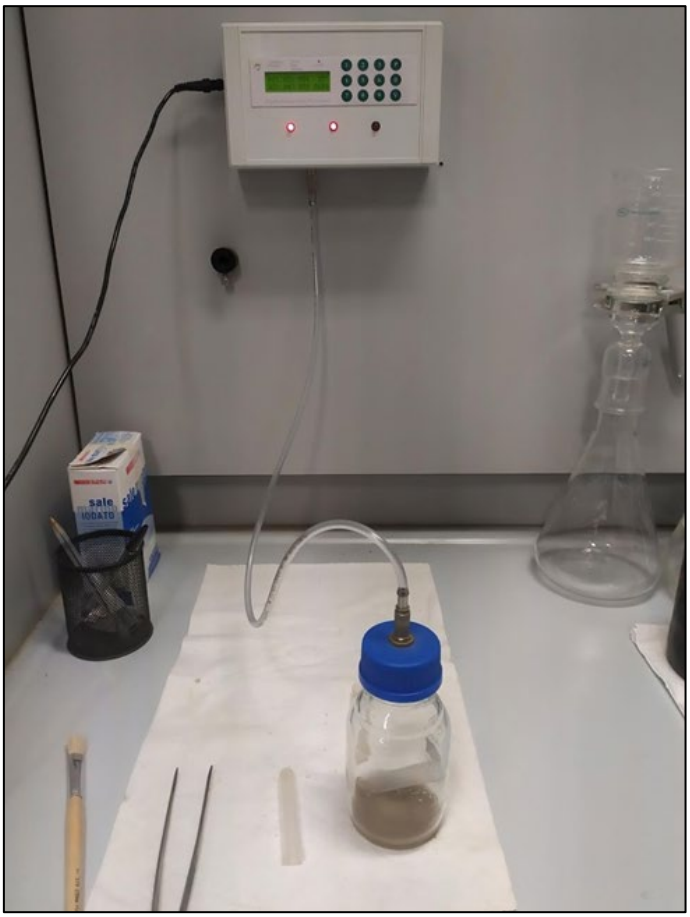

Figure 4: instrumentation used for calcimetric analyses.

The procedure performed for carrying out the analysis is as follows:

1. The samples to be analyzed, previously ground, were dried in an oven at 105 ° C for 24 hours. This allowed the elimination of the humidity present in the sediments, which could have partially inhibited the reaction.
2. The instrument was calibrated using 0.5 g of pure calcium carbonate.
3. Exactly 0.5 grams of sample were weighed (using an analytical balance to at least three decimal places) and introduced into the glass container.

4. 5ml of hydrochloric acid (diluted to 10%) were introduced into a test tube which was delicately inserted into the glass container, resting it against the walls of the container; at this point, the container was hermetically closed.
5. Given the measurement input to the instrument, the test tube inside the container has been turned upside down allowing the acid to react with the sample and release carbon dioxide.

The analysis time is 15 minutes for each sample. The instrument is designed in such a way as to memorize the readings of carbon dioxide volume taken at well-defined time intervals, corresponding to 60, 300, and 900 seconds.

The reason for this temporal division of the test is that the different types of carbonates (calcite, dolomite, etc.) react at different times. The first carbonate to react is calcite (calcium carbonate), which reacts more or less completely in the first 60 seconds; dolomite (mixed carbonate of calcium and magnesium) begins to react after the first 60 seconds and takes several minutes to react completely. Recording the carbonate content at different time intervals, therefore, allows for determining the abundance of different types of carbonates present in the sample.

X-ray Energy Dispersion Spectrometry (SEM-EDS)

The analytical technique of X-ray energy dispersion spectrometry was used to determine the chemical composition of the samples.

X-ray energy dispersion spectrometry by scanning electron microscope (SEM-EDS) is an elementary microanalysis technique widely used in various fields of study. The characteristic peaks of X-rays from excited electrons provide information for the identification and quantification of all elements of the periodic table (except hydrogen, helium, and lithium) present as major elements (10%), minor elements (between 10% and 1%) and trace elements (<1%). The detection limits generally vary between 0.1-0.3% depending on the elements of interest, the matrix, and the operating conditions of the instrument (Newbury & Ritchie, 2013).

Analyses were conducted using a Zeiss EVO MA15 scanning electron microscope (Carl Zeiss AG, Oberkochen, Germany), equipped with an INCA 300 x-ray energy dispersion spectrometer (Oxford instrument, Abingdon, UK). The characteristics of the instrumentation are the following:

- Magnification range: 5 - 1.000.000x.
- Chamber dimensions: 365 mm (Ø) x 275 mm (h).

- Usable acceleration voltages: 0.2-30 Kv.

Each sample to be analyzed was ground to obtain powders. Each sample was subsequently pressed through a press, using boric acid support to obtain tablets for the analyses.

To obtain the chemical composition of the samples, each sample was divided into four square areas using the smartSEM software (Zeiss). Each area was analyzed individually and subsequently, the entire area containing the squares was analyzed. This was done to verify the repeatability of the analysis. The obtained elemental composition (expressed in percentage weight - wt.%), was subsequently converted into oxide percentage (wt. %) through a conversion algorithm.

Mass spectrometry

Mass spectrometry is a powerful analytical technique used to quantify known materials, identify, and quantify unknown compounds.

The process underlying this technique consists of the conversion of the sample into gaseous ions, with or without fragmentation. These are subsequently characterized based on the ratio between mass and charge (m / z) and their relative abundances.

A mass spectrometer generates a series of ions starting from the sample to be analyzed; subsequently, it separates these ions based on the “m / z” ratio and records the relative abundances of each type of ion. The fundamental parts that make up a mass spectrometer are:

- A sample introduction system for introducing the material to be analyzed into the ion source while maintaining the vacuum required by the technique.
- The ion source for the production of gaseous ions from the substance to be analyzed;
- A mass analyzer to identify the characteristic mass components of ions based on the mass/charge ratio.
- A detection system to reveal and quantify the relative abundance of ions identified through a conversion dynode with a secondary electron multiplier and multi-channel plate (Kaklamanos, Aprea and Theodorisis, 2020).

In this study the following mass spectrometry techniques were used: “Isotope Ratio Mass Spectrometry” (IRMS) for the measurement of the carbon isotope ratio; "Inductively Coupled Plasma Mass Spectrometry" (ICP-MS) for the quantification of heavy metals.

Isotope Ratio Mass Spectrometry

The IRMS technique allows you to accurately measure the small differences in the abundance of the isotopes ^{2}H / ^{1}H, ^{13}C / ^{12}C, ^{15}N / ^{14}N, and ^{18}O / ^{16}O of the substances under analysis.

One of the most popular tools for IRMS analysis, applicable to a wide range of disciplines and for a great variety of materials, is the EA-IRMS (Elemental Analysis - Isotope Ratio Mass-Spectrometry). Solid samples are introduced into the elemental analyzer (EA) through tin capsules and the analysis proceeds as follows:

- The sample is burned, and the gases formed are introduced into the ion source of the IRMS.
- The gases are ionized and then separated using an isothermal gas-chromatographic column and using a "purge and trap" system column.
- Final revelation in the magnetic sector analyzer (Kaklamanos, Aprea and Theodorisis, 2020).

For the IRMS analyses, an elementary analyzer “Elementar Vario Micro Cube” was used in line with an “ISOPRIME 100 mass spectrometer, operating in continuous flow mode. This system allows temperature variations of the combustion module above 1050 ° C, functional for the extraction of components at different destabilization temperatures (Natali, Bianchini, et al., 2018). The elemental carbon concentration is expressed as a lost percentage (wt%). The isotope ratio is expressed in the notation δ (‰): δ (‰) = [1000 · (R_{sample} - $R_{standard}$) / $R_{standard}$)], where R_{sam} is the isotopic ratio of the sample and $R_{standard}$ is the isotopic ratio of the international isotope standards Pee Dee Belemnite (PDB) for Carbon and air N_2 for Nitrogen.

For the IRMS analyses, the previously ground and dried samples were introduced (about 10 mg) into small tin containers. These were closed to form small spheres, such as to be able to be introduced into the autosampler system.

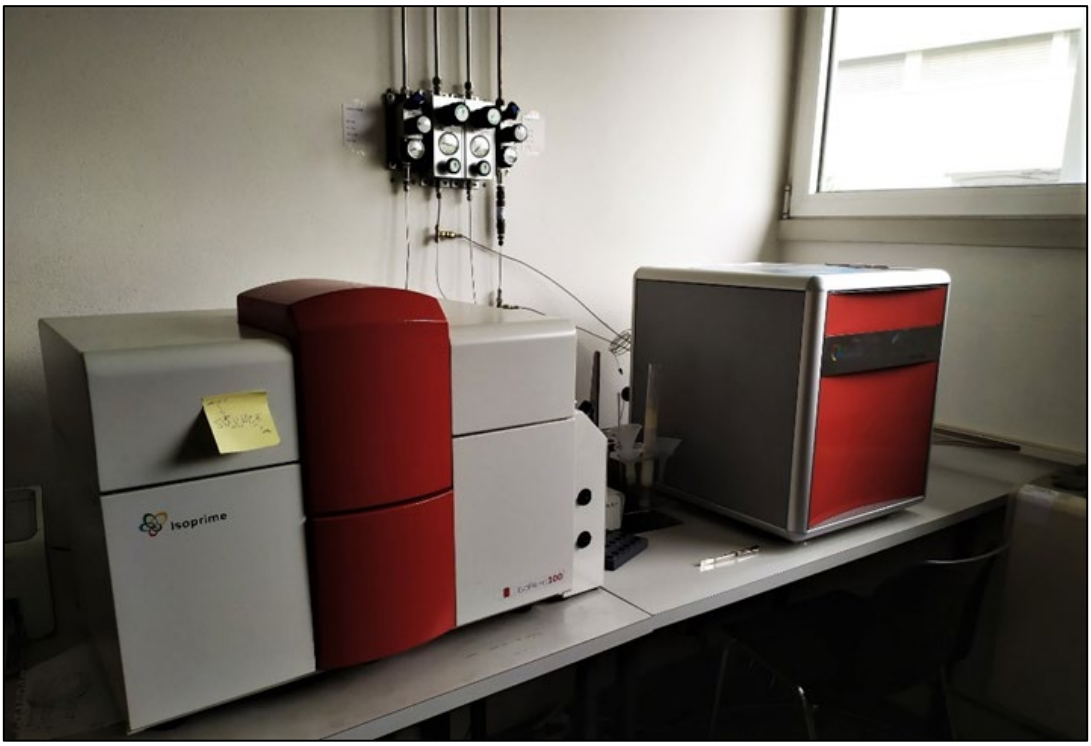

Figure 5: EA-IRMS instrumentation. On the right, there is the elementary analyzer "Elementar Vario Microcube"; on the left there is the "Isoprime100" mass spectrometer.

Inductively Coupled Plasma-Mass Spectrometry (ICP-MS)

The ICP-MS technique was used to determine the concentration of metals.

Through this technique, it is possible to identify the presence of inorganic metallic material at concentrations below 1 ppb.

The ICP-MS works using an inductively coupled plasma torch, which consists of three concentric quartz tubes, capable of producing an ionization of the substances under examination. The ions produced are then separated and detected by the mass spectrometer.

For the ICP-MS analyses the samples were subjected to acid attack using the following procedure:

1. 0.2 g of each previously pulverized and dried sample were introduced into a PTFE beaker. To this were added 6 ml of hydrofluoric acid (ultra-pure) and 3 ml of nitric acid

(ultra-pure). The beakers were covered with paraffin and left to stand under the extractor hood for 24 hours.

2. After 24 hours the samples were placed for 15 minutes in an ultrasonic bath to homogenize the solutions.
3. Through a heated plate, the solutions were brought to a temperature of 195 degrees causing evaporation.
4. Once the incipient dryness was reached, the beakers were removed from the hot plate and allowed to cool. At this point, 3 ml of hydrofluoric acid and 3 ml of nitric acid were added, and the beakers were placed back on the plate heated to 195 ° C.
5. Once the incipient dryness was reached, the beakers were placed to cool. Further addition of 4 ml of nitric acid was then carried out and the drying operation was repeated.
6. Once the incipient dryness was reached, the beakers were left to cool. At this point, a fourth and final addition of 2 ml of nitric acid was made. The solutions were racked into labelled flasks. By adding ultra-pure water, the solutions were subsequently diluted up to a volume of 100 ml.

The solutions were then subjected to analyses, that were carried out by using an X Series (Thermo-Scientific, Bremen, Germany) inductively coupled plasma mass spectrometer.

Test sites

Bibione

Geographic framework

Bibione is part of the Municipality of San Michele al Tagliamento, located in the Province of Venice. San Michele al Tagliamento borders the municipalities of Morsano al Tagliamento, Ronchis, Latisana and Lignano Sabbiadoro, Fossalta di Portogruaro, Portogruaro and Caorle and is bordered by the Adriatic Sea to the south and the Tagliamento River to the west.

Bibione is a peninsula, bordered by the Tagliamento river to the east, the Lugugnana canal to the north, and the Litoranea Veneta to the west, while the Adriatic Sea to the south. At its northern end is the Val Grande Natural Park, a lagoon area with low salinity waters. To the east, at the Punta Tagliamento lighthouse, there is the mouth of the Tagliamento river. To the west, there is the lagoon where Porto Baseleghe is located.

The coast of Bibione is about 10 kilometers long and is low and sandy.

Figure 6: Satellite image of Bibione.

Climate

The area of the municipality of San Michele al Tagliamento falls within the coastal strip of the Venetian plain: although it is part of the Mediterranean climate, it has a high degree of continentality, with frigid winters and hot summers. Precipitation is distributed fairly evenly throughout the year, except in winter, which is the driest season. In the intermediate seasons, the Atlantic perturbations prevail, in summer, however, there are frequent thunderstorms. Temperatures follow, as usual, the seasonal trend: the highest are observed during the summer, with an average of 28 ° C and the lowest between December and January, with an average of 3-4 ° C.

For what concern the rainfall, they substantially have two peak periods corresponding to the spring season (April with about 95 mm) and the late summer-autumn period (with about 120

mm). The least rainy season is winter, with a minimum in February (51 mm), while in summer rainfall is around 65 mm.
The Bibione area is significantly affected by the influence of the sea and the wetlands behind it, making it possible to consider it as a warm temperate microclimatic area. The diurnal-nocturnal temperature variations are not of particular importance if not near the coast, due to the accumulation and thermal release of the water masses.
The prevailing winds blow from the north, coming from the alpine areas and northern Europe. Characteristic is the Bora wind, even if, especially in the western part, it is affected by the winds from the southwest.

Geological framework

The area of San Michele al Tagliamento is in the Venetian-Friulian plain, falling within the Neogene-Quaternary foreland of the eastern south-alpine chain, with south-eastern vergence, which, starting from the Pliocene, is shared with the northern Apennine chain to northeastern vergence.
The Veneto-Friuli plain represents the Tertiary-Quaternary sedimentary filling of the foreland subsidence basin relating to the south-alpine and north-Apennine chains (Doglioni, 1993). The expansion activity towards the north of the Apennine foredeep reached the southern sector of the Venetian plain starting from the upper Miocene, leading it to a rotation towards the south, recorded as far as the Venetian Lagoon (Carminati et al. 2003).
The Alpine front is buried below the Venetian Plain, although in the Friulian sector some of the outermost thrusts partially emerge in the middle of the plain, creating some tectonic terraces that touch both the Middle Pleistocene and the alluvial sediments of the Last Glacial Maximum (LGM) (Zanferrari et al., 2008).
Below the Plio-Quaternary sediments they tell a rather complex geological history of the area:
The palaeogeography of this area, throughout the Jurassic and Cretaceous periods, was represented by the Belluno Basin-Friulian Carbonatic Platform (FCP) system, which was established in the Lower Jurassic, in an extensional and transtensive context linked to the opening of the tethidean basin.

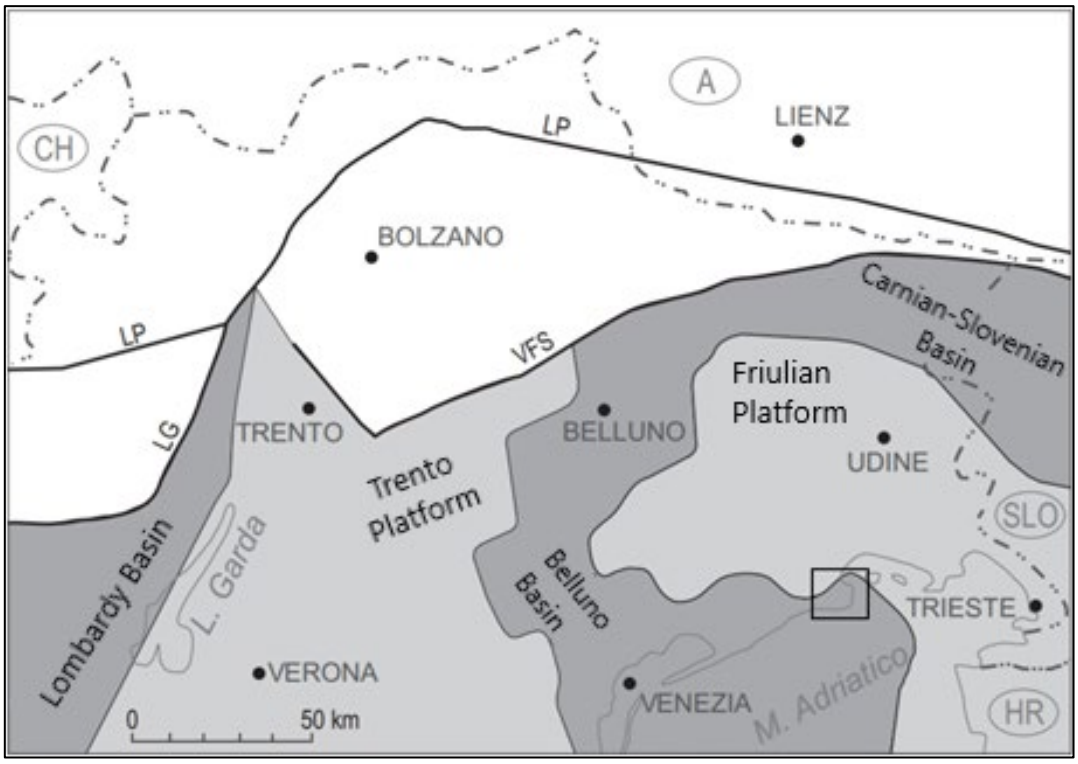

Figure 7: Paleogeographic scheme of the South-Alpine between middle Jurassic and the endo of Cretaceous. In the square is highlighted the Bibione Area. Source: Zanferrari et al., (2008) – modified.

The Bibione area falls within the basin area of the carbonate system considered (Zanferrari et al., 2008).

Starting from the end of the Cretaceous period, the Dinaric event that led to the structuring of the Dinarides subjected the carbonate platform to a yo-yoing process: at first, there was a general uprising that led to the emergence and extinction of the FCP; in a second moment, the flexuration of the foreland towards the east, leads to the drowning of the north-eastern sectors of the platform, reaching bathyal bathymetry.

Starting from the upper Oligocene, the indentation of the Adriatic plate below the Alpine system s.s. and the simultaneous right-hand passing along the Periadriatic Lineament (Massari, 1990; Ratschbacher et al., 1991; Fodor et al., 1998), led to the formation of the SSE chain with folds and

thrust of the Southern Eastern Alps (Doglioni and Bosellini, 1987; Castellarin and Cantelli, 2000). During this event (Insubric event) the Venetian-Friulian plain and the Adriatic offshore came to be in a position of the distal foreland, with a peripheral rise at the current coast. The foreland basin slowly extended towards WSW and reached the current coastal area only in the Burdigalian.

Starting from the Serravallian (Castellarin et al., 1992) the southeastern Alpine chain was structured.

From then until today, the southern alpine foreland is shared between the two chains (Fantoni et al., 2002; Di Giulio et al., 2006). In reality, the effects of the structuring of the north-Apennine chain are completely prevalent and now this region belongs to the Apennine foreland (Zanferrari et al., 2008).

The current appearance of the Veneto-Friuli plain is the result of the late Pleistocene-Holocene evolution of the rivers that characterize it and of the phases connected with the glacial period called Last Glacial Maximum (LGM). These areas of fluvial influence are defined as "alluvial megafans" (Fontana et al., 2004; Fontana, 2006; Fontana et al., 2008): they are depositional systems in the shape of large fans that originate at the end of the mountainous area. The particle size of the sediments of these systems decreases both towards the coast and towards the edges of the megafans. These are predominantly controlled by glacio-eustatic dynamics, as they guide both the alluvial processes and the position of the mean sea level.

As for the area under study in more detail, it constitutes the western distal portion of the megafan of the Tagliamento river. In this area, the ancient alluvial plain was buried or remodelled following the formation of the Caorle lagoon and the delta systems.

Regarding hydrogeology, the Coastal Hydrogeological System has been identified with the area next to the coastline affected by the Middle Holocene marine transgression. The limit between this system and those upstream has been conventionally placed in correspondence with the maximum marine ingression line: the coastal sands that make up the Holocene coastal sandy aquifer are deposited within this limit. From the hydrostratigraphic point of view, it is possible to divide the coastal hydrogeological system into several parts. Within the first 16 meters of depth, a sandy sedimentary body extends along the entire coastal arc, identified as a Holocene coastal sandy aquifer. The base of this aquifer was conventionally placed at the lower limit of the regressive littoral deposits, consisting of mainly sandy sediments corresponding to beaches,

littoral ridges, and dunes. The top of the coastal aquifer emerges along the entire provincial coastal arc represented by the undifferentiated coastal unit and the Bibione unit at the mouth of the Tagliamento (Fabbri et al., 2013).

The Holocene coastal sandy aquifer consists of coastal deposits corresponding to beaches, coastlines, and dune systems, formed by fine and medium sands and silty sands, with the presence of bioclasts. In the interdunal depressions, alternations of clayey silts and silty-clayey sands are found, with variable percentages of organic matter and sometimes peat (Fabbri et al., 2013).

Geomorphology

Bibione is located on the right wing of the delta of the Tagliamento. The areas occupied by brackish waters have been greatly reduced and remodelled by human interventions; currently, they are represented by the Valle Grande and Vallesina of Bibione, as well as by the nearby lagoon of Caorle (Bondesan and Meneghel, 2004).

The mouth of the Tagliamento is an example of a bialar cusp delta, whose relatively larger western wing reaches 9 km in length. The Tagliamento delta was formed about 2000 years ago. The setting of the latter did not take place with a gradual dynamic, but with rapid increases interspersed with erosive phases and phases of stability (Marocco, 1888, 1889).

The delta of the Tagliamento underwent, between 1644 and 1868, profound changes caused both by natural factors and by anthropic factors related to the embankment, burying works, reclamation, and continuous river regimes. Over the years the delta has been subjected to severe erosion and as many nourishment phenomena (Zunica, 1971).

Comparing the shorelines reported in the surveys of 1891, 1978 1985, it can be observed the evolution of the left-wing of the Tagliamento with an accentuated development of the eastern lobe of the mouth, in contrast to the erosion of the stretch of coast that extends up to Lignano Riviera. Towards the east, however, as far as the Bocca di Lignano, a strong progression of the beach stands out also in this case, at a secular level (Brambati, 1987).

The evolutionary trend of the coast is represented by a marked erosive phase in the sector near the mouth, whose material, following the direction of the main drift current, undergoes transport towards the west. A part of it is deposited on the western part of the lobe, in correspondence with the more urbanized part. Another part, on the other hand, participates in the expansion (towards the west) of the "Bocca di Porto Baseleghe" system (Fontolan, 2011).

The entire delta area, starting from the 1960s, has been subjected to an intense process of anthropization for urban, residential, and tourist purposes. The houses are developed in a strip near the beaches and their construction involved the excavation of the dune reliefs.
Urban development has also entailed the creation of important nautical centres which have been developed in the close vicinity of the lagoon mouths (in the case of Bibione, the nautical centre is that of Porto Baseleghe). The terminal part of the Tagliamento was fixed by the creation of a marina (equipped with a shipyard, workshops, residential areas, recreational areas, sports facilities, bars, and restaurants) which uses the river entrance as an access channel (Gordini et al., 2006).

Results of analyses

As regards the coastal area of Bibione, the sampling was carried out on the whole area, from the mouth of the Tagliamento river to the inner part of the Baseleghe Lagoon, where the Port of Baseleghe is located.

Sampling was performed in different environments to study the differences between sediments from different coastal environments. The sampling areas are as follows:

- Baseleghe Lagoon: the sampling concerned the navigable section of this area. Some samples were also taken on the beaches and the banks of the canal.
- Dune / Backshore: the samples were taken in the emerged beach areas. The sediments of these areas are washed by seawater only on occasions of severe storms.
- Shoreline: the samples taken in these areas represent sediments that are continuously exposed to the waves arriving on the coast.
- Seabed: the samples were taken in areas of the seabed, about 500 meters from the coast.

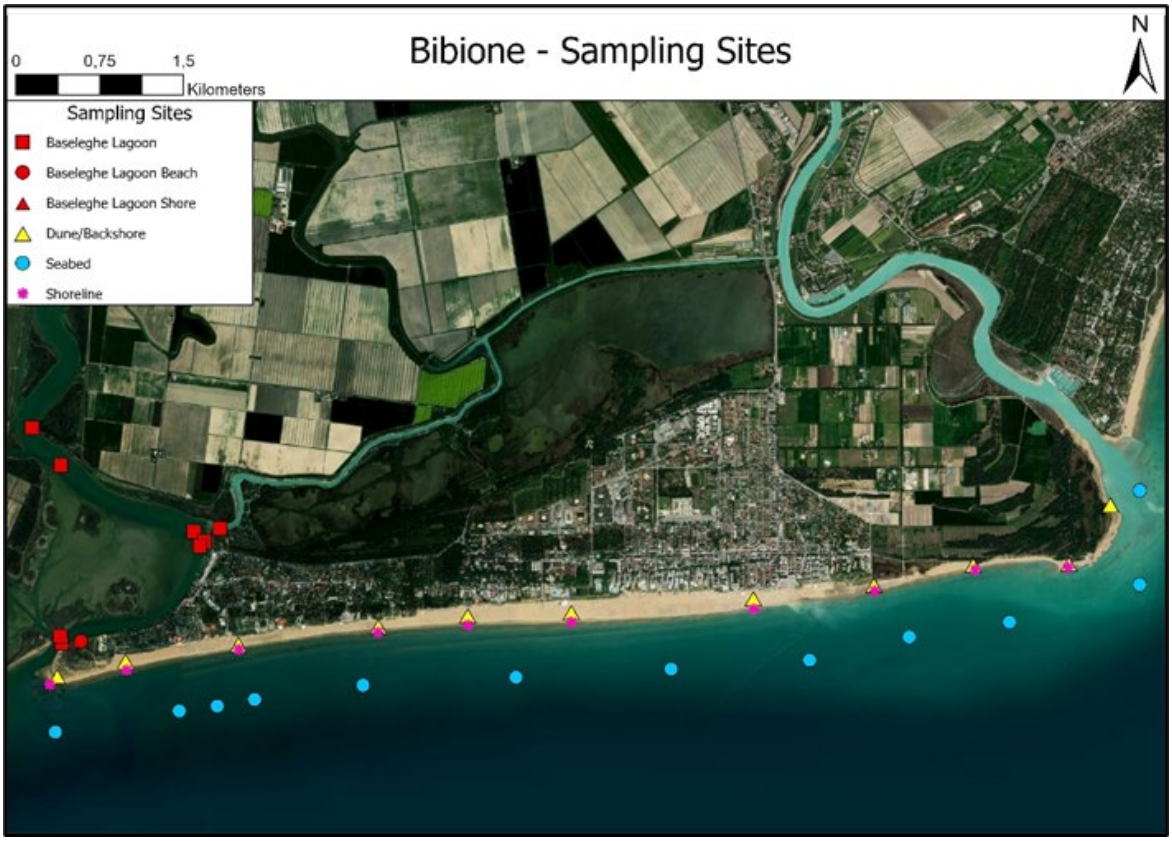

Figure 8: Satellite image of the Bibione area. The zones and the relative sediment sampling points are reported.

In the matter of texture of the sediments, two main sediments domains have been identified based on the results of textural analyses, such as the sediments of the coastal area (sensu stricto) and the sediments of the Baseleghe lagoon:

- The sediments of the Baseleghe lagoon are essentially made up of silty and clayey sediments, in which the sand content is relatively low. Using the sediment classification scheme proposed by Shepard (1954), these samples can be classified as clayey silt, sand-silt-clay (a mixture in which the three terms are more or less equivalent, but in this case very displaced towards the vertex of the silt), silty sands and finally sands (Figure 9). The presence of some samples displaced towards the vertex of the sands will be discussed in the following pages.

- The sediments coming from the coastal area in sensu stricto are all classified as sands, in which silt and clay are present in very low percentages (if not completely absent).

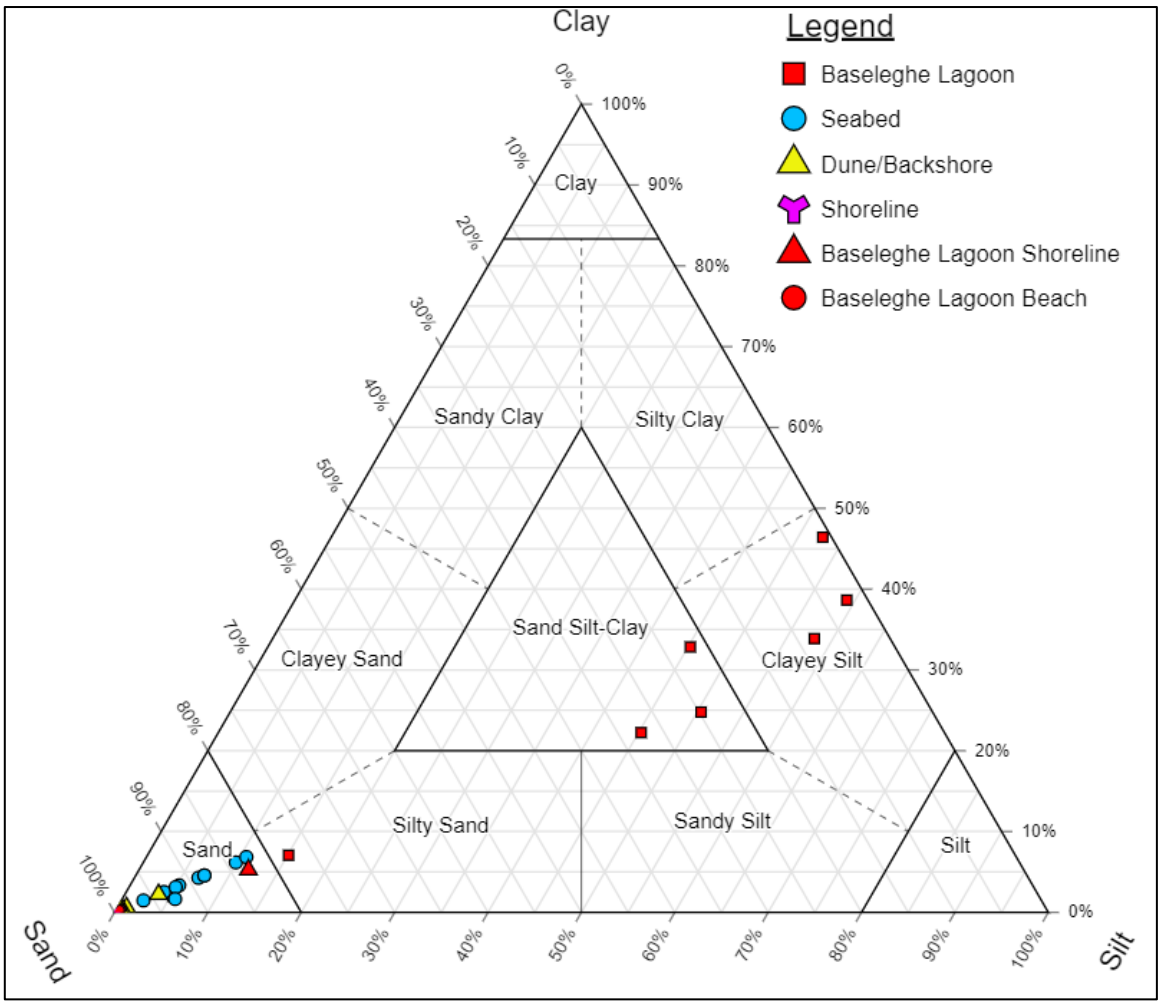

Figure 9: Shepard's sediment classification scheme (1954) on which the textural compositions of the samples are plotted.

Textural differences were also observed within the two domains described above. The most evident concern, as previously mentioned, is the sediments coming from the Baseleghe lagoon, in which it has been observed that some samples show a much higher sand content than others (Figure 5).

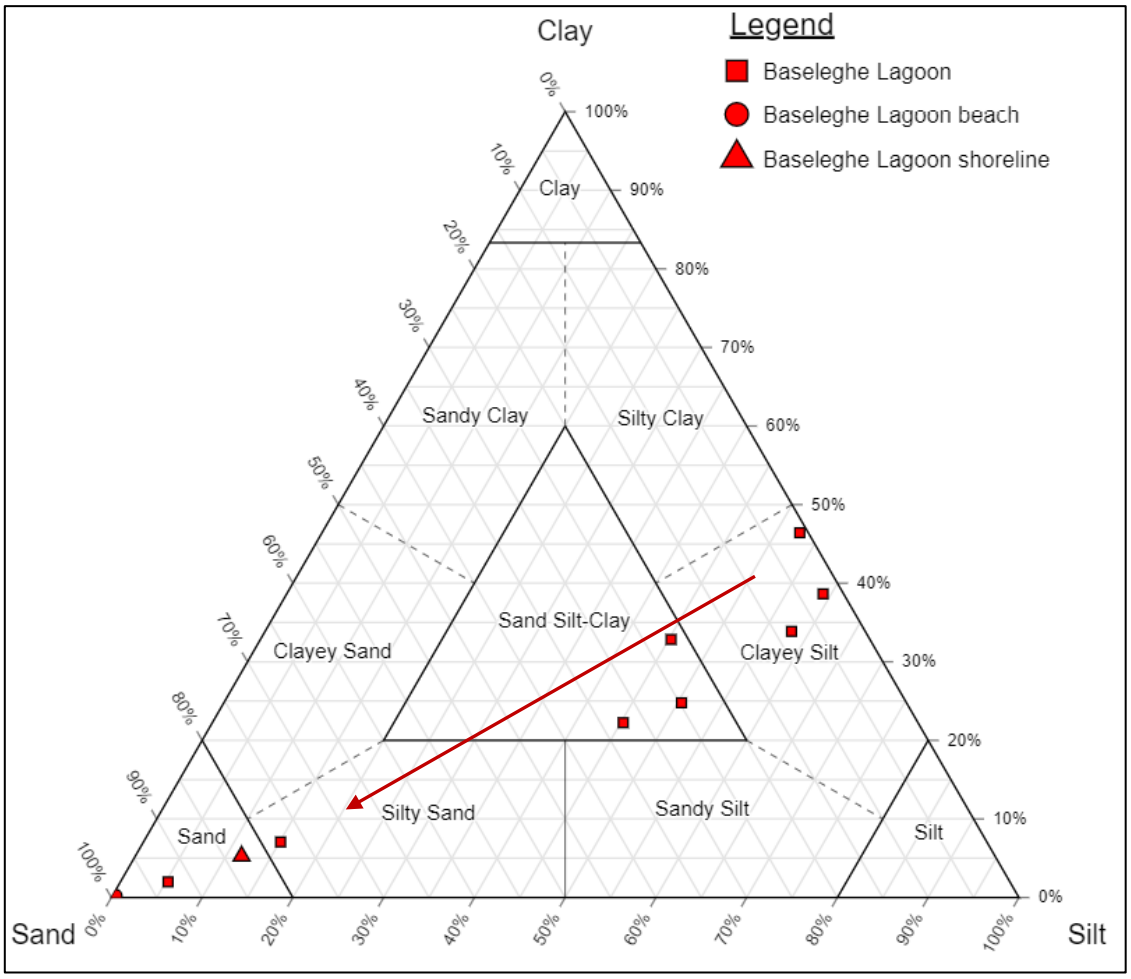

Figure 10: Shepard's sediment classification scheme (1954) on which the textural compositions of the samples from Baseleghe lagoon are plotted. The red arrow indicates the increase in sand content.

The sand content in the samples, determined through textural analyses, was plotted on a map and then a deterministic "Inverse Distance Weighting" (IDW) interpolation was performed through the ArcGIS software. The results of this interpolation (Figure 11) showed that the sand content, in the context of the Baseleghe lagoon, increases towards the mouth of the lagoon (reaching the values of the coastal zone) while it decreases towards the internal areas of the lagoon.

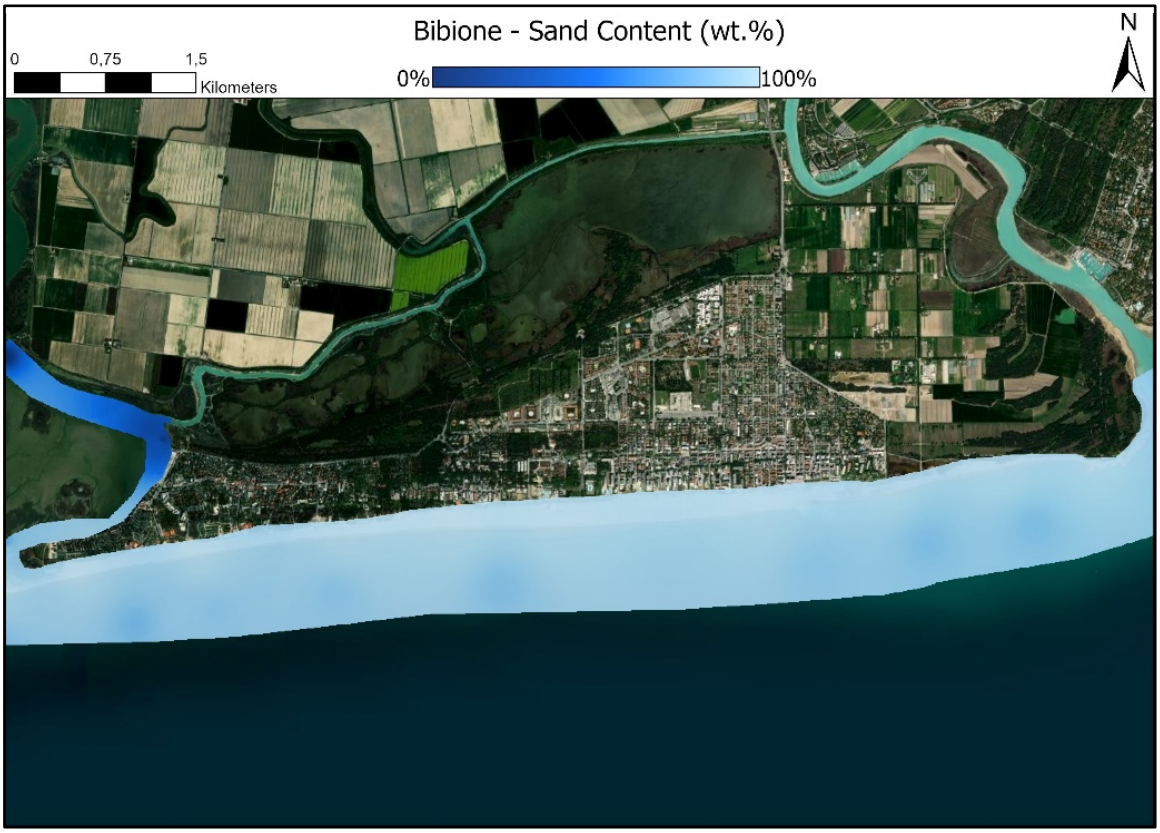

Figure 11: Result of the IDW interpolation concerning the sand content in the samples of the Bibione coastal area.

What was observed could probably be because approaching the mouth of the lagoon, the energy and influence of the sea (waves and tides) increase making it possible to transport sandy sediments that require more energy (compared to silty and clayey ones) to be taken over by the water. On the contrary, in the innermost areas of the lagoon where the influence of the sea becomes less effective, the silty and clayey sediments reflect the lower energy that characterizes these environments.

For what concern the domain of sediments from the coastal area in sensu stricto, slight textural differences are visible between the samples from the beach and those from the seabed, in which the latter showed a slightly lower sand content (in favour of sediments with a lower particle size

class) than the others, reflecting the lower energy conditions that exist, above all, concerning the shoreline environment.

Regarding the composition of the sediments, first, these were found to consist mainly of carbonates, in which the carbonate content varies from a minimum of 55% up to a maximum of 97%. Furthermore, in these samples, it was observed that there is a slight predominance of sediments of a dolomitic nature compared to the calcites ones and it agrees with previous studies carried out in this area (Gazzi et al., 1973).

Also in this context, a clear compositional difference was observed between the sediments of the Baseleghe lagoon and the sediments of the coastal area (s.s.): the sediments of the lagoon are distinguished from the others, as they are characterized by significantly lower carbonate content values. it has also been observed that the sediments closest to the lagoon mouth show higher carbonate content (contrary to those of the innermost areas) with values similar to the sediments of the coastal area. This behaviour (as seen previously about the sand content) is probably due to the context of greater energy in which this area of the lagoon is located, allowing the transport of sediments from the coastal zones towards those of the lagoon.

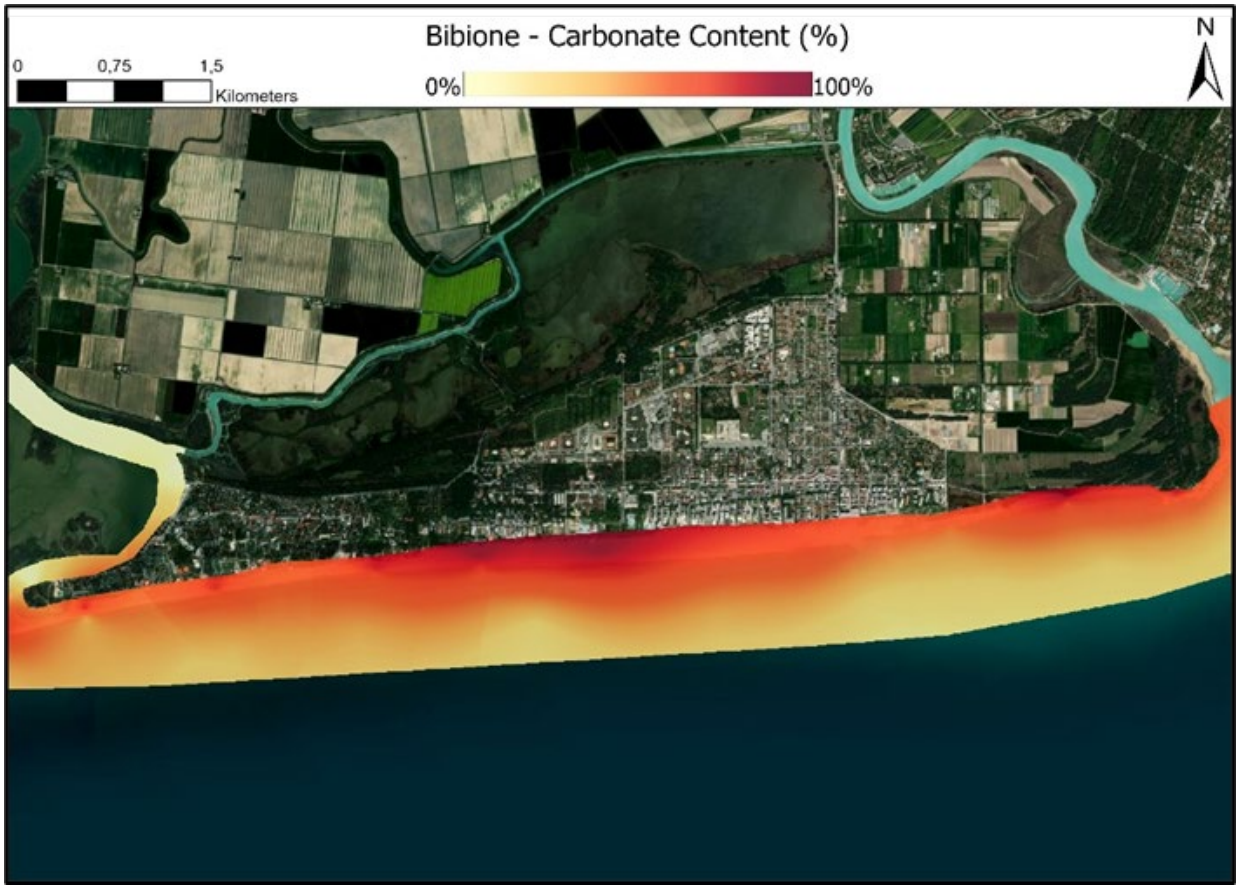

Figure 12: Result of the IDW interpolation concerning the carbonate content in the samples of the Bibione coastal area.

From the compositional point of view, it was also observed, that in the lagoon context the lower carbonate contents correspond to higher contents in terms of SiO_2 and Al_2O_3. Considering that the granulometry of the sediments in this area is basically silty and clayey, then it is likely that the greater content of SiO_2 and Al_2O_3 (Figure 13) is due to a greater quantity of phyllosilicate minerals (of which the clayey fractions are composed).

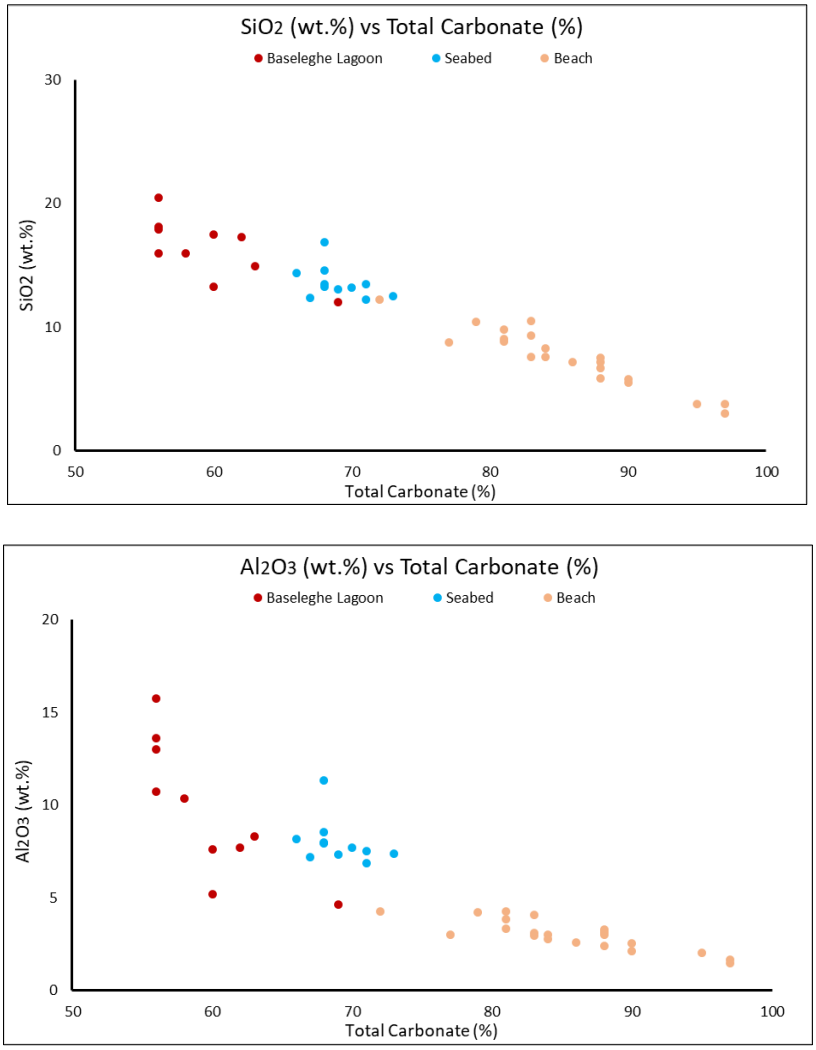

Figure 13: Scatter plots showing SiO_2 (top) and Al_2O_3 (bottom) vs. total carbonate content.

An interesting aspect that has been noted concerns the carbonate content in the different environments of the coastal zone. To observe variations in compositional terms, comparisons were made between the composition of the samples along profiles ranging from the backshore to the seabed: it was observed that the total carbonate content decreases along with these profiles, showing minimum values always in the seabed samples. This decrease was observed in

all terms concerning the carbonate content: total carbonate, calcite, dolomite, CaO, MgO, L.O.I (Figure 14).

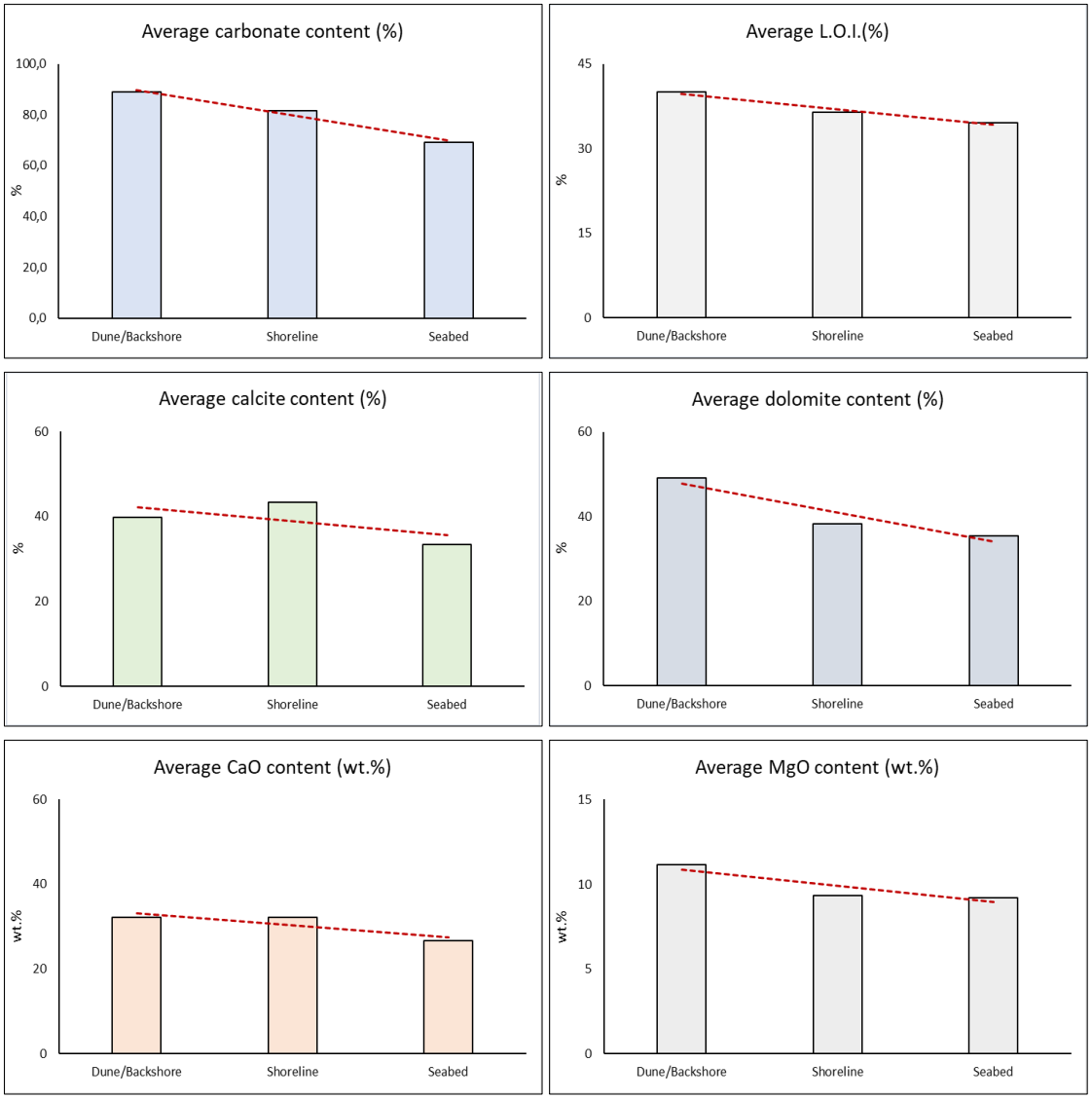

Figure 14: Bar graphs showing the averages of the contents of total carbonate, L.O.I., calcite, dolomite, CaO, and MgO in the samples from the different environments of the coastal area of Bibione.

The above shows substantial differences between the dune/backshore environment and that of the seabed that can be resumed as follow:

- decrease of total carbonate content of about 24%.
- decrease in the difference between total carbonate and $CaCO_3$ by approximately 28%.
- decrease in the average MgO content of about 18%.
- decrease in the average content of CaO of about 18%.

Considering that the seabed sediments had greater abundances of finer textural fractions than those of the shoreline and, especially than those of the backshore, it is possible to hypothesize that the observed decrease of carbonate terms depends on the particle size differences between these environments. However, the correlation indexes between the abundance of the different particle size fractions and those of carbonate terms, partially justify the observed variations (Figure 15). In fact, only total carbonate content CaO content showed a good degree of correlation with the abundance of the different particle-size fractions; while MgO, dolomite, and calcite contents were poorly correlated. It could be therefore hypothesized that another factor could be co-responsible for the observed variations.

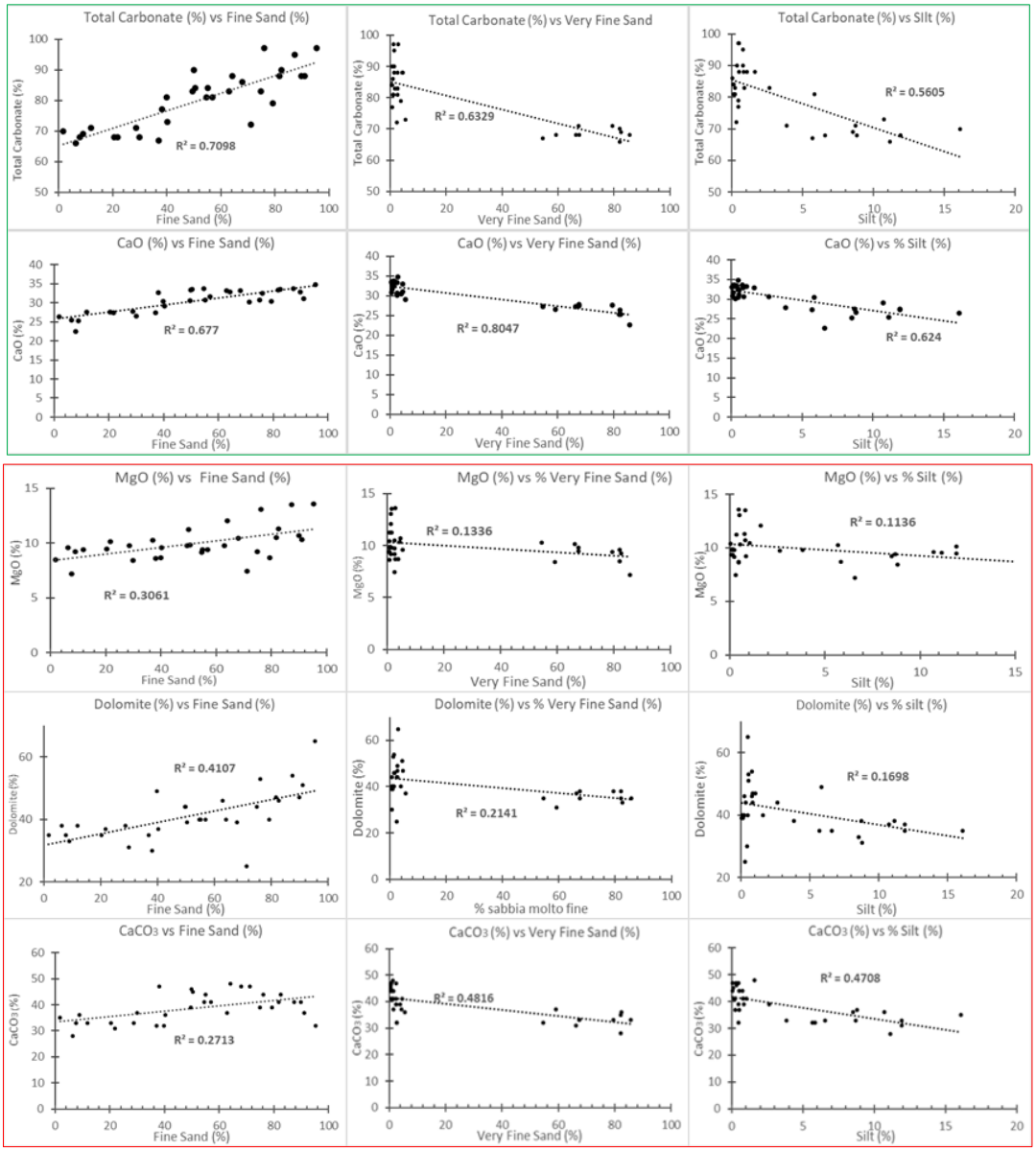

Figure 15: Scatter graphs showing the contents of total carbonate, CaO, MgO, dolomite, and calcite, compared with the abundances of the different particle size fractions. The graphs with the green outline are those in which there is a good degree of correlation between the terms considered; graphs with red outlines are those in which there is a low degree of correlation.

A factor, that could be co-responsible for generating the variability observed in the various environments, is related to the possible dissolution of carbonate sediments.
Considering that the backshore environment is not in contact with water (except during storms and rainy weather conditions) it is conceivable that the observed decreases, especially in the seabed sediments, may also be due to the dissolution of carbonates at contact with water. In the sediments of the seabed, which are constantly in contact with seawater, the longer contact times would allow the greater dissolution of the carbonates. Among the three environments considered, the intermediate values of decrease are observed in the shoreline samples: in this area, the contact time of the sediments with the water varies depending on the tides and wave motion. So, the smaller decrease in the shoreline area compared to the seabed would be justified.
In this context, although the sediments of the backshore environment only come into contact with water during severe storms, it must be taken into account that climate change is leading to an increase in intense short-lived phenomena (3, 6, 9, 12 hours) in which large amounts of rainfall in very short periods (Monai, 2009).
The increase in these phenomena could affect the contact times between water and sediments on rainy days. Although the granulometry of the backshore sediments still allows rapid infiltration of rainwater, intense events could negatively affect this parameter, leading to longer contact times and consequent greater leaching of carbonates. However, it should be emphasized that the contact times that would be established would not be comparable to the water-sediment ones in the shoreline area and, even more so, in the seabed area.
Leaching on carbonate sediments could represent a problem, especially in a climate change context:
One of the many effects that are causing climate change is the acidification of the oceans; ocean acidification is a predictable result of the high concentration of atmospheric CO2, leading to the solubilization of this species in ocean water with the consequent decrease in the surface ocean pH (Doney et al., 2009). The average pH of the oceans has decreased by 30% (due to the increase in atmospheric carbon dioxide) since the industrial revolution. With current emission rates, it is estimated that the pH of the oceans could decrease by an additional 150-200% (Turley, 2013). Recent studies have shown that marine acidification could cause marine carbonates to enter dissolution regimes much faster than predicted by previous studies

(Naviaux et al, 2019).

In this regard, comparisons have been made on the variation of seawater pH in recent years in the northern area of the Adriatic Sea. The data recorded daily by the Italian national tide-gauge network were processed to obtain annual averages and information on the possible acidification processes of the sea in this area of the Adriatic. For these evaluations, the tide-gauge stations of Venice and Trieste were taken into consideration, which is the closest to the Bibione site. The comparison has shown that, in recent years, there has been a decrease in the average pH of the seawater in this area (Figure 16).

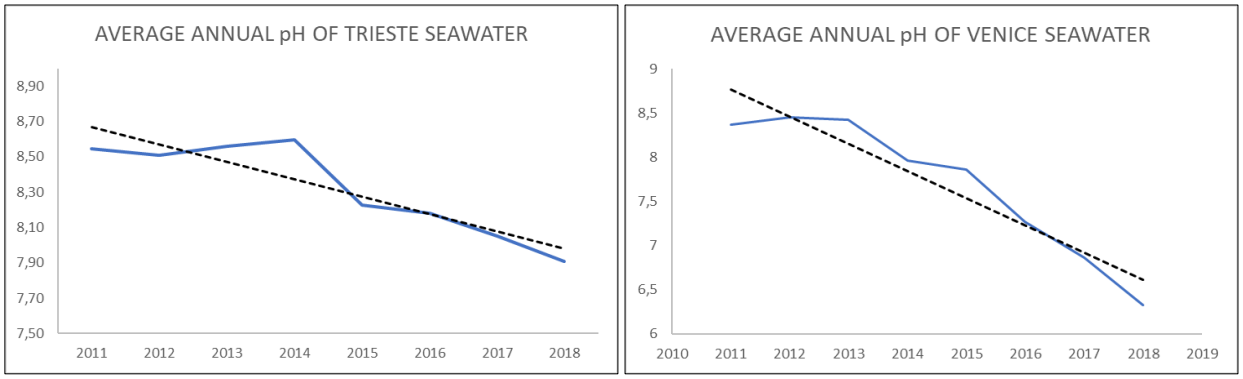

Figure 16: Average annual pH of the seawater of Trieste (left) and Venice (right), calculated using the data recorded by the Italian national tidal-gauge network.

Based on the above, the dissolution of carbonates could represent an additional factor to the problem of coastal erosion that already afflicts the Bibione area, especially in the future. Moreover, this could add to the increase in extreme events such as heavy rains and heavy sea storms in connection with climate change.

As regards the concentration of heavy metals in the sediments, The analytical results were subsequently compared with the legal limits established by the Italian legislation in "Table 1 of Annex 5 to Title V of Part IV of Legislative Decree no. 156 of 2006" (Figure 17; Figure 18). From this comparison it emerged that all the samples analyzed had concentrations lower than the legal limits for "sites for public, private and residential green use", testifying to the excellent quality of these sediments.

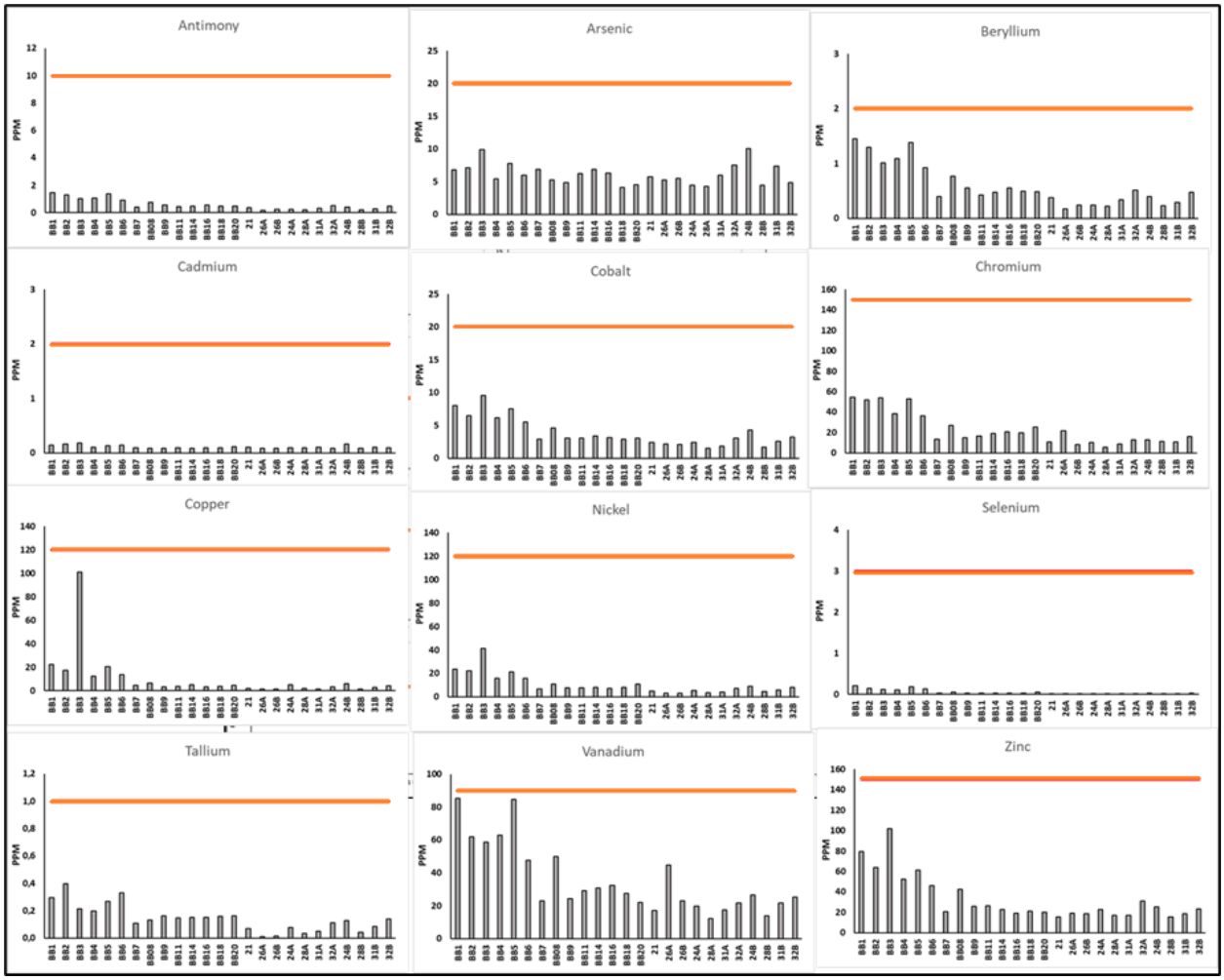

Figure 17: Bar graphs showing the concentrations of different heavy metals (arsenic, antimony, beryllium, cadmium, cobalt, chromium, copper, nickel, selenium, thallium, vanadium, and zinc) in the sediments sampled in 2019. Orange lines indicate the limit values of Italian law for "sites for public, private and residential green use "provided for in "Decree Law 152 of 2006".

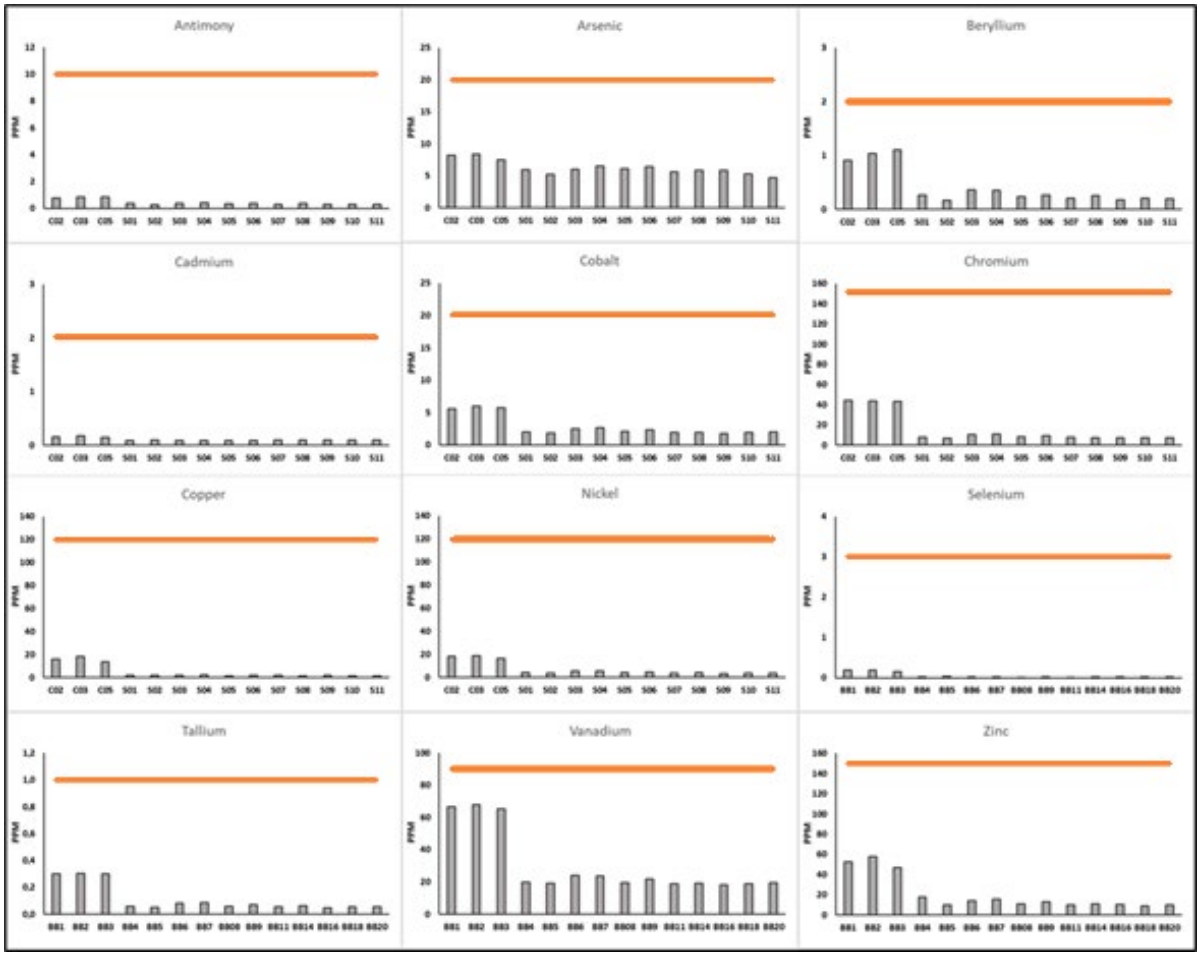

Figure 18: Bar graphs showing the concentrations of different heavy metals (arsenic, antimony, beryllium, cadmium, cobalt, chromium, copper, nickel, selenium, thallium, vanadium, and zinc) in the sediments sampled in 2020. Orange lines indicate the limit values of Italian law for "sites for public, private and residential green use "provided for in "Decree Law 152 of 2006".

Despite the good general quality of the sediments, both 2019 and 2020 samples, it was observed that the samples coming from the inner area of the Baseleghe lagoon show the highest values of the concentrations of heavy metals (remaining however below the legal limits). Many studies have shown that the heavy metal content is inversely proportional to the particle size of the sediments, accumulating in the fine sediments (Davies et al. 1991, Sakai et al. 1986, Thorne and

Nickless 1981, Wakida et al., 2007). Considering the above, the concentration values of heavy metals were compared to the abundances of the different particle size fractions of the investigated samples. Indeed, it emerges that the concentrations of metals show high correlation indices with the abundances of finer fractions. In particular, the highest values are found in the comparison with the granulometry belonging to the class of clays and secondarily to that of silt. In the beach areas, sediments show very low percentages of the finer fractions compared to those of the seabed areas and (especially) of those of the lagoon. This would explain why the concentrations of heavy metals are always higher in the lagoon samples.

Final Considerations

What emerged from this study is that the sediments of the coastal area of Bibione are mainly carbonate sands, probably attributable to the solid transport of the Tagliamento river. The carbonate nature of these sediments is likely associated with the rock formations that make up the south-eastern Alpine arc, through which the river flows (and has flowed in previous geological times). These characterize the sediments of alluvial deposits in the portion of the Venetian-Friulian Plain belonging to the Tagliamento river and, therefore, the sediments that today characterize the coastal area of Bibione. The Baseleghe lagoon differs from the coastal area (sense strict) as the carbonate content is relatively lower. Here the fine fractions are predominant and there is probably a high content of phyllosilicate minerals.

High variability of the carbonate content was observed, particularly between the dune/backshore environment and that of the seabed. These differences could be due, on the one hand, to the selectivity of the sediments based on the particle size fractions and, on the other hand, to the dissolution of the carbonate sediments.

The analyses on heavy metals concentration did not reveal any criticalities and no values above the legal limits. It emerged, however, that the area that could be more subject to pollution problems would be the Baseleghe lagoon. This is most likely due to the type of sediments that make up the lagoon area.

Spinut (Split)

Results of analyses

As regards the Spinut site, the sediment sampling was carried out in both the marina area managed by the company PSD Spinut (seabed sediments sampling) and on the small beach west of the port (beach sediment sampling).

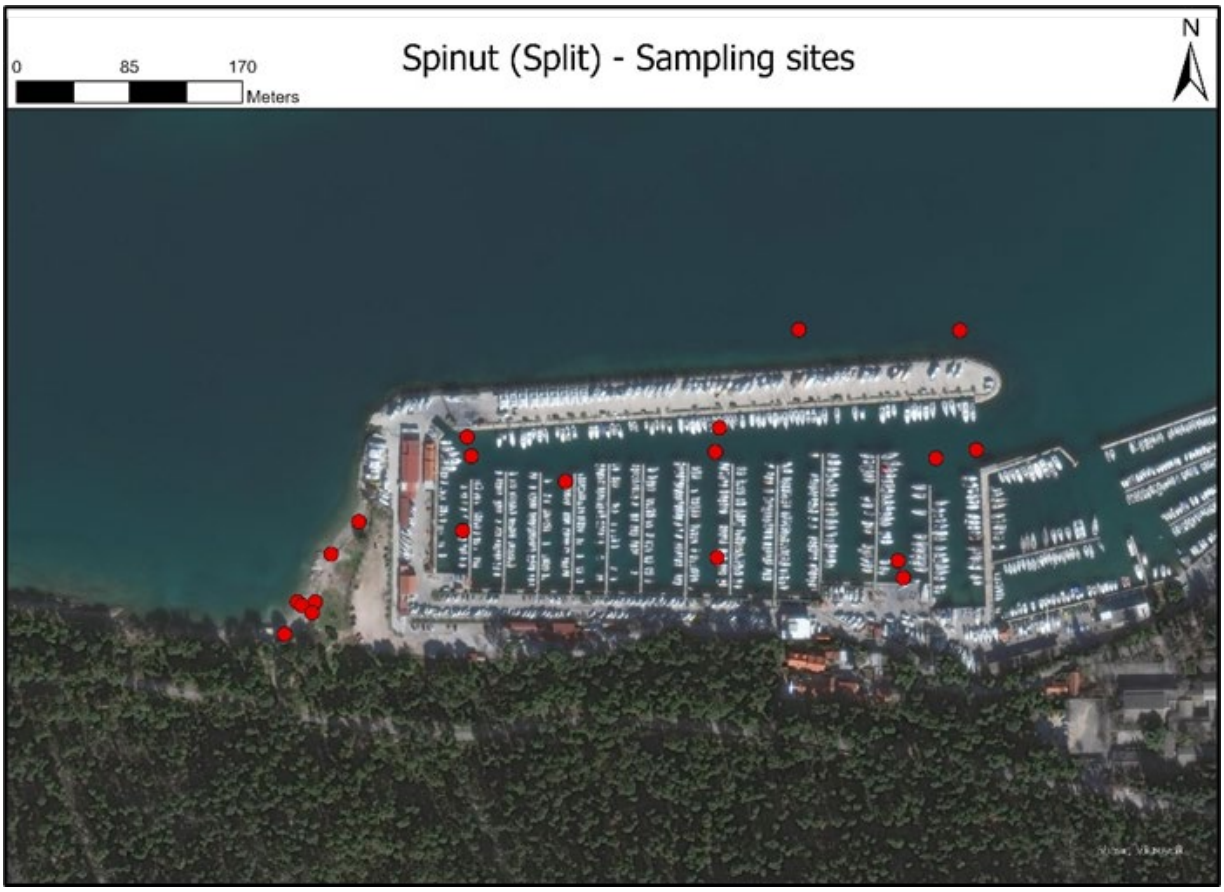

Figure 19: Satellite image of the Spinut coastal area, where the samples were taken. The red dots indicate the sampling points.

Concerning the granulometry of the sediments, there are clear differences between those coming from the beach and those coming from the seabed.

The sediments of the seabed present, in some cases, percentages of all the granulometric classes (gravel, sand, silt, and mud). The presence of percentages of gravel in some samples made it necessary to use two types of classification schemes: the Shepard classification scheme (1954) and the Folk' classification scheme (1959). The latter is used to classify sediments containing gravel. Samples containing gravel fall under the different points of the classification scheme, therefore they can be classified as Mud, sandy mud, muddy sand, sandy muddy gravel, and gravel. The samples in which there is no gravel, classified according to the Shepard scheme can be defined as sands, silty sands, sandy silts, and clayey silts.

On the other hand, Beach sediments are made up almost exclusively of sediments of the granulometric size of gravels, with very low percentages of sand (about 1%).

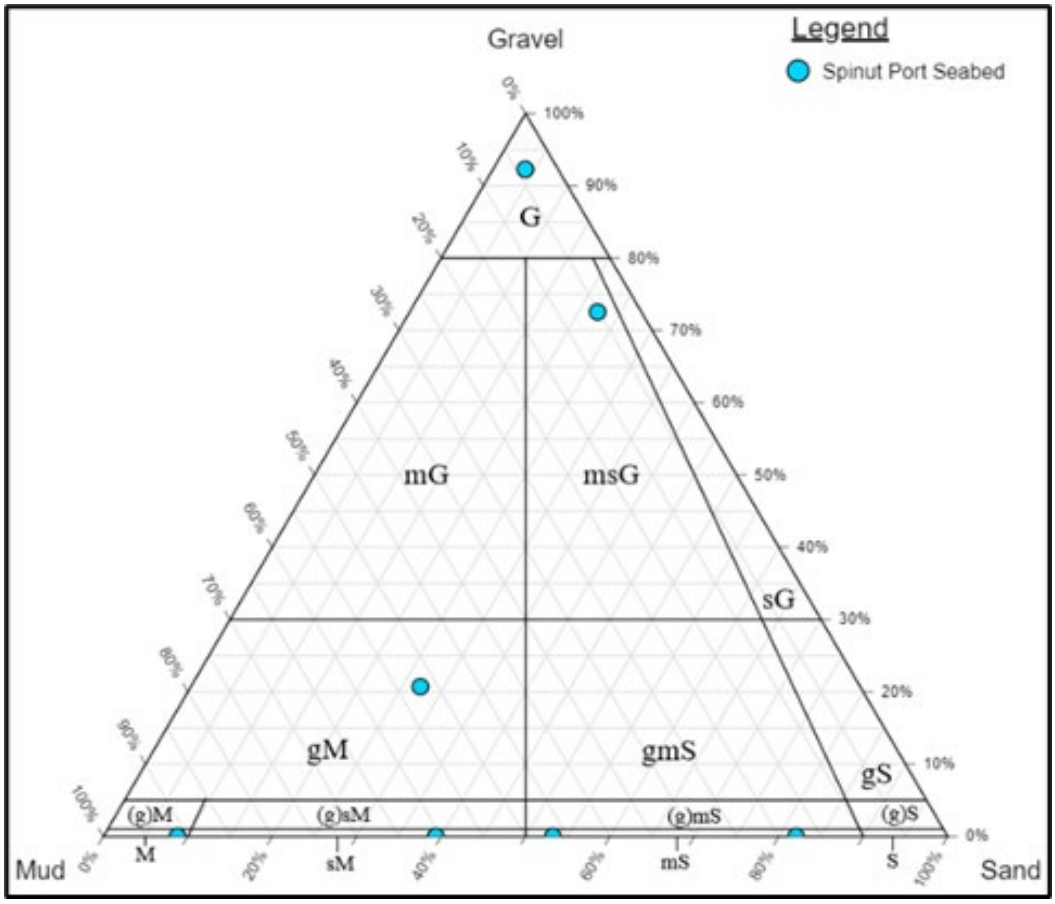

Figure 20: Folk 's classification diagram:: G: gravel; mG: muddy gravel; msG: muddy sandy gravel; sG: sandy gravel; gM: gravelly mud; gmS: gravelly muddy sand; gS: gravelly sand; (g) M: slight gravelly Mud; (g) sM: slight gravelly sandy mud; (g) mS: slight gravelly muddy sand; (g) S: slight gravelly Sand; M: mud; sM: sandy mud; mS: muddy sand; S: sand.

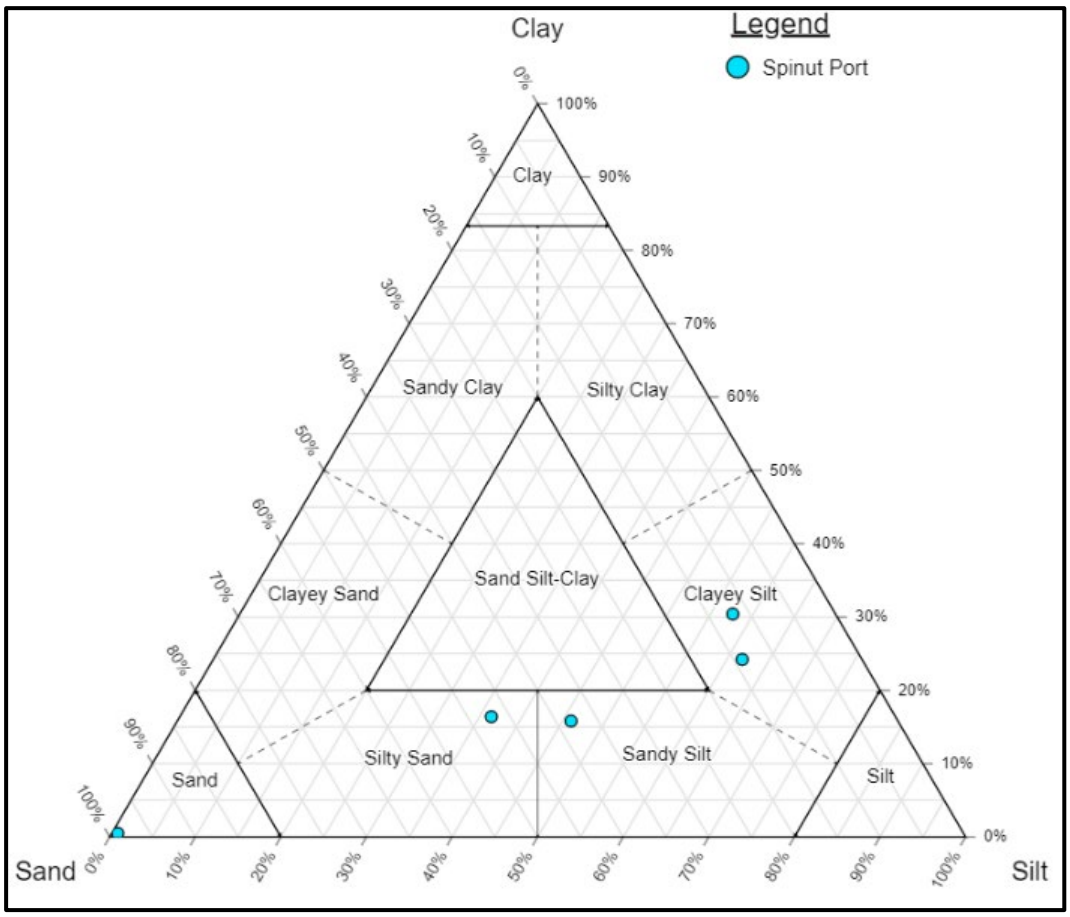

Figure 21: Shepard's classification diagrams.

Observing on maps (Figure 21; Figure 22) the distribution of the sand and mud contents in the samples coming from the internal area of the marina, it is noted that the sand content reaches its maximum values in the areas closest to the port exit where there is a connection with the open sea; on the contrary, the sand content reaches minimum values in the innermost areas of the port. On the other hand, the mud content follows a trend more or less opposite to that of the sand content.

This could be because in the areas closest to the port exit, as there is greater energy (waves, tides, etc.), the water can take charge and deposit coarser sediments. On the contrary, the low-

energy environment allows the deposition of sediments with finer particle size in the more internal and sheltered areas.

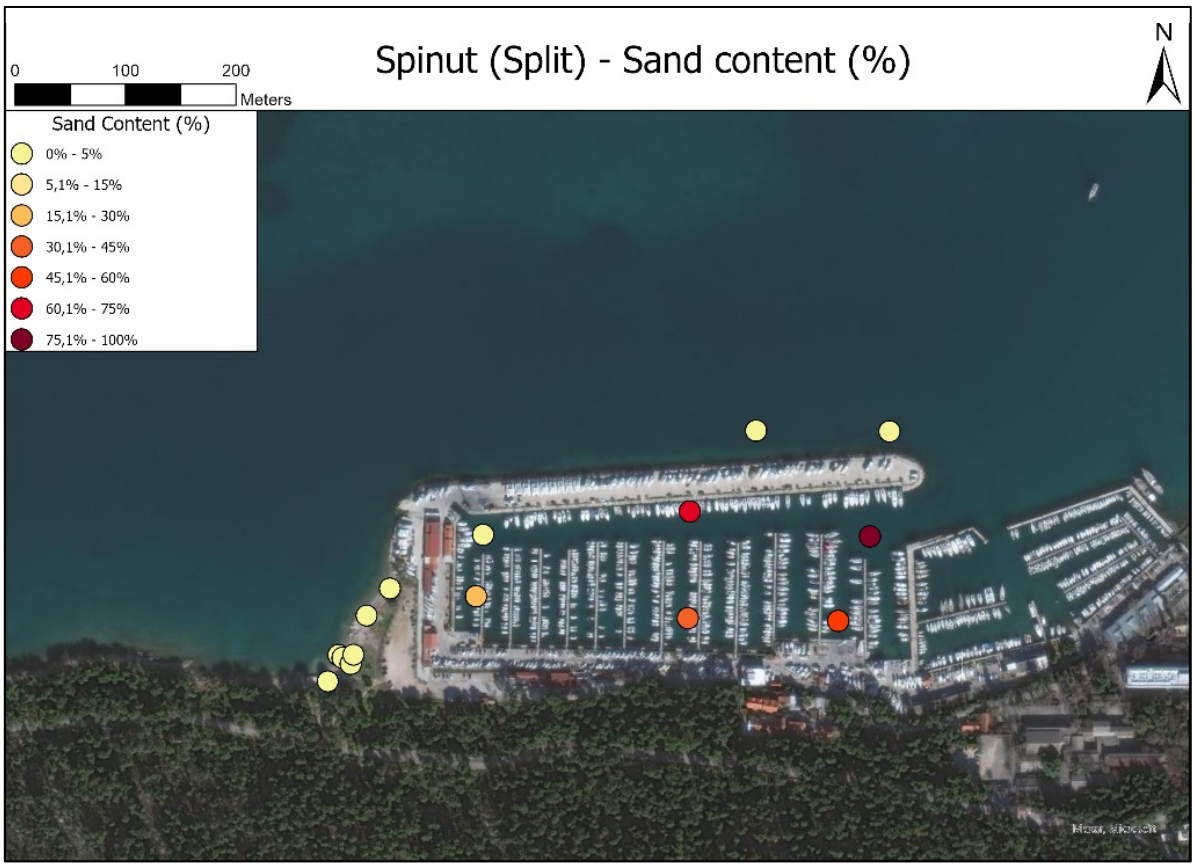

Figure 22: Satellite image of Spinut port area on which sand contents in the sample are shown.

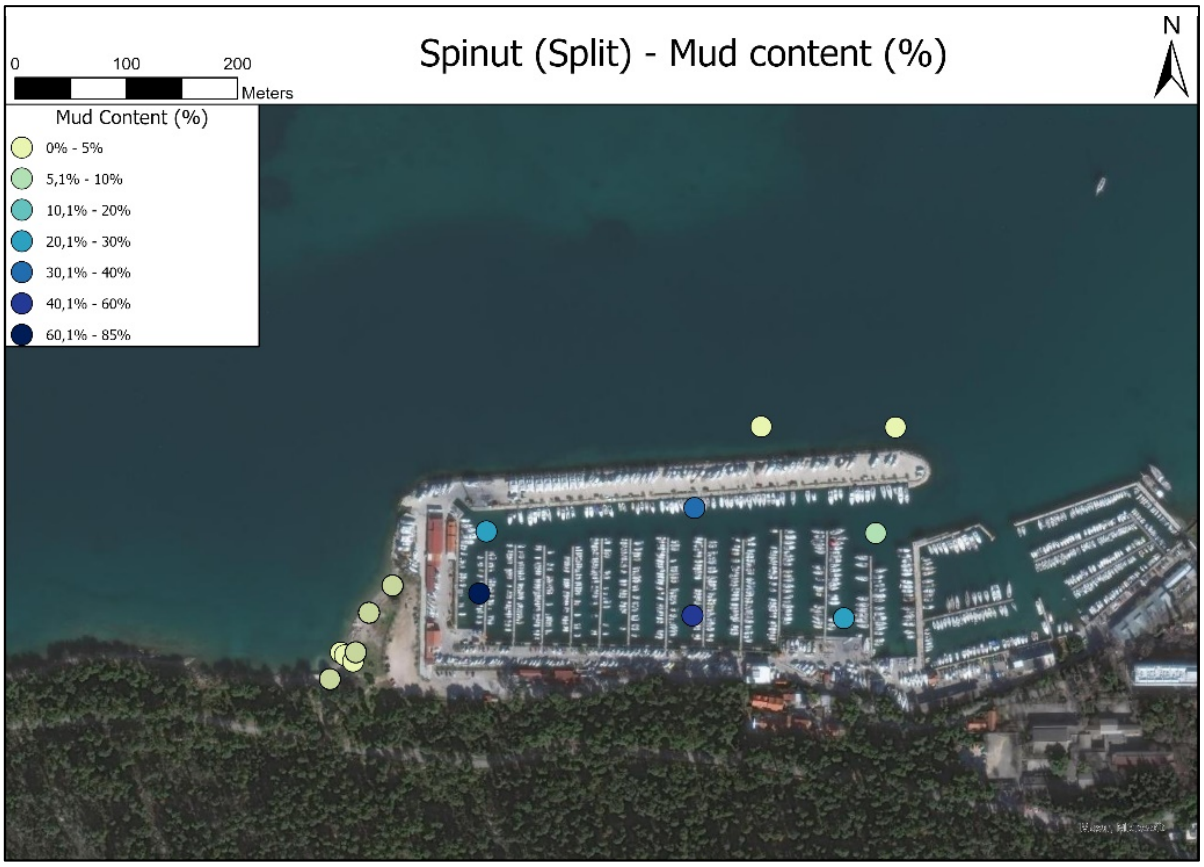

Figure 23: Satellite image of Spinut port area on which mud contents in the sample are shown.

From a compositional point of view, the samples from the beach are almost exclusively made up of carbonate sediments, in which the total carbonate content varies between 90 and 96%. Considering the low quantities of MgO (<1%) it is likely that the sediments are made up almost exclusively of calcium carbonate (calcite).

The seabed samples are also made up mainly of carbonate sediments but have lower percentages, between 58 and 87%. The wide compositional range also reflects the wide particle size range of the samples. Samples with a higher content of muddy sediments contain higher quantities of clay minerals which determine a more silicate composition of the samples (Figure 23).

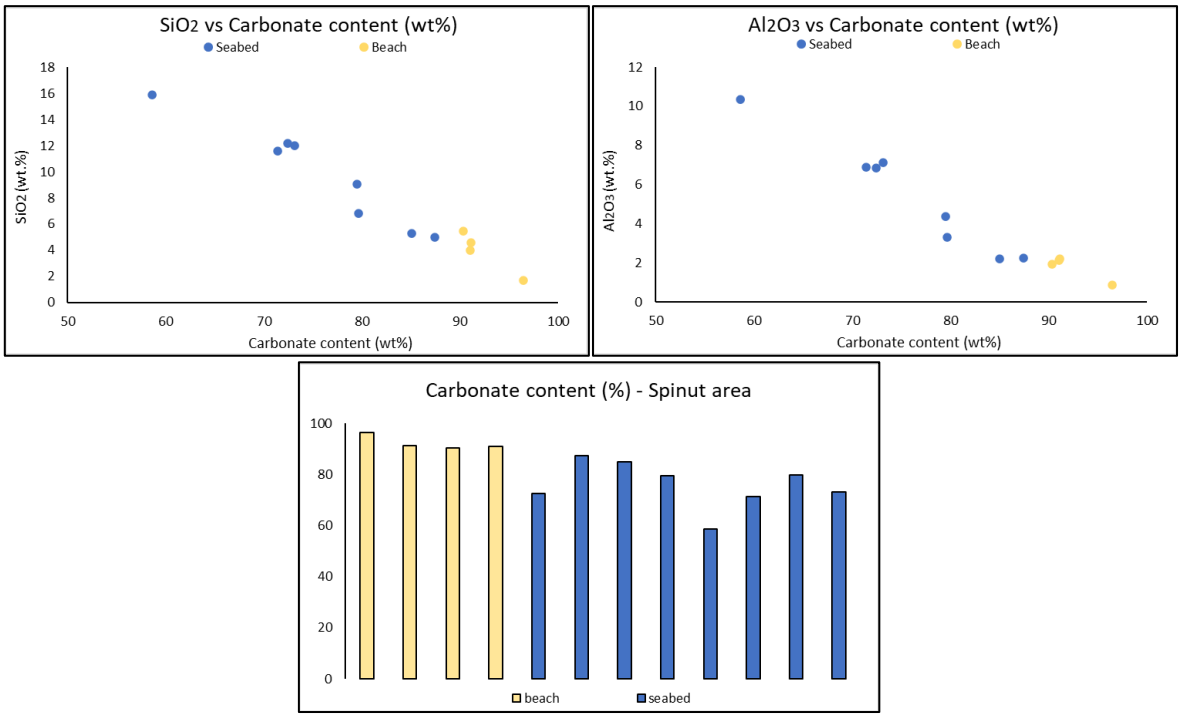

Figure 24: Comparison graphs of the carbonate content in the Spinut area samples. Top left: SiO2 vs Carbonate content scatter plot; Top right: Al2O3 vs Carbonate content scatter plot; Bottom: bar graph showing the carbonate content in the various samples.

Regarding the concentration of heavy metals in the samples studied, the values determined through the analyses we compared with the legal limits established by the Italian law in "Table 1 of Annex 5 to Title V of Part IV of Legislative Decree no. 156 of 2006" (Figure 24; Figure 25). Comparison with the limit values revealed that the thresholds were exceeded in some samples for a small group of heavy metals. The exceeding of the thresholds involved in some cases both the limits for "sites for commercial and industrial use" and the limits for "sites for public, private and residential green use". The number of samples and the heavy metals in which limit exceedances were observed are as follows:

- Antimony: one sample exceeds the limit threshold for "sites for public, private and residential green use".
- Arsenic: one sample exceeds the limit threshold for "sites for public, private and residential green use".

- Copper: four samples exceed the limit threshold for "sites for public, private, and residential green use" and one sample also exceeds the limit threshold for "sites for commercial and industrial use".
- Lead: one sample exceeds the limit threshold for "sites for commercial and industrial use".
- Zinc: one sample exceeds the limit threshold for "sites for commercial and industrial use".

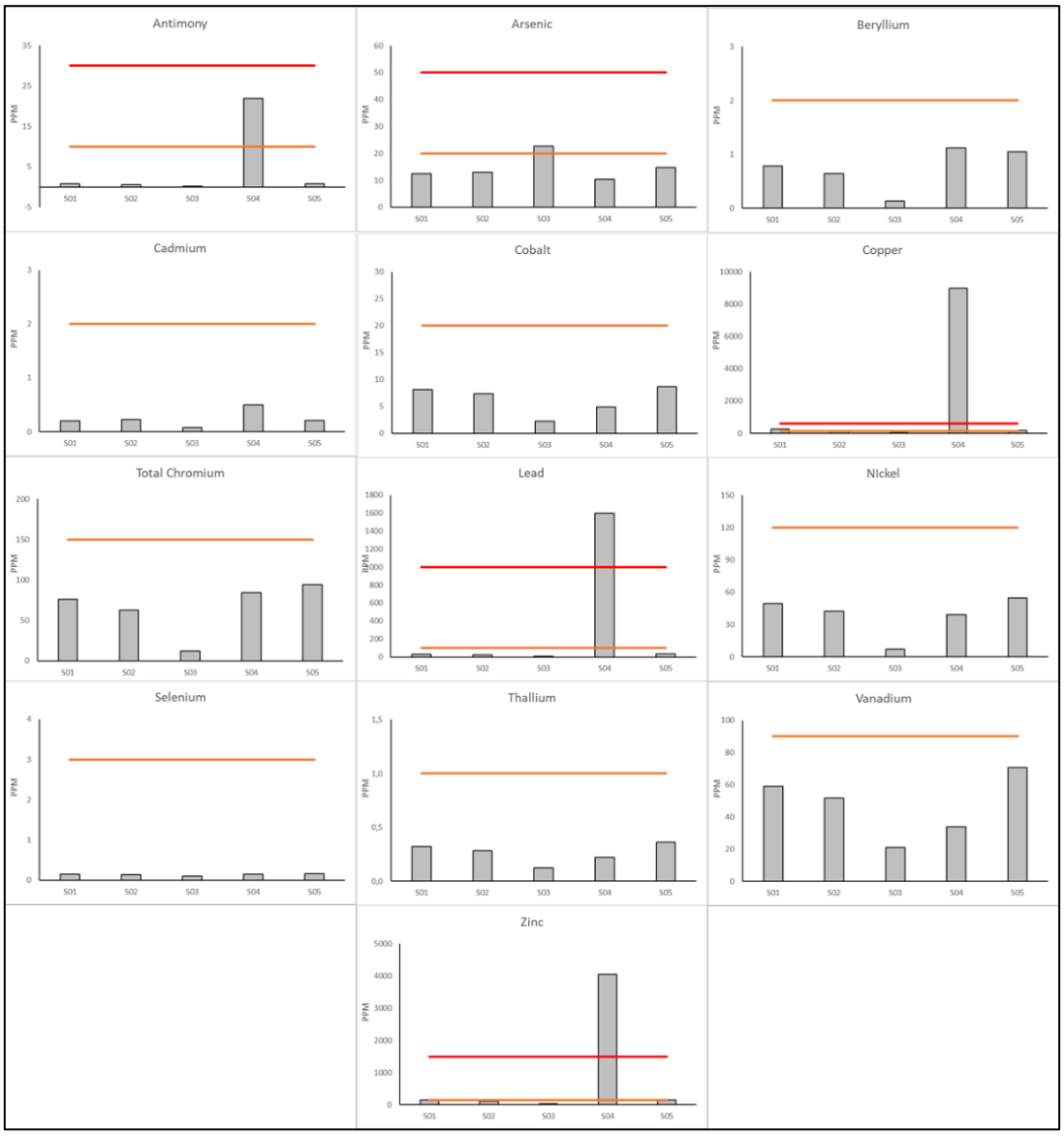

Figure 25: Bar graphs showing the concentrations of different heavy metals (arsenic, antimony, beryllium, cadmium, cobalt, chromium, copper, nickel, selenium, thallium, vanadium, and zinc) in the sediments of the seabed of Spinut coastal area, compared with the limit values of Italian law for "sites for public, private and residential green use "provided for in "Decree Law 152 of 2006".

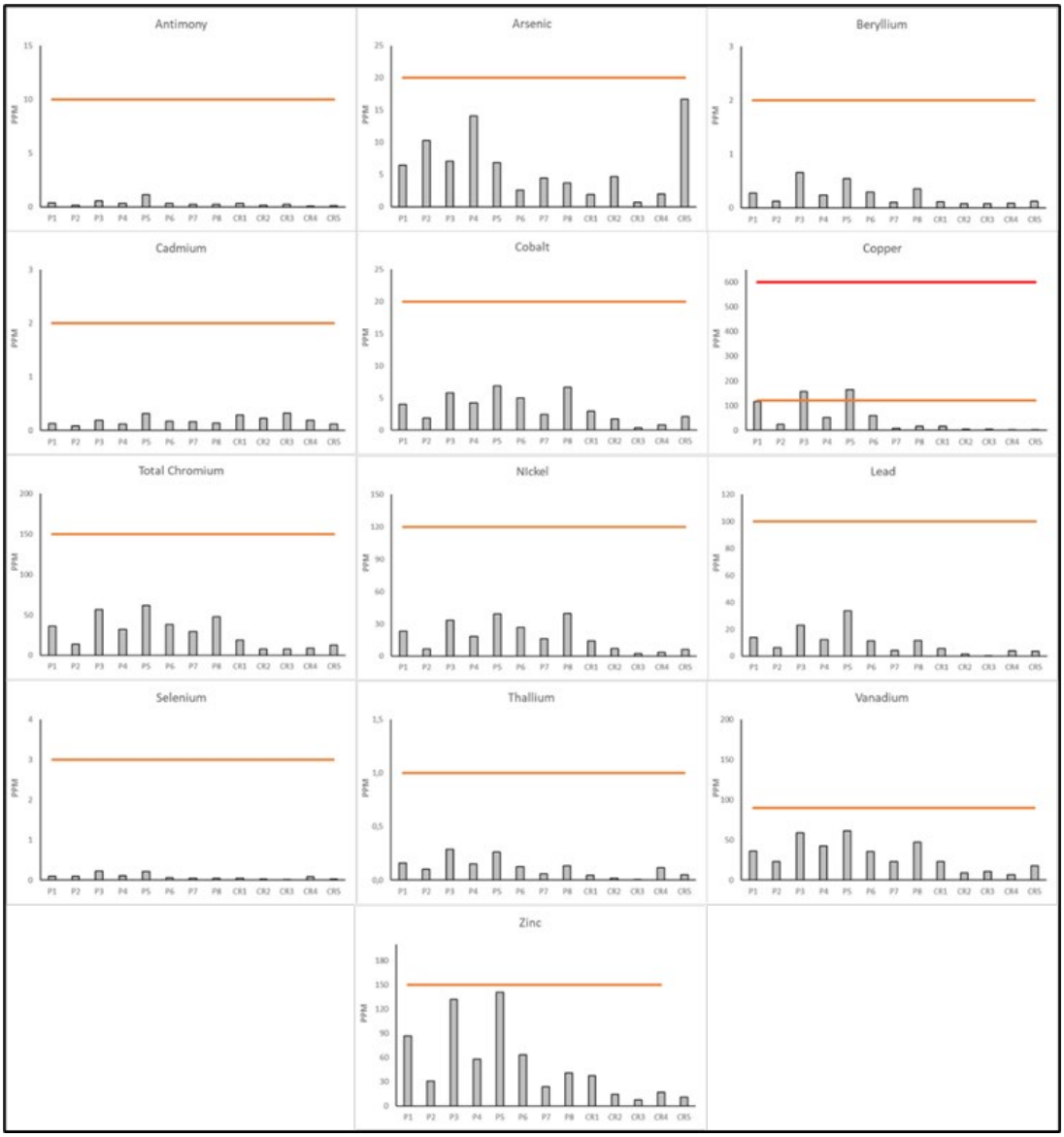

Figure 26: Bar graphs showing the concentrations of different heavy metals (arsenic, antimony, beryllium, cadmium, cobalt, chromium, copper, nickel, selenium, thallium, vanadium, and zinc) in the sediments of the seabed of Spinut coastal area, compared with the limit values of Italian law for "sites for public, private and residential green use "provided for in "Decree Law 152 of 2006".

The concentration values of heavy metals have been plotted on a map, so it was possible to observe that there was a sample (located in the south-east area of the port) responsible for the exceedances of the concentration limit values of Antimony, Lead, Copper, and Zinc (Figure 26; Figure 27; Figure 28; Figure 29; Figure 30). This sample also exhibited the highest copper concentration (14 times higher than the limits for "sites for commercial and industrial use") among the samples in which the concentration limits were exceeded. In this context, however, it is possible to observe that the limits were exceeded in samples located in the innermost areas of the port. The only sample in which, there was an overrun of the limits for the concentration of arsenic, on the other hand, was in the area of connection with the open sea.

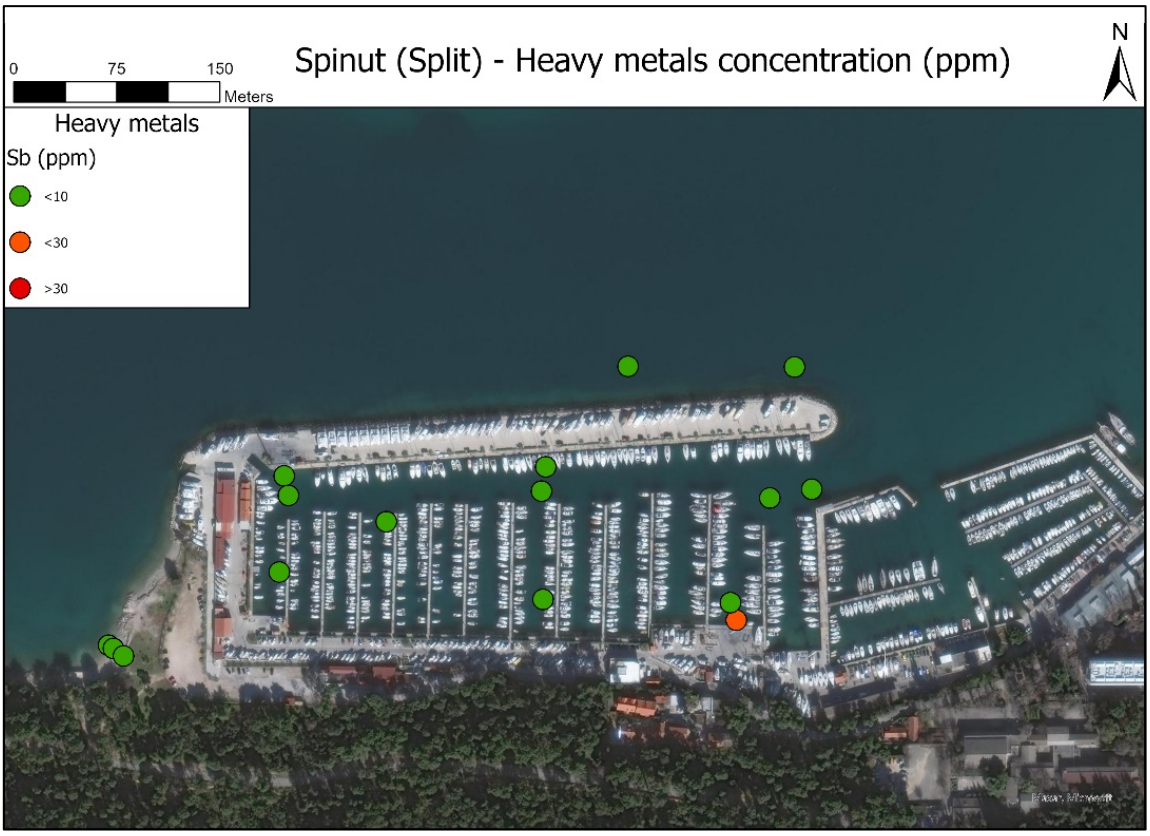

Figure 27: Satellite image showing the sampling points coloured according to the following criterion: green: samples in which the concentration of antimony is lower than the limit value for "sites for public, private and residential green use"; orange: samples in which the antimony concentration is below the limit value for "sites for public, private and residential green use" but below the limit value for "sites for commercial and industrial use"; red: samples in which the antimony concentration is higher than the limit value for "sites for commercial and industrial use".

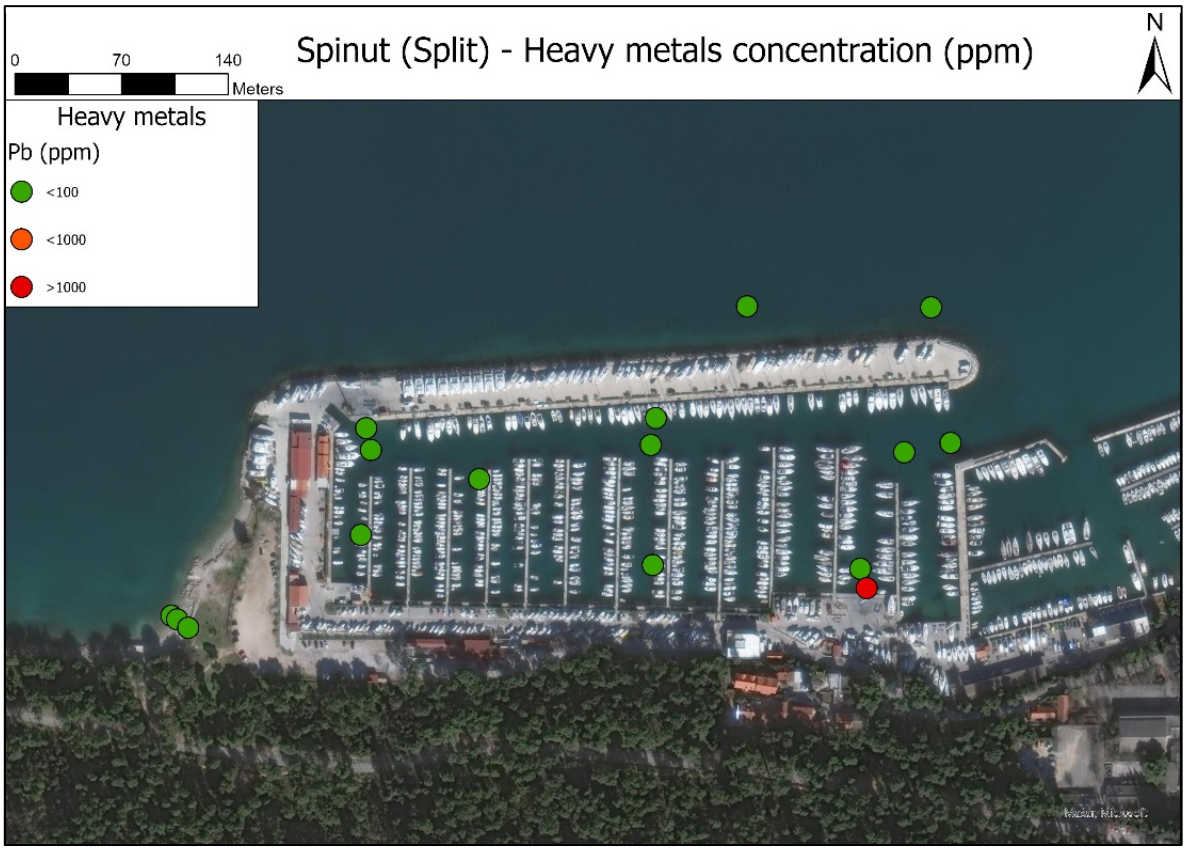

Figure 28: Satellite image showing the sampling points coloured according to the following criterion for Lead concentration: green – concentration lower than the limit value for "sites for public, private and residential green use"; orange - concentration is over the limit value for "sites for public, private and residential green use"; red: concentration higher than the limit value for "sites for commercial and industrial use".

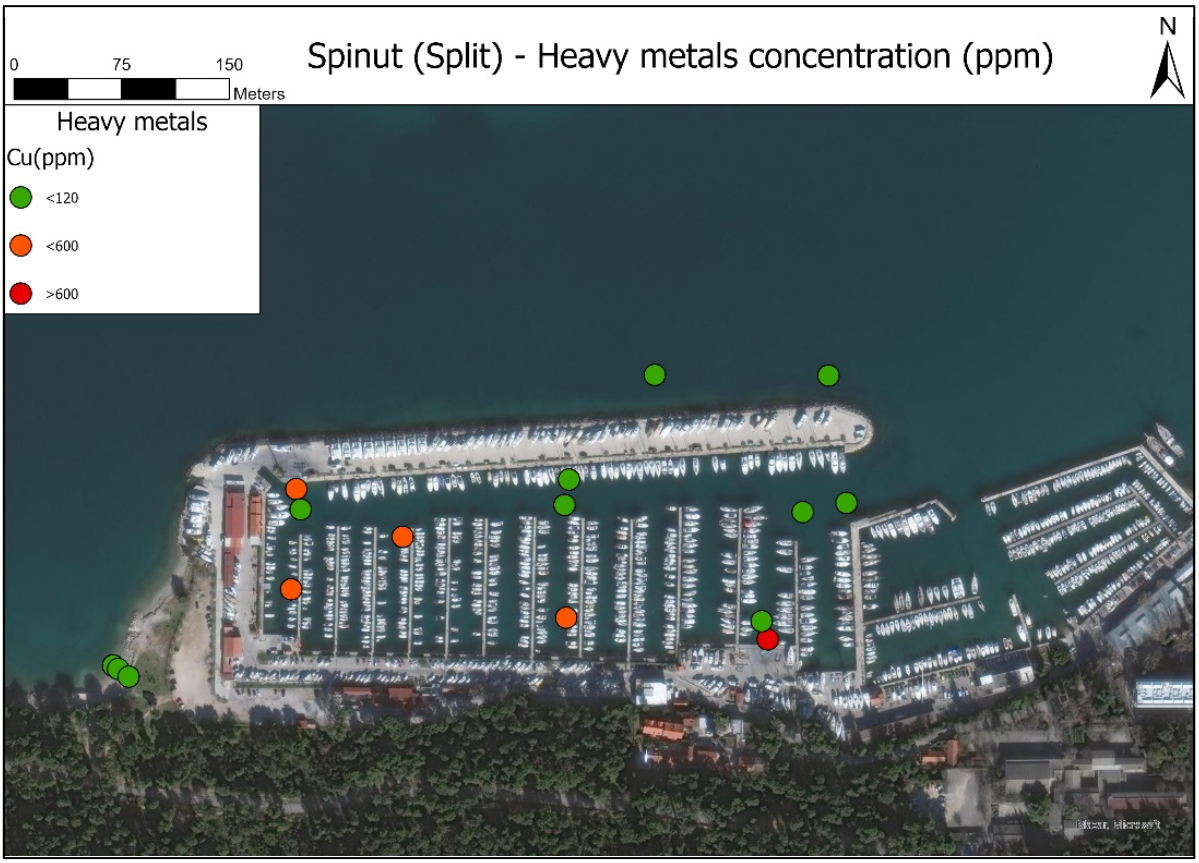

Figure 29: Satellite image showing the sampling points coloured according to the following criterion for Copper concentration: green - concentration lower than the limit value for "sites for public, private and residential green use"; orange - concentration is over the limit value for "sites for public, private and residential green use"; red - concentration higher than the limit value for "sites for commercial and industrial use".

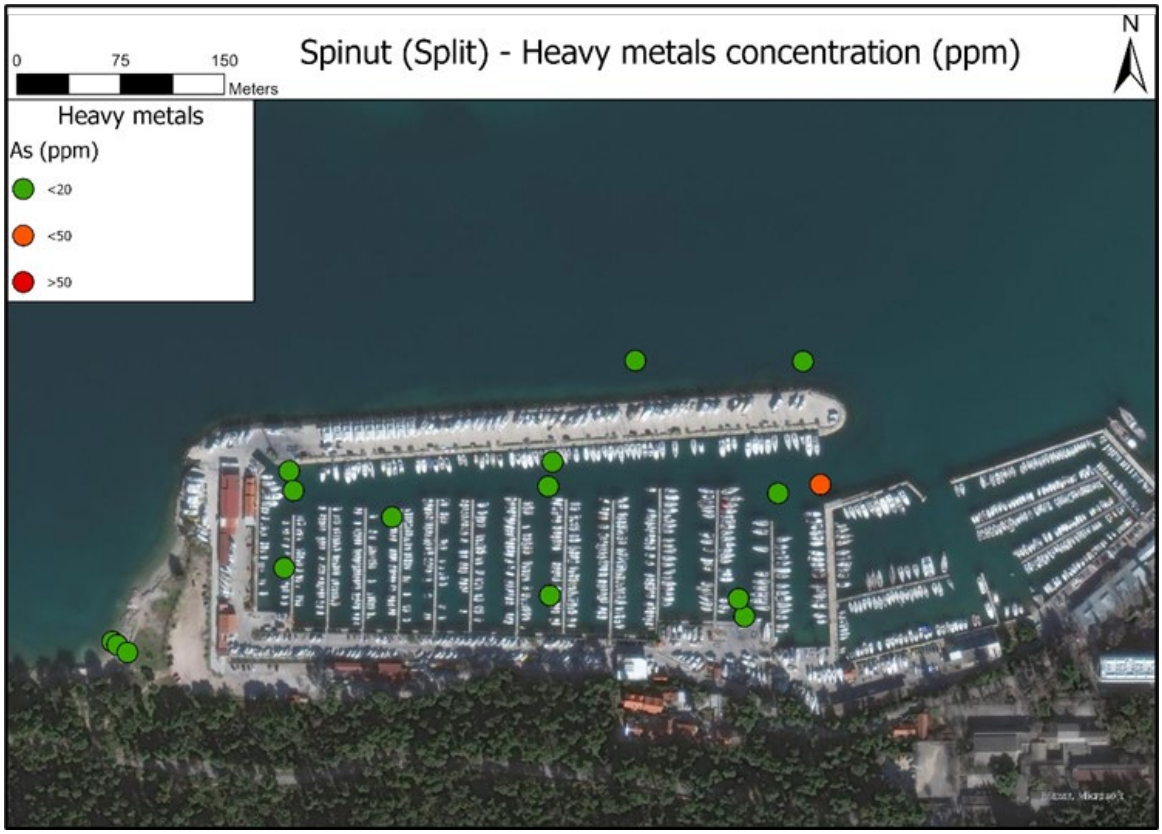

Figure 30: Satellite image showing the sampling points coloured according to the following criterion for Arsenic concentration: green - concentration lower than the limit value for "sites for public, private and residential green use"; orange - concentration is over the limit value for "sites for public, private and residential green use"; red - concentration higher than the limit value for "sites for commercial and industrial use".

Similar results were also obtained from the analysis of the samples taken in the year 2021. Considering that heavy metals tend to accumulate in sediments with a higher clay component, the correlation indexes (C.I.) between the concentration of some of the heavy metals (Copper, Lead, Zinc) both with the percentage abundance of clay and the percentage of aluminium was calculated. Results indicated that there was a good correlation (> 0.85) between the terms considered when the C.I. was calculated by excluding the sample with concentrations well above

the limits. When the C.I. was calculated including the latter sample as well, the values were close to 0. What is seen about the values of the correlation indexes provides two indications:

- At the point where the sample was taken that shows numerous exceedances of the concentration limits of heavy metals, the concentration values have no dependence on the quantity of clay present but are rather due to a phenomenon of punctual contamination near the sampling point,

- The exceeding of concentration limits for copper is more related to the greater quantity of clay present in the sediments of the innermost areas of the port as widely seen in the literature (Davies et al. 1991, Sakai et al. 1986, Thorne and Nickless 1981, Wakida et al., 2007)., where metals dispersed in the water due to the activities of the port can be deposited.

Port areas generally represent a source of pollutants due to the different activities that are carried out. The main sources of pollution in ports include vessel batteries, ship-borne oil discharges, dry-docking operations, discharging of bilge oil, urban runoff, domestic wastewater discharges, and atmospheric deposition across the air-sea interface (Mali et al., 2017). After being transported into the aquatic ecosystems, these contaminants are absorbed by suspended solids and accumulate in port sediments where they become even more resistant to degradation. (Zakaria et al., 2002; De Luca et al., 2005). When the concentration of these contaminants trapped in port sediments increases significantly, they are leached to the surrounding water column, thereby leading the to degradation of the quality of the aquatic ecosystems (Lee et al., 2001, Tsapakis et al., 2006, Ameer and Linden, 2008, Oliveira et al., 2012, Ribeiro et al., 2013, Civeira et al., 2016, Mali et al., 2015, Mali et al., 2016).
The concentrations of heavy metals in the control sampling points outside the port area, however, indicate that there are no problems outside the port.

Final Considerations

The sediments of the marina Spinut area show strong differences between those coming from the beach and those from the seabed.
The beach sediments are mostly gravelly and are made up of more than 90% of calcium carbonate (calcite).

Seabed sediments are characterized by all granulometric classes, so various samples can be classified, from a granulometric point of view, according to a wide range of classes: sands, silty sands, sandy silts, and clayey silts according to Shepard (1954) in the samples without gravel component, while mud, sandy mud, muddy sand, sandy muddy gravel, and gravel according to Folks (1959) in the samples with gravel component. These samples have a lower carbonate content, which varies between 58% and 87%. On the other hand, silica and aluminium have a higher content, probably due to the greater quantities of clay minerals in the finer granulometric fractions.

As regards the concentration of heavy metals, one sampling point was found to be particularly critical, as extremely high concentration values of lead, copper and zinc were determined. In this area, it is likely that a punctual type of contamination has occurred, the cause of which is not known.

Other samples showed that the limits were exceeded, especially in copper concentrations. In these, the concentration values are well correlated with the abundance of clay, indicating that the metal that ends up in the water due to port activities tends to accumulate in these areas.

Ancona

Geographic framework

Ancona is an Italian municipality located in the Marche region, of which it is also the regional capital. It is also the capital of the Province of Ancona. The town is bordered by the municipalities of Agugliano, Camerano, Camerata Picena, Falconara Marittima, Offagna, Osimo, Polverigi, Sirolo, and on the east side is bordered by the Adriatic Sea.

The coast northwest of the port of Ancona (fig. 1) is low and sandy, and the coast southeast of the port is high and rocky. The urban area is characterized by an alternation of hills and valleys, with an east-west direction.

Figure 31: Satellite image of the Ancona Area. The red line shows the boundary between the municipalities of Ancona and Falconara Marittima.

Climate

The climate is Mediterranean. The average monthly temperatures are at their lowest in January (1°/2°C) and peak in July/August (26°/28°C). The city is located north enough to suffer in part some influences typical of northern Italy (such as the fog in winter and early spring), as well as the typical influences of the Adriatic side (such as cold eruptions from Russia).

Winter, from December to February, is quite cold. There are quite mild periods, in which the Atlantic currents prevail, during which there can also be rainy days. When the warm wind from the southwest (Garbino) blows, which descends from the Apennines, the temperature can reach and exceed 20 ° C even in the middle of winter. In periods of good weather, fog can form. On the other hand, winds from Eastern Europe, sometimes even in March, can bring cold periods, in which snow can also fall. Given the location on the coast, frosts are generally not intense, and on the coldest nights of the year, the temperature does not go below -4 / -5 ° C.

Summer, from June to August, is hot and sunny, with rare rainy days and some thunderstorms coming from the Apennines. The breeze blows from the sea in the afternoon. However, there can be very hot and sultry periods. Moreover, occasionally the Garbino wind can bring some hot days.

The proximity to the sea increases the level of humidity in the winter and, to a lesser extent, in the summer. For the same reason, Ancona has medium-strength winds throughout the year with one of the strongest being the Bora, a cold, dry wind blowing in violent gusts, especially in the winter.

Other winds are the warm Scirocco and the Maestrale, which usually bring good weather. The rainiest months are September and October.

Rainfall amounts to 820 mm per year: they are therefore at an intermediate level. In the least rainy months (January, July) 45 mm of rainfall, and in the wettest (November) 85 mm fall.

Geological framework

From a regional geology point of view, the Ancona area is in the external domain of the central Apennines (belonging to the thrust and fold Apennine chain) where the Miocene, Pliocene, and Pleistocene terrains are widespread. In these deposits, the Neogene deformation phases that have affected this sector of the chain are recorded with good continuity, which is made evident by a strong lithological, sedimentological, and stratigraphic variability (Cello and Tondi, 2011). These terrains rest on top of a carbonate succession referable to as the Umbria-Marche

succession. This, starting from the lower Jurassic, was deposited in a pelagic environment, connecting to the south with a carbonate platform environment (Lazio-Abruzzo platform) which in the lower Jurassic also characterized the Umbria-Marche area (Colaccichi et al., 1970; Centamore et al., 1971; Pialli, 1971).

The sedimentation of this succession continued up to the Paleogene, first in response to the extensional processes induced by the tethidean rifting and then by the phenomena of thermal subsidence and crustal thinning (Cello et al., 1996: Marchegiani et al., 1997, 1999). The succession presents a very strong variability, due to a different pelagic environment, in response to the deformation phases that over time have conditioned the deposition of sediments (Centamore et al., 1971). Starting from the Miocene, the Umbria-Marche succession was involved in the structuring of the Apennine chain. The latter migrated over time towards the Adriatic foreland and involved the Ancona area only starting from the Pliocene. In this area, the geological structures linked to the formation of the Apennine structure are generally buried under the turbidite sequences that have been deposited starting from the Miocene (Bally et al., 1986). The only exception is the coastal area between Ancona and Mount Conero, where the Cretaceous-Pliocene carbonate and siliciclastic deposits emerge.

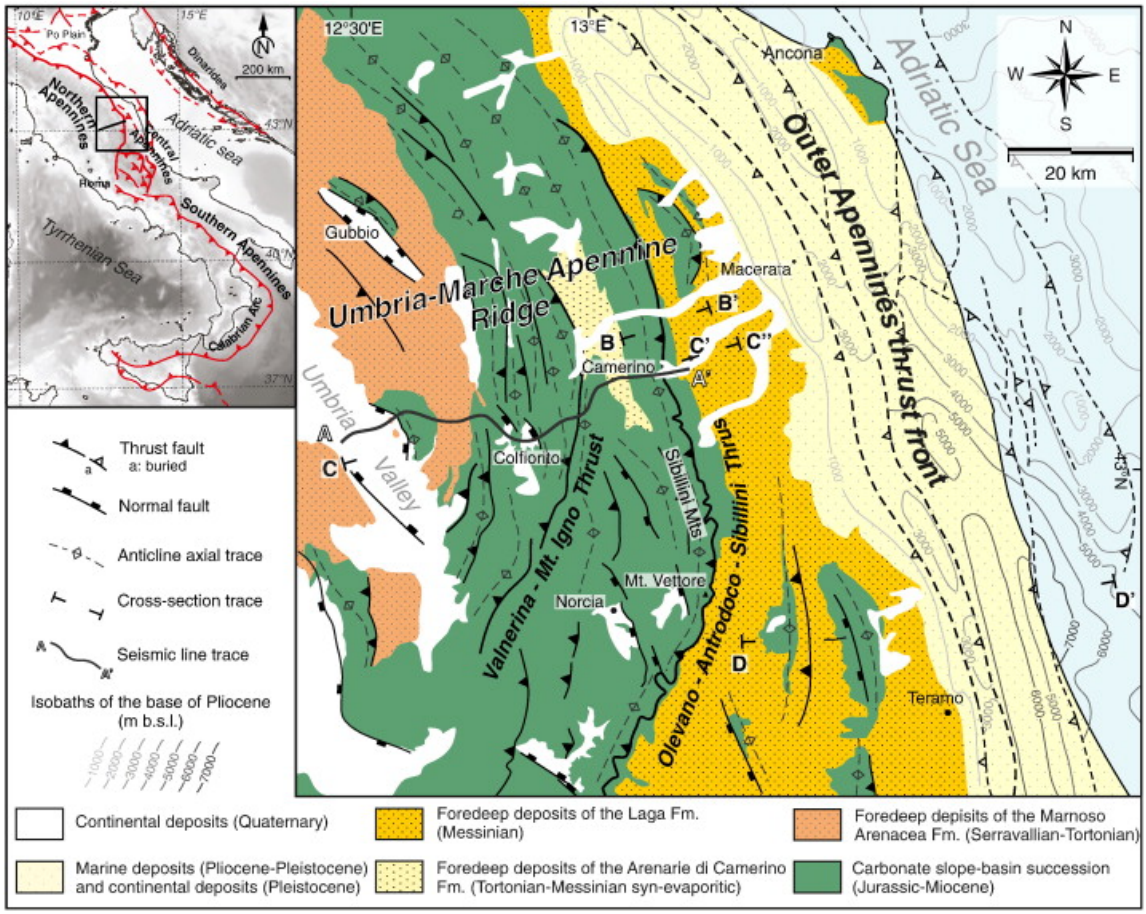

Figure 32: Structural sketch map of the southern sector of the Northern Apennines transected by the arc-shaped Umbria–Marche Apennine Ridge (Scisciani et al., 2014).

Between the end of the lower Pliocene and part of the middle Pliocene, in the Ancona area, a condensed succession of mainly clayey was deposited, followed (in discordance) by an arenaceous-pelitic series of the lower Pleistocene (Cello and Tondi, 2011).

Starting from the middle Pleistocene, following a rise on a regional scale, the entire Marche area has emerged. This allowed climatic agents to shape the landscape and produce the deposition of floods, eluvium-colluvial layers, marine deposits, and landslide deposits (Cello and Tondi, 2011).

From a tectonic point of view, the Ancona area is the result of different tectonic phases (Crescenti et al. 1983; Cotecchia, 2006; Cello & Tondi, 2011). One of the last phases, the compressive phase

of the lower-middle Pliocene, gave rise to the main structures present in the area, which are approximately NW-SE oriented folds (Cello & Coppola, 1989; Crescenti et al., 1983) associated with thrusts (Cello and Tondi, 2011). Among these folds, the most important structure is the syncline of Tavernelle, with the axis running approximately parallel to the coastline and exerting the main structural constraint on the layout of the entire area. The results following this tectonic phase are numerous NW-SE oriented normal faults, which have been interpreted as collapsed structures at the front of the thrust or the rear of the anticlines associated with the thrust (Cello & Coppola, 1989).

The orientation of these structures is consistent with the direction of the tectonic movements, slightly towards the NE, which are still active today. The normal faults that cut the Montagnolo hill with a local orientation about EW, are considered collapsing structures: these have strongly brought down the sediments towards the sea, with a maximum displacement between 50 and 150-200 meters (Crescenti et al., 1983; Cello and Tondi, 2011).

The last tectonic phase (Pleistocene - Present) is responsible for the transversal faults with anti-Apennine orientation NNE-SSW (Crescenti et al. 1983; Cello & Coppola 1989; Cello & Tondi 2011) which are found in the coastal area. These structures cut and displace the previous folds, giving life to isolated structures (Nanni, 1980). Moreover, these structures are probably still active and are probably seismogenic sources (Cello and Tondi, 2011).

From a hydrogeological point of view, the aquifers present in the territory are represented by arenaceous-pelitic lithofacies interspersed with Pleistocene pelites. These bodies usually have a discrete lateral continuity, emerging on the main watersheds and have medium-high permeability. The aquicludes are represented by clayey marl, marly clays, and clays which are located on the top of the arenaceous units. The position of the aquifers suggests the possibility of finding conditions of confined aquifers in the area. The occurrence of groundwater in terrigenous deposits as evidenced by the presence of springs fed, for the most part, by modest shallow aquifers closely linked to the pluviometry trend.

Geomorphology

The current geomorphological structure of the Ancona area is influenced by numerous factors including the neotectonic evolution, the climatic events of the Quaternary, the geological characteristics of the subsoil, and the most recent anthropic activity.

The main morphogenetic processes are due to the action of surface running waters and gravity. The latter is particularly active to the east and west of the city of Ancona, giving rise to extensive landslides. In the context of the morphogenesis of the area, the result of the intense uplift of the Apennine chain starting from the upper Pliocene is fundamental (Dramis et al., 1992; Coltorti et al., 1996). This uplift has induced a rapid and general deepening of linear erosion, alternating with phases of lesser intensity due to the different climatic conditions that have occurred since the middle Pleistocene (Cello and Tondi, 2011). The alternation of the climatic phases of the past, characterized by cold periods and temperate periods, are linked respectively to moments of prevalent sedimentation and prevalent linear erosion, recognizable along the valley axes where the alluvial deposits are arranged at decreasing altitudes compared to the current valley floor (Coltorti et al., 1991; Dramis et al., 1992).

The intense urbanization and anthropization of the coastal area have almost completely covered the pre-existing forms. The coastal morphology itself appears to have been strongly altered, for example through the construction of protective reefs (Cello and Tondi, 2011). The anthropogenic activity represents one of the main control factors of recent and current morphogenesis, introducing in the evolutionary framework of the area processes of erosion and accumulation much faster and more intense than those due to natural causes (Farabollini et al., 2000).

On 13th December 1982, at about 10.45 p.m., the city of Ancona was hit by a catastrophic landslide on the north-facing slope of the Montagnolo, moving from about 170 meters a.s.l. (above sea level) down to the sea. The slope portion affected by mass movement extended over about 3.4 km^2 and along the shore, it is about 1.7 km wide. The deformation phase lasted only a few hours. Many buildings were damaged beyond repair, and some completely collapsed. Lines of communications such as the Flaminia Road and the railway were interrupted, lifted, and moved towards the sea. This impressive landslide has an ancient origin; after its early activation, the phenomenon has moved sporadically, coincident with significant rainfall events or earthquakes (Sciarra, Pasculli & Calista, 2006). The areas most affected included Borghetto, Posatora, and Torrette; involved 342 hectares of urban and suburban land, damaged two hospitals and the Faculty of Medicine of the University of Ancona, and damaged or destroyed 280 buildings, for a total of 865 houses.

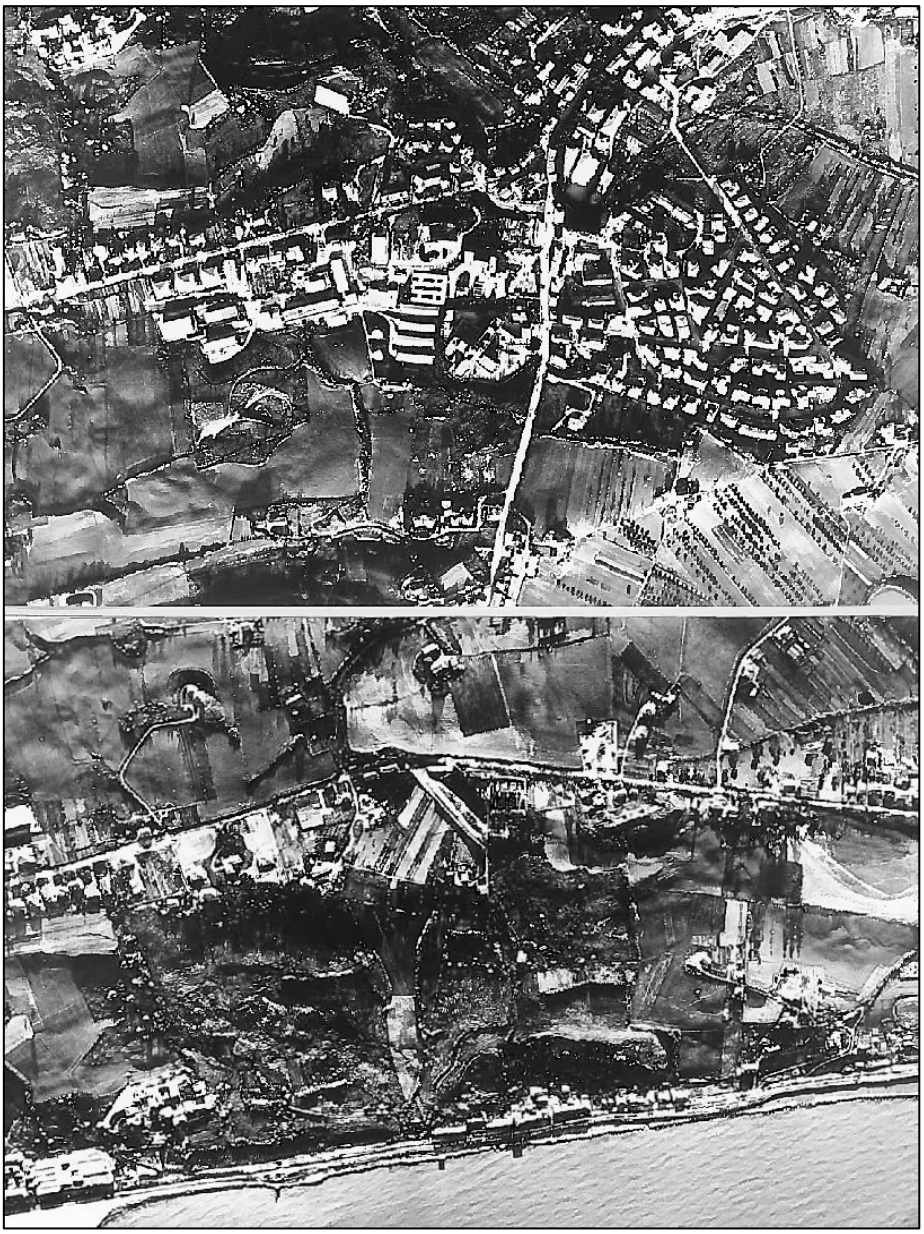

Figure 33: Aerial photos of the area hit by the landslide, before and after the event. Source: https://www.comuneancona.it/ankonline/ankonmagazine/2021/12/10/13-dicembre-39-anni-fa-la-frana-di-ancona-le-immagini-i-ricordi-nuovi-interventi-per-il-monitoraggio/. Accessed on March 7th, 2022.

Results of analyses

For the Ancona site, sampling was carried out both in the Torrette-Palombina area and in the "Marina Dorica" tourist port area. As regards the Torrette-Palombina area, the sampling was performed in three different environments: backshore, shoreline, and seabed. The samplings in the area of the "Marina Dorica" port concerned the sediments of the seabed and were carried out both inside the port and in the external area.

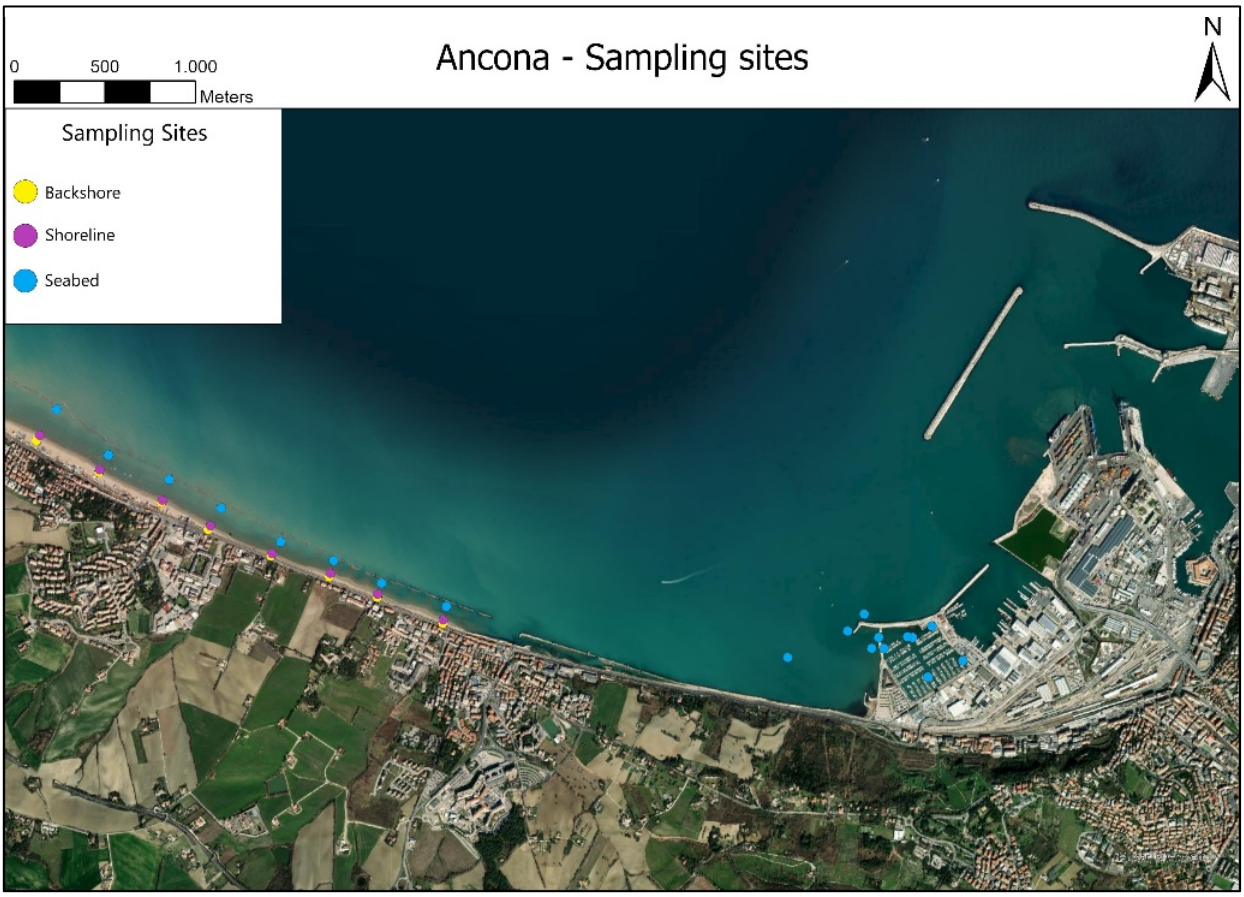

Figure 34: Satellite image of the Ancona area with sampling point plotted.

As for the samples taken in the Torrette-Palombina area, from the point of view of the grain size of the sediments, these mainly consist of sand, although, the content slightly decreases in the seabed sediments in favour of muddy granulometry. In general, however, according to the

Shepard classification scheme (1954), these sediments can be classified as sands (Fig 35). Only two seabed samples, towards the south-eastern area of the investigated area, showed a higher content of silt and clay but, in any case, not exceeding 16 (Figure 34).

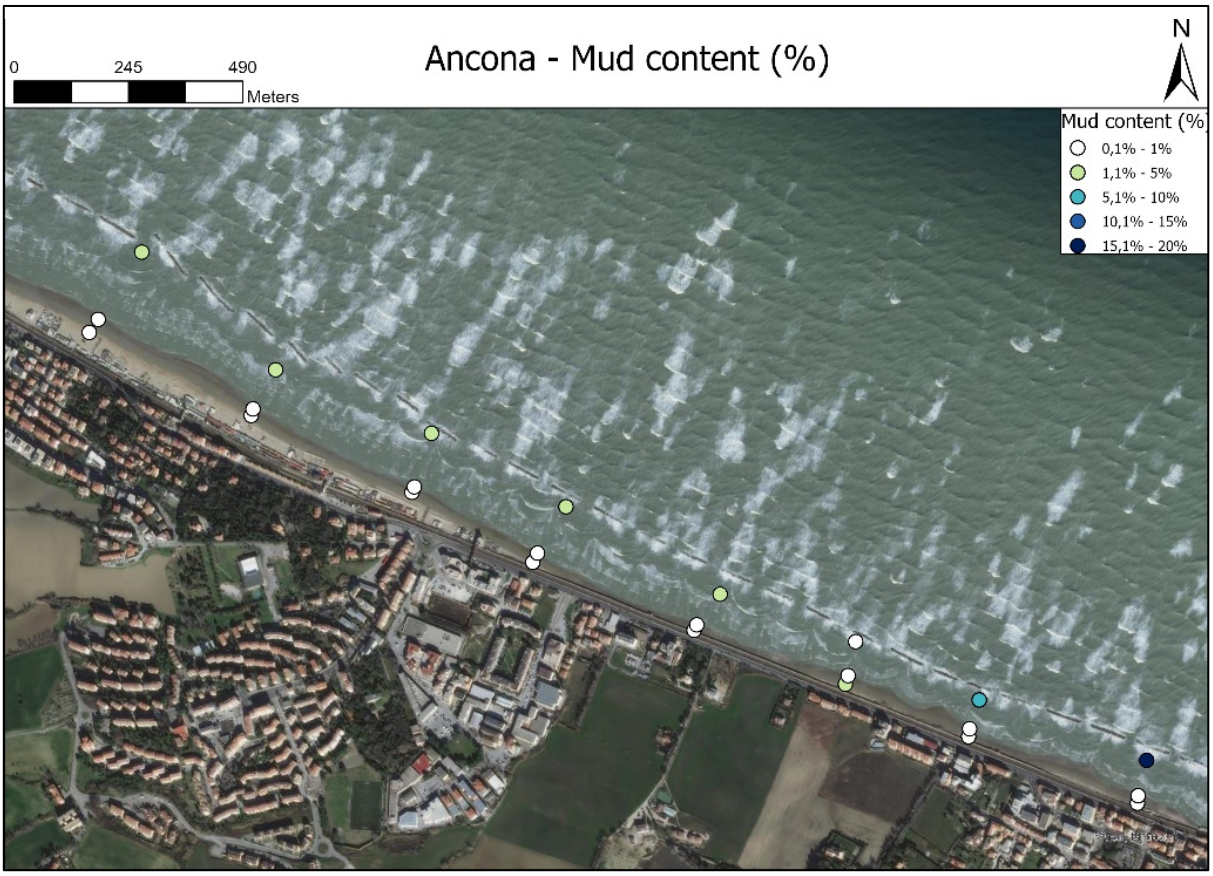

Figure 35: Satellite image of Torrette-Palombina area on which sand contents in the sample are shown.

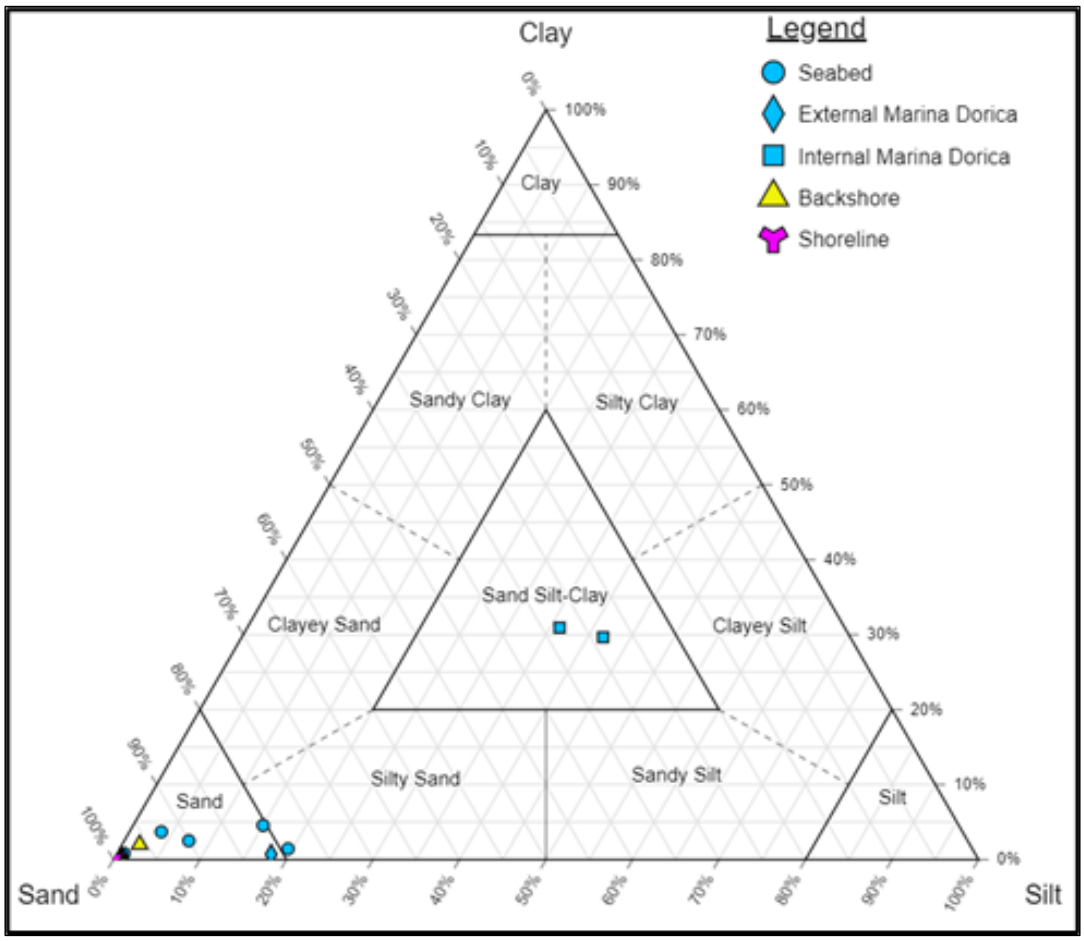

Figure 36: Shepard's sediment classification scheme (1954) on which the textural compositions of the samples are plotted.

The sediments sampled in the port area of Marina Dorica have much higher muddy granulometry contents than those in the Torrette / Palombina area. The sediments of this area, according to the classification scheme of Shepard (1954), can be classified as observing on the map the abundance of the different classified as silty clays, silt clayey, silt, sand-silt-clay, silty sands, and sands.

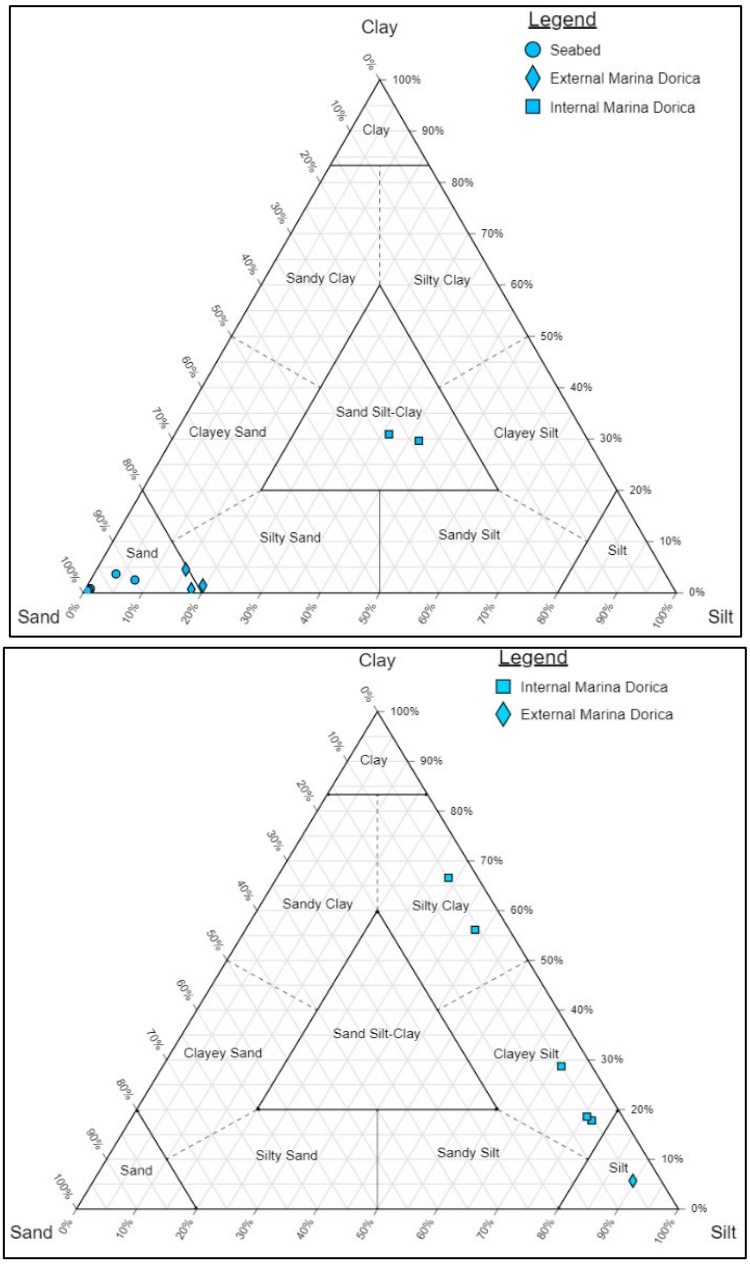

Figure 37: Shepard's sediment classification scheme (1954) on which the textural compositions of the samples are plotted.

From the observation of the distribution of the different grain size classes in the marina area, it was possible to note that the silt and clay content decreased from the internal areas of the port to those closest to the connection with the open sea (Figure 37; Figure 38). This is likely due to the energy of the different environments, which are very calm in the innermost and sheltered areas (allowing the deposition of very fine sediments), and become more energetic towards the outside, where the influence of the sea is stronger, allowing the deposition of coarser sediments than the others. In the external areas, however, the sediments of the seabed near the cliffs of the piers are mainly made up of sand. This is probably due to the higher energy environments that exist due to the waves impacting the cliffs and which do not allow the settling of muddy sediments. Finally, it was possible to observe the presence of a sample, located at the eastern end of the map, which is almost exclusively made up of silt, probably due to the depth of the seabed which is little affected by wave motions and allows the deposition of silty sediments.

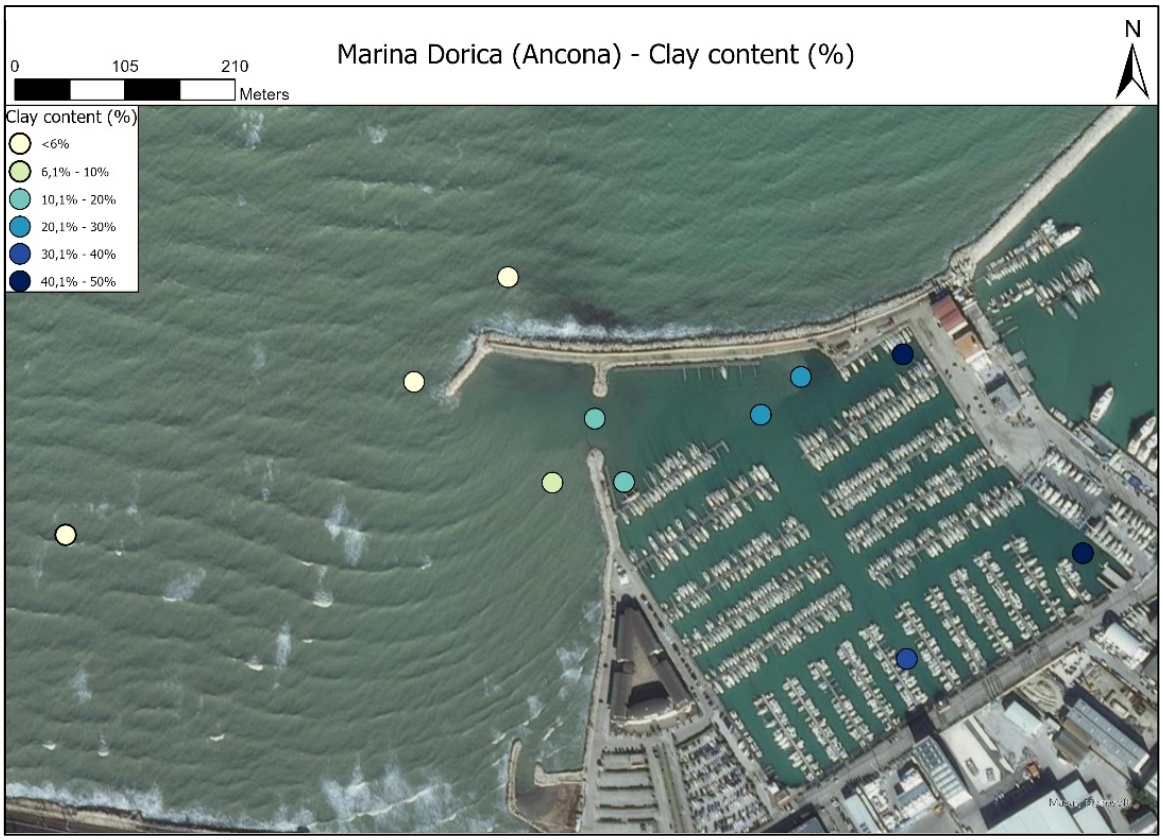

Figure 38: Satellite image of Marina Dorica port area on which clay content in the samples is shown.

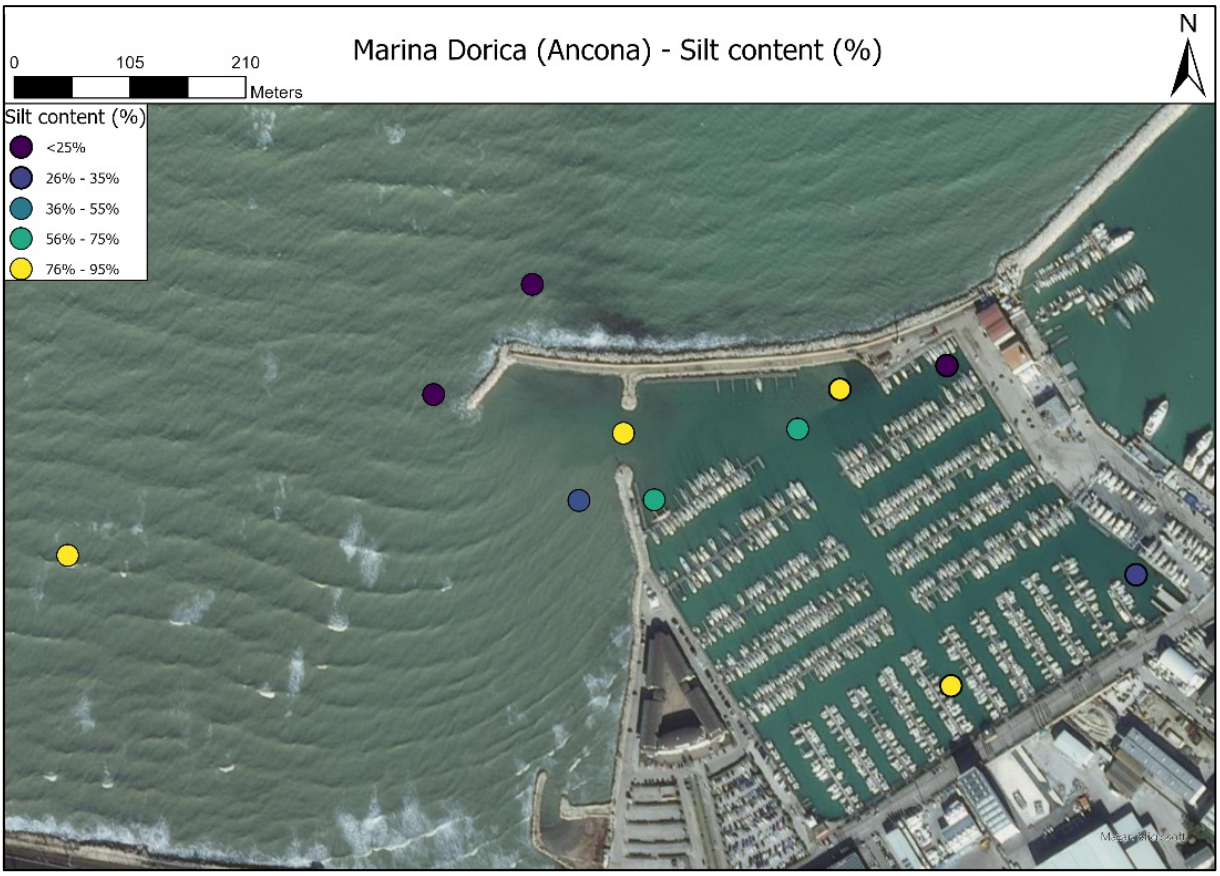

Figure 39: Satellite image of Marina Dorica port area on which silt content in the samples is shown.

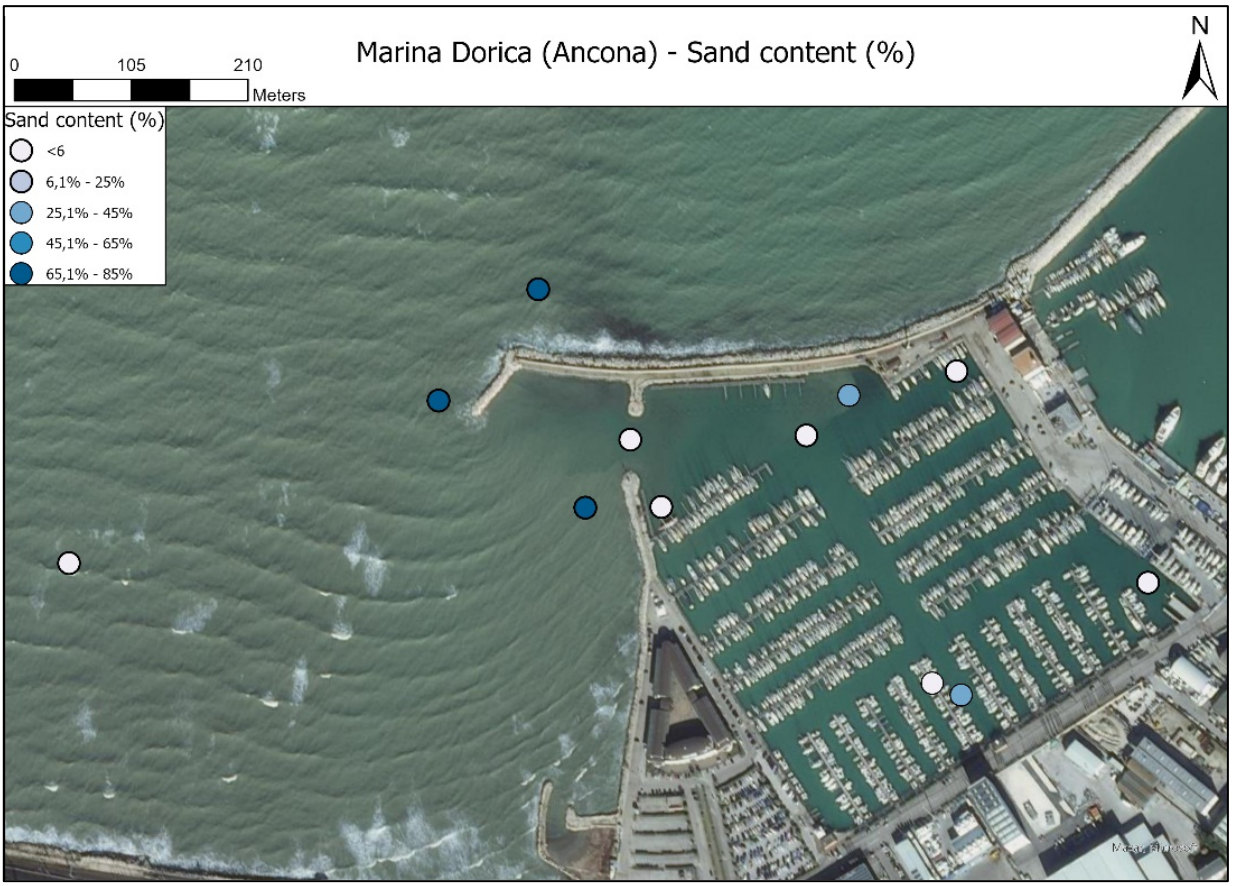

Figure 40: Satellite image of Marina Dorica port area on which sand content in the sample is shown.

The sediments of the coastal area of Torrette-Palombina are mainly made up of carbonates, in which the content varies from a minimum of 65% to a maximum of 76%. The highest values occur on the beach where there is a very low quantity of muddy sediments, while the lowest values occur in the sediments of the seabed in favour of more silicate compositions probably due to a greater quantity (albeit modest) of clayey sediments. In general, throughout the area, there is a fair amount of siliciclastic sediments as the silica and aluminium content varies from minimum values of 16% (in beach sediments) up to maximum values of 30% (in seabed sediments).

As for the sediments in the area of the “Marina Dorica” tourist port, the samples have carbonate contents significantly lower than those observed in the Torrette-Palombina area. The carbonate content, in fact, is between 44% and 58%. This is probably due to the more clayey granulometry of these sediments, which therefore contain a greater quantity of phyllosilicate minerals, which adds to the general high quantity of siliciclastic sediments.

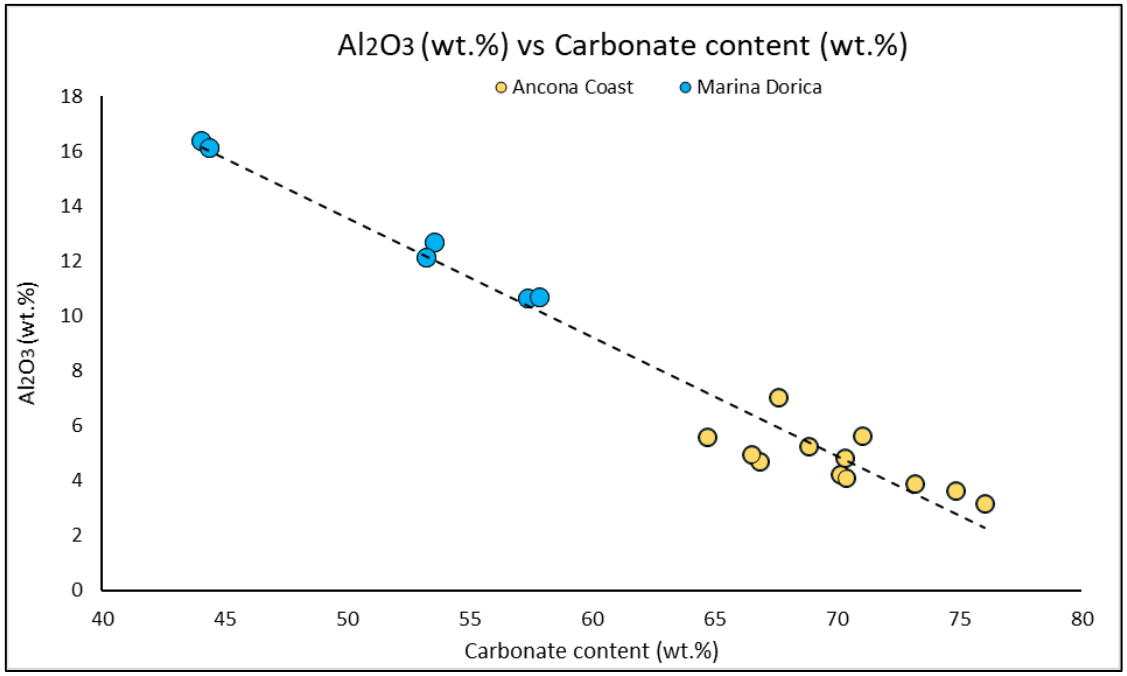

Figure 41: Scatter plot in which the values of the carbonate content vs Al_2O_3 content are plotted.

As regards the concentration of heavy metals in sediments, analyses were carried out on the samples collected in the "Marina Dorica" area. The analytical results were subsequently compared with the legal limits established by the Italian legislation in "Table 1 of Annex 5 to Title V of Part IV of Legislative Decree no. 156 of 2006".

In general, good quality of the sediments emerged, although exceedances of the threshold limits for "public, private and residential green sites" were identified in two samples, as regards the concentrations of copper and zinc (Figure 9). Furthermore, in these two samples, the highest

concentrations of all other heavy metals are always found (although these do not exceed the limits).

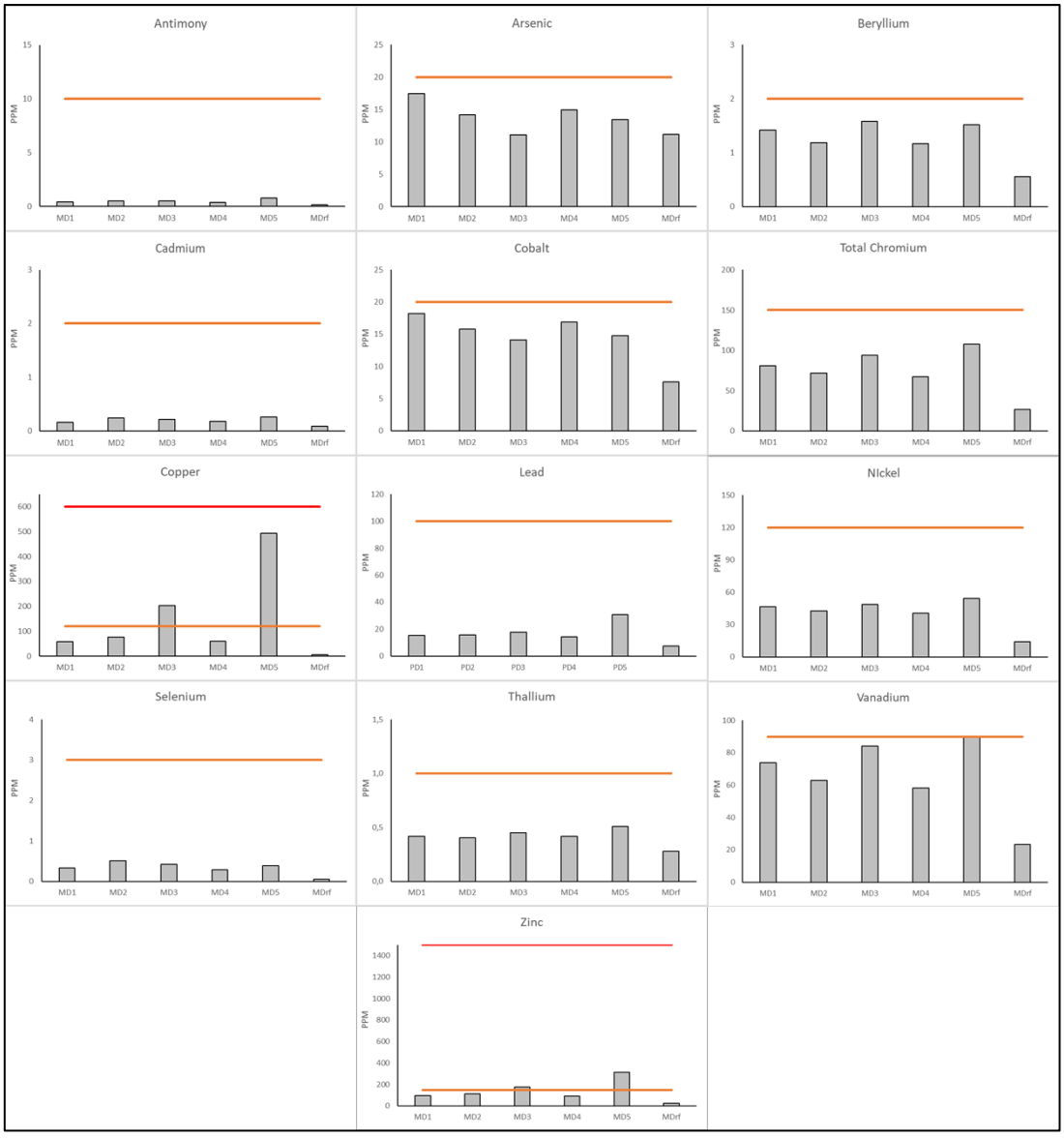

Figure 42: Bar graphs showing the concentrations of different heavy metals (arsenic, antimony, beryllium, cadmium, cobalt, chromium, copper, nickel, selenium, thallium, vanadium, and zinc)

in the sediments of the seabed Marina Dorica port area, compared with the limit values of Italian law for "sites for public, private and residential green use "provided for in "Decree Law 152 of 2006".

Plotting the distributions of heavy metal concentrations on a map, it was possible to observe that the samples with high concentrations of heavy metals were those with the greatest abundance of clayey sediments (Figure 10; Figure 11). Considering the large scientific literature that testifies to the affinity of heavy metals with clayey granulometry (Davies et al. 1991, Sakai et al. 1986, Thorne and Nickless 1981, Wakida et al., 2007), it is likely that these high concentrations are due to the abundance of clayey sediments, favouring the accumulation of heavy metals. In a port area where activities are widely recognized as possible sources of heavy metal dispersion (e.g., Mali et al., 2017), this scenario is quite likely. The concentrations of heavy metals, however, are well below the legal limits in the areas outside the port, indicating that the only problems are related to specific areas of the port.

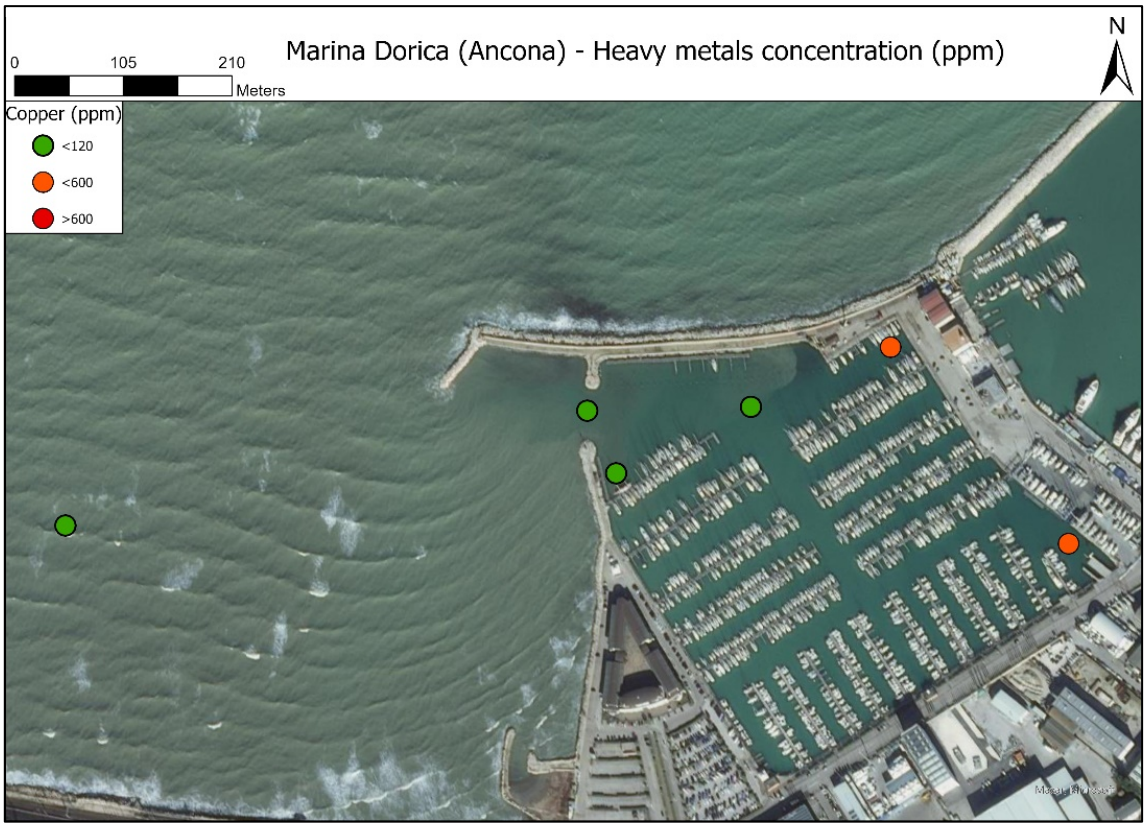

Figure 43: Satellite image showing the sampling points coloured according to the following criterion: green: samples in which the concentration of Copper is lower than the limit value for "sites for public, private and residential green use"; orange: samples in which the Copper concentration is below the limit value for "sites for public, private and residential green use" but below the limit value for "sites for commercial and industrial use"; red: samples in which the Copper concentration is higher than the limit value for "sites for commercial and industrial use".

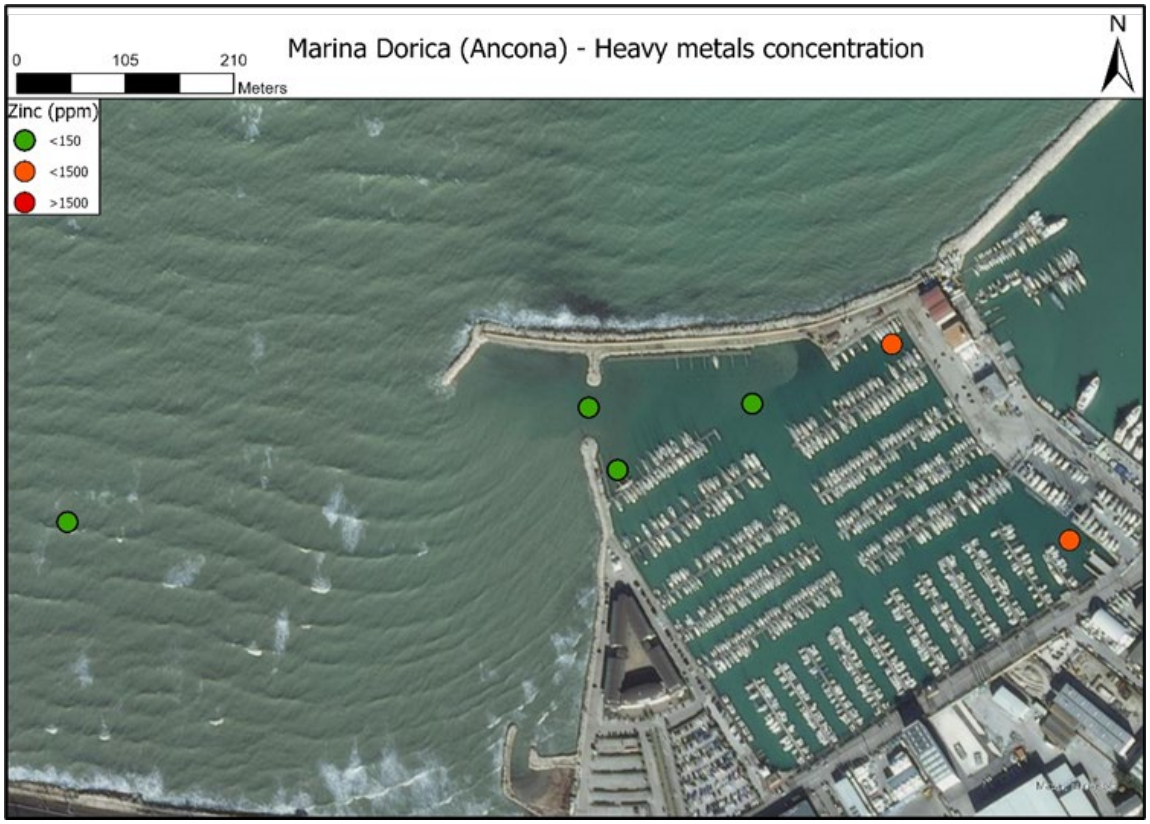

Figure 44: Satellite image showing the sampling points coloured according to the following criterion: green: samples in which the concentration of Zinc is lower than the limit value for "sites for public, private and residential green use"; orange: samples in which the Zinc concentration is below the limit value for "sites for public, private and residential green use" but below the limit value for "sites for commercial and industrial use"; red: samples in which the Zinc concentration is higher than the limit value for "sites for commercial and industrial use".

What was seen through this study, indicates that the heavy metals dispersed in the waters of the port tend to accumulate in the most sheltered areas, where the seawater is unable to take charge of the sediments, so it is unable to lead to a dilution of the concentration of heavy metals.

Final Considerations

The sediments of the Ancona area show strong differences between the coastal area of Torrette-Palombina and the port area of "Marina Dorica".

As for the sediments of the Torrente-Palombina area, these have basically sandy granulometry both in the beach areas and in the seabed areas. Slight increases in the content of muddy fractions have been observed in the seabed located in the southeast area. From the compositional point of view, these sediments are mainly made up of calcium carbonate (calcite), which the percentages are between 65% and 76%. Siliciclastic sediments are fairly abundant, in fact, the percentage of Silica and Aluminium is between 16% and 30%.

As regards the port area of "Marina Dorica", these sediments have a higher content of muddy sediments than that seen in the other area. The sediments of the interior of the port see an increase of silt and, above all, clay towards the more internal and sheltered areas of the port. On the contrary, in the external areas, close to the piers, the mud contents are much lower in favour of a higher abundance of sands. Also, from the compositional point of view, these sediments differ from those of the other areas, since the contents of calcium carbonate are decidedly lower (44-58%), in favour of a higher content of silica and aluminium. This is probably due to the greater quantity of clayey sediments in the seabed of this area.

As far as the concentration of heavy metals is concerned, although the general quality of the sediments was found to be good, it was found that the copper and zinc concentration limits were exceeded in the samples coming from the innermost areas of the port. This is probably due to the large quantity of clayey sediments that allow a greater accumulation of heavy metals.

Podstrana

Results of analyses

As for the Podstrana test site, sampling was carried out in the Strožanac area. The samples were taken both inside the marina Strožanac (seabed sediment sampling) and on the nearby beach located south of the marina (beach sediment sampling).

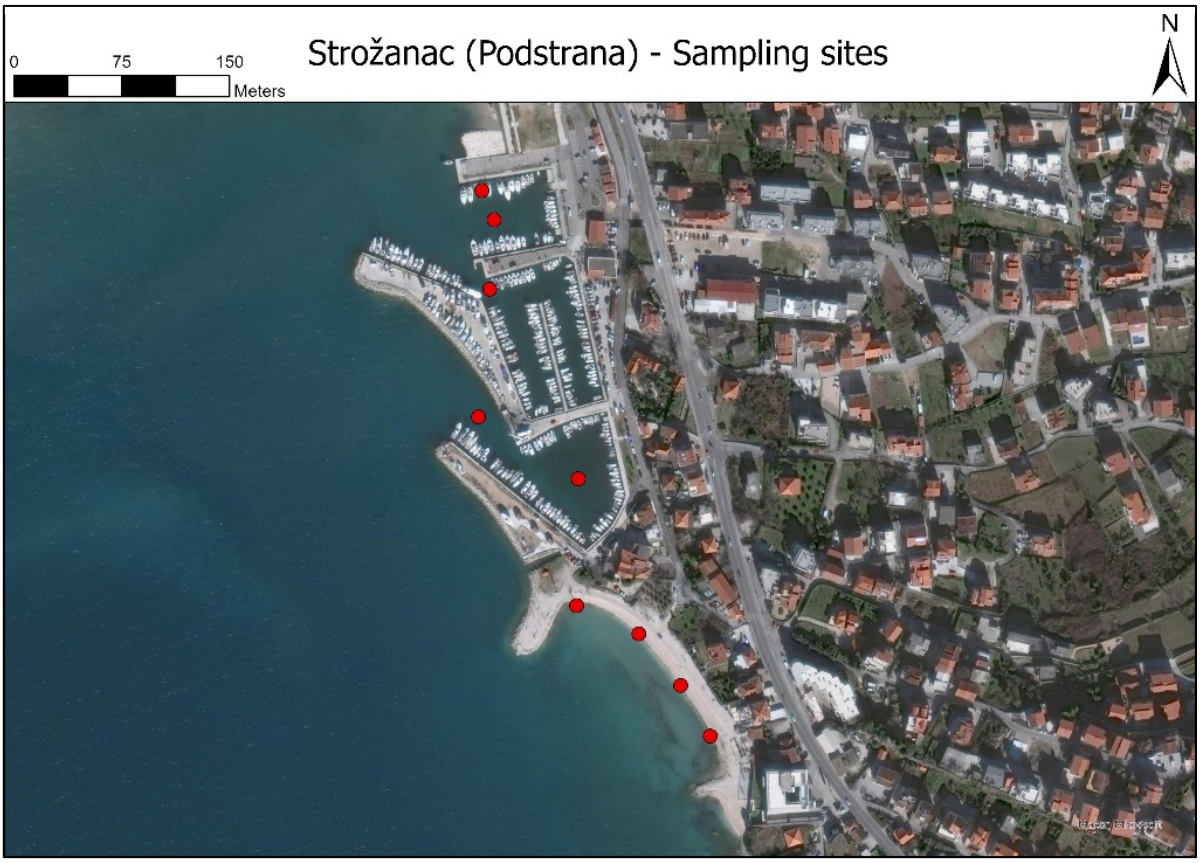

Figure 45: Satellite image of the Strožanac area, where the samples were taken. The red dots indicate the sampling points.

The results of the textural analyses have highlighted very strong differences between the sediments of the beach and those of the seabed in the marina area. Moreover, these differences would seem not to be due to the simple distribution of sediments due to the different energies

of the depositional environments (finer grain sizes in lower energy environments such as the seabed away from the coast; coarser grain sizes in higher energy environments such as shorelines). In this context, as will be shown below, beach sediments exhibit characteristics that are incompatible with a beach generated by natural processes.

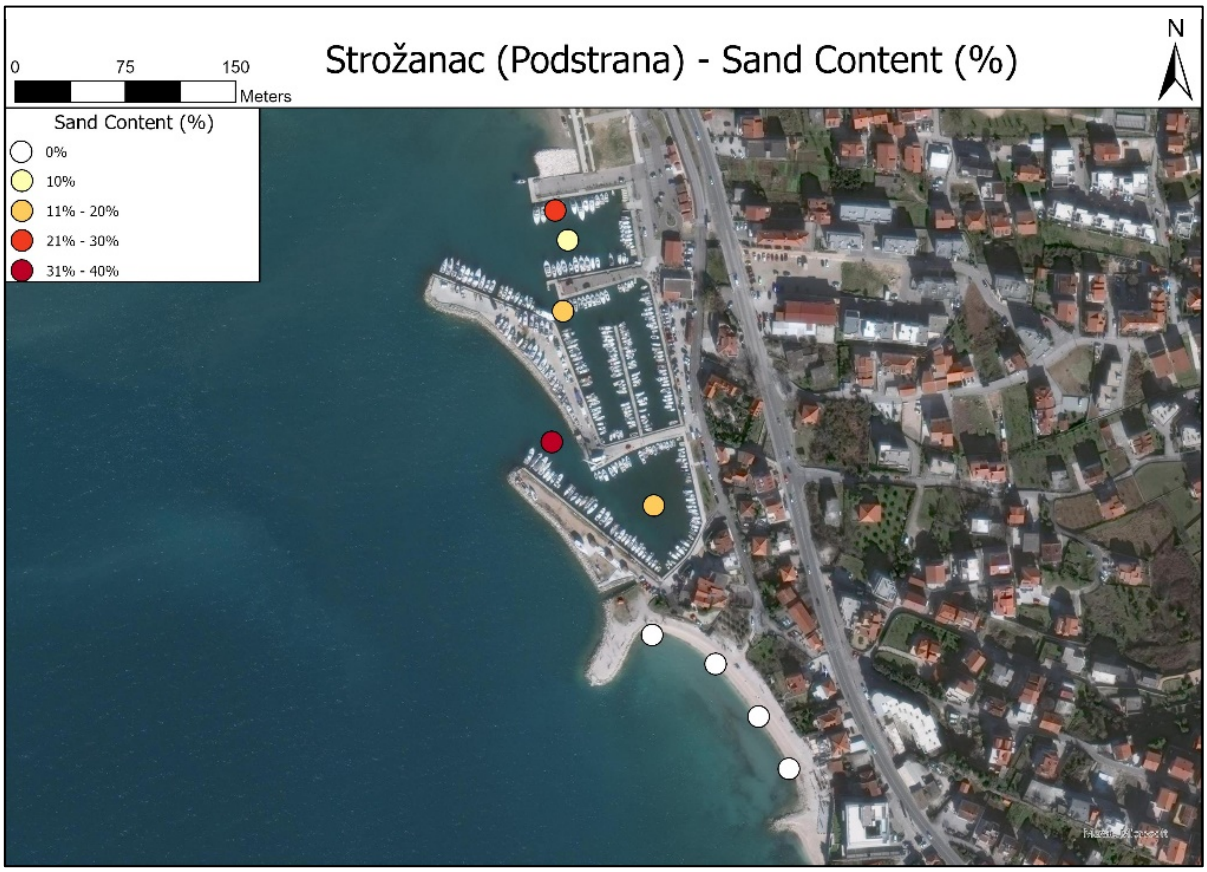

Figure 46:Satellite image of Strožanac area on which sand contents in the sample are shown.

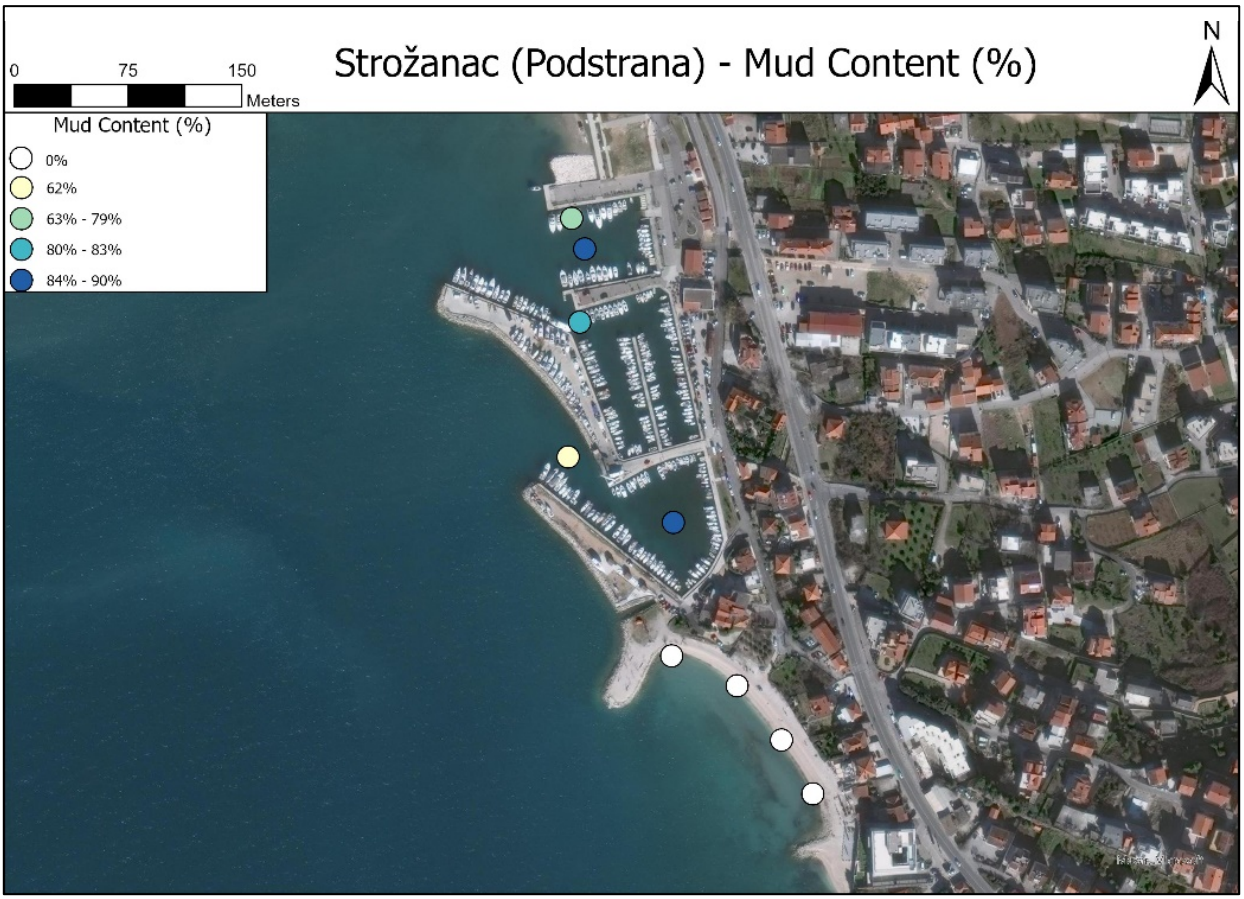

Figure 47:Satellite image of Strožanac area on which sand contents in the sample are shown.

Seabed sediments showed sand contents up to 40% and mud contents up to 85%. According to Shepard's (1954) sediments classification system, the analyzed samples can be classified as clayey silts and sandy silts.

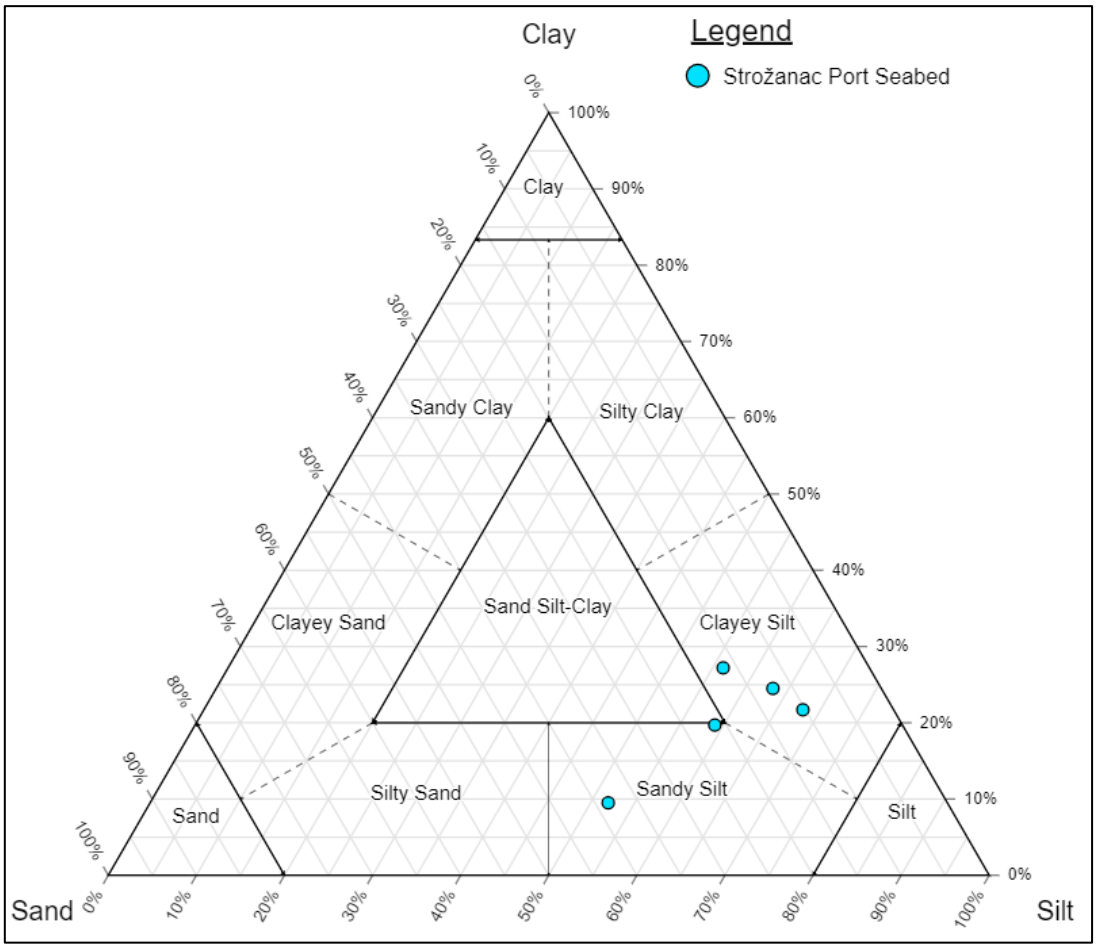

Figure 48: Shepard's sediment classification scheme (1954) on which the textural compositions of the samples are plotted.

Sediment samples from the beach can be classified as gravel according to Shepard's (1954) classification diagram. The results of the analyses showed that these sediments are extremely well sorted, with sorting values (expressed according to the sigma scale) below 0.250. More specifically, the results showed that on average about 95% of the grains constituting the samples are pebbles with a size between -3 and -2 Phi (ie between 16 and 4 mm).

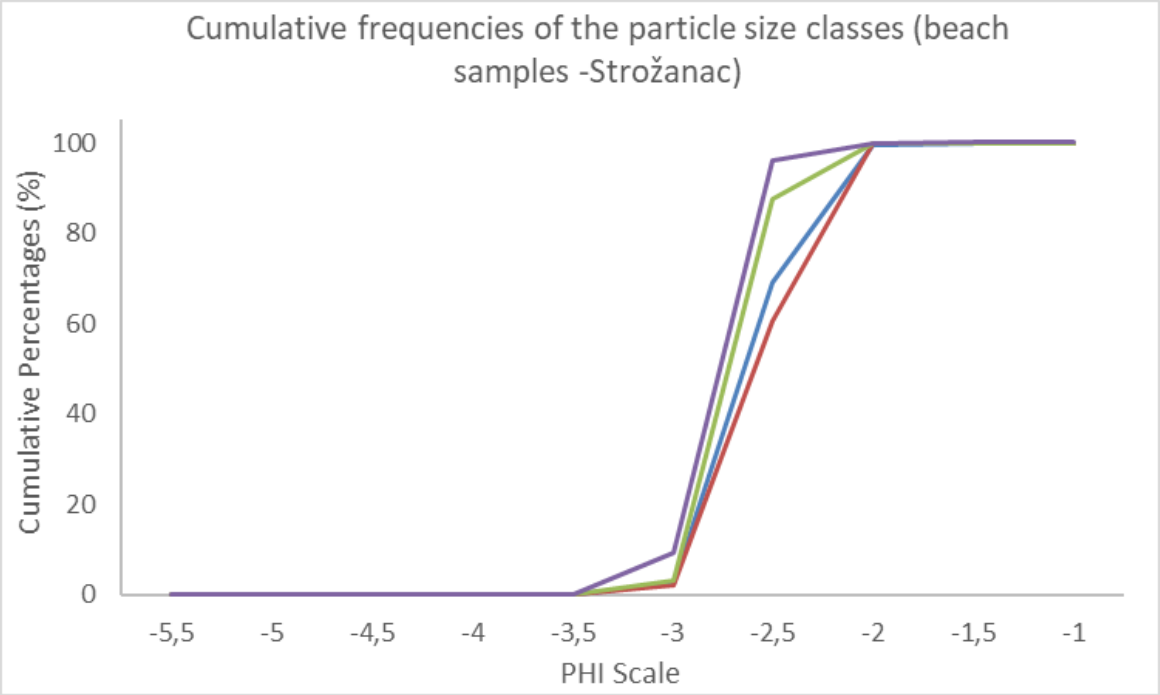

Figure 49: Cumulative curves in which the cumulative frequencies are plotted relative to the textural analyses carried out on the beach samples through the sieving method.

The sediments, therefore, show an almost total absence of texture variability, indicating a probable anthropogenic origin of the beach.

From a compositional point of view, the sediments of the beach consist almost entirely of carbonate, in which the carbonate content is abundantly higher than 90%. Considering the very low concentrations of MgO (<1%) it is possible to state that the sediments are made up of calcium carbonate (calcite). On the other hand, as regards the sediments of the seabed of the marina Strožanac, the carbonate content of the sediments is considerably lower, with values between 40 and 55% (Figure 49). This is probably due to the particle size of these sediments, which, as seen above, are essentially clayey silts and sandy silts. These, therefore, favour a shift towards more silicate compositions due to the greater quantity of phyllosilicate minerals (clay minerals).

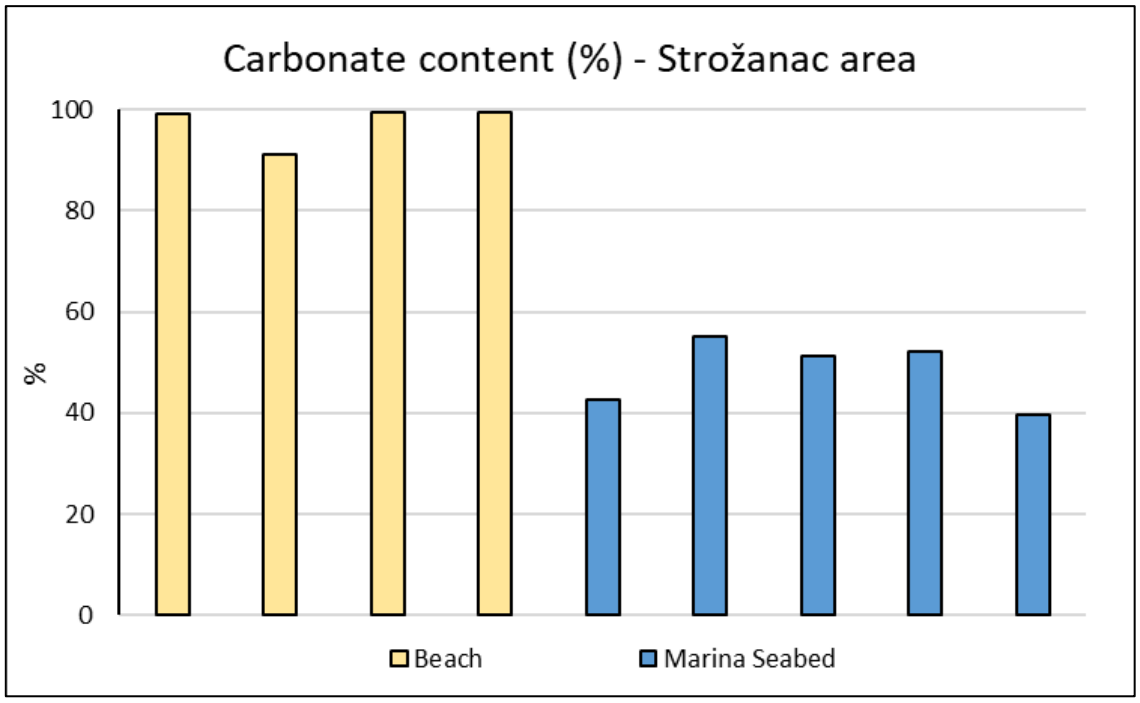

Figure 50: Bar graph showing the percentage values of the carbonate content in the sediments of the Strožanac area.

As regards the analyses of the concentration of heavy metals in the sediments, these were performed only on the seabed samples. This is because, as widely reported in the literature, the concentration of heavy metals strongly decreases as the particle size increases. In particular, these have a strong tendency to accumulate in silty sediments and, even more, in clayey sediments (Davies et al. 1991, Sakai et al. 1986, Thorne and Nickless 1981, Wakida et al., 2007). Considering the gravelly granulometry of the beach sediments it is unlikely that these can host high concentrations of heavy metals and for this reason, it was decided to carry out the analyses only on seabed sediments, where there is a high quantity of silty and clayey sediments.

The analytical results were compared with the legal limits established by the Italian law in the "Table 1 of Annex 5 to Title V of Part IV of Legislative Decree no. 156 of 2006":

The concentrations of metals in the Seabed samples investigated resulted both below the limits for “sites for commercial and industrial use “and the limits for "sites for public, private and residential green use". The latter have much lower threshold limits than the other category.

The analyses have, therefore, shown that although the sediments are located on the seabed of a port area in which there is a strong potential for contamination, they showed an excellent quality from the point of view of the concentration of heavy metals (Figure 50).

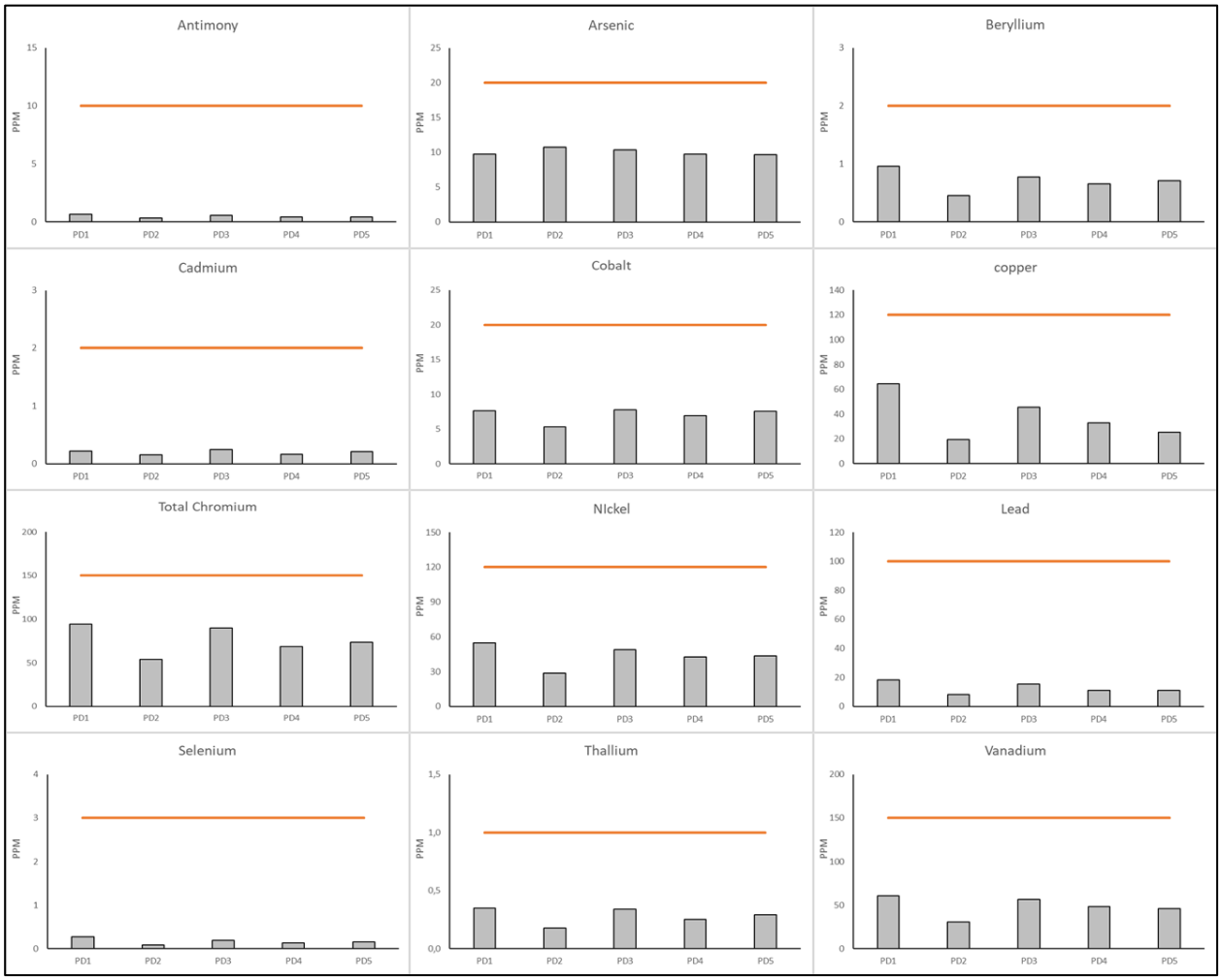

Figure 51: Bar graphs showing the concentrations of different heavy metals (arsenic, antimony, beryllium, cadmium, cobalt, chromium, copper, nickel, selenium, thallium, vanadium, and zinc) in the sediments of the seabed of marina Strožanac, compared with the limit values of Italian law for "sites for public, private and residential green use "provided for in "Decree Law 152 of 2006".

Final Considerations

The results of the analyses of sediments in the Strožanac area indicate, first, that the beach located in the southern area of the marina Strožanac could probably be of anthropogenic origin. The sediments of this area, in fact, have an extremely high sorting with practically identical granulometry throughout the beach (dimensions between 4 and 16 mm). Also, from the compositional point of view, these sediments are quite identical, showing carbonate contents higher than 90%; the carbonate is likely almost all represented by calcite.

Seabed sediments in the Strožanac marine area can be classified, from a textural point of view, as clayey silt, and sandy silt. In these sediments, the carbonate content is between 40% and 55%. This is most likely due to silty-clay sediments which host more quantity of clay minerals, thereby increasing the silica and aluminium contents.

From the point of view of the concentration of heavy metals, the sediments of the beach, thanks to their gravel granulometry, should not present problems regarding contamination or pollution by heavy metals. On the contrary, the sediments of the seabed in the marina Strožanac, being made up of silty/clayey sediments and being in an area potentially exposed to heavy metal pollution phenomena, present a higher risk. However, the analyses have shown that there is no condition of heavy metal pollution.

Sacca di Goro

Authors

Geographic Framework

Sacca di Goro is a shallow coastal lagoon located in the southern part of the Po River delta with a surface area of 26 km^2, an average depth of about 1.5 m that is variable in relation to the river and sea water inflows (Simeoni et al., 2000). The Sacca di Goro is connected by two mouths to the Northern Adriatic Sea which variably inflow according to the tidal dynamics (Natali et al., 2016).

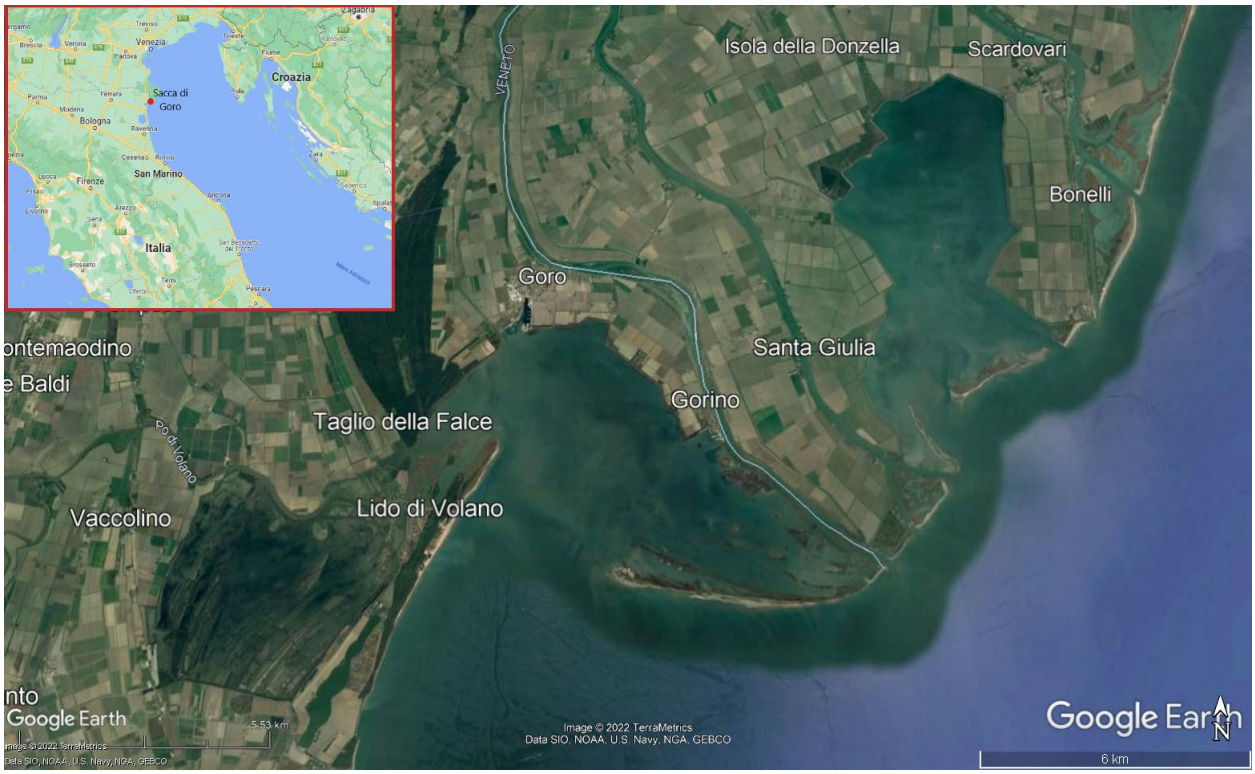

Figure 52: Satellite image of Sacca di Goro area.

Climate

The area of the Pò delta falls within the cold temperate climate zone. In this area, however, the conditions are mitigated by the presence of the sea which tends to give the area more Mediterranean climatic characteristics.

The temperature variations in this zone are generally below 22 ° C, with temperatures above 23 ° C in July and below 2 ° C in January. Average annual rainfall has very low values, less than 600 mm and can be considered on the verge of desertification. The maximum rainfall tends to be concentrated in the winter period while rainfall is scarce in the spring (Ciavola et al., 2000).
In the summer period, the Scirocco winds from the south-east are the most dominant, while in the winter the dominant winds blow from the west (Ciavola et al., 2000).

Evolution of Sacca di Goro

The Goro lagoon is part of the Po delta system and is separated from the sea by a sand spit (Scanno di Goro).
The evolution of the Sacca di Goro has been and is strongly influenced by the evolution of the delta apparatus of the Po River. In turn, the morphology of the latter is controlled by two fundamental factors: the structural trend of the subsoil and climate changes.
As regards the geology of the subsoil in the area under examination, the major structure (belonging to the Apennine chain) is the "Ferrara ridge", which represents a differential subsidence area, which probably led to the northward migration of the Po River in the last 3000 years (Bondesan, 1985).
The climatic changes that have taken place in the last 3000 years, on the other hand, have contributed significantly to shaping the territory, favouring the succession of marine and continental conditions.
Around 3000 BC, at the end of the last glaciation, the sea level reached its maximum, making the coastline several kilometers to the west of the current shorelines (Bondesan, 1986; 1990).
In the following 5 millennia, the sea level remained more or less the same, but the accumulation of sediments determined the gradual increase of the alluvial plain causing the coastline to move towards the east (Bondesan, 1986; 1990).
The modern Po delta was formed due to an important hydraulic project by the Venetians. The latter, in fact, between 1598 and 1604 diverted the main ramp of the Po until it flowed south-east into the ancient Goro pocket, which was increasingly buried. This work decisively conveyed the natural evolution of the delta (Gabbianelli et al., 2000).
Towards the end of 1600, the new delta was centered on the branch of the Po di Viro and stretched towards the sea for about 7 km (Gabbianelli et al., 2000).

In the following years, some anthropic interventions directed the terminal shaft of the river to the south. In 1750 the area of the mouth of the Po di Goro was advanced by about 10 km and that of the Abbot branch by 6 km (Ciabatti, 1966). In 1800, in the cartography of the time, the first hints of an inlet near the Po di Goro appear, which will develop first as Rada di Goro and subsequently, into the homonymous Sacca di Goro (Simeoni et al., 1998).
Due to the lower solid contribution to the sea due to the end of the "Little Ice Age", starting from the first half of the 20th century the advancement rates decreased significantly. The continuous advancement of coastal arrows precludes the Sacca di Goro from the direct action of the seafavouringng the deposit of fine materials inside it (Gabbianelli et al., 2000).

The sediments of the Sacca di Goro

An in-depth study campaign of the sediments of the Sacca di Goro was carried out between 2003 and 2005 by Bertelli and Vaccaro (2007), in which 95 sediment samples were analyzed, taken over the three years of investigation.
The sediments of the Sacca di Goro have a granulometric range that goes from sands to clays. Sandy sediments are found in greater quantities near the sea mouths and locally near the town of Gorino (Figure 51); true north-east, on the other hand, the percentage of fine fraction progressively increases (Figure 52), passing from percentages of sand higher than 97% to percentages lower than 5% (Bertelli and Vaccaro, 2007).

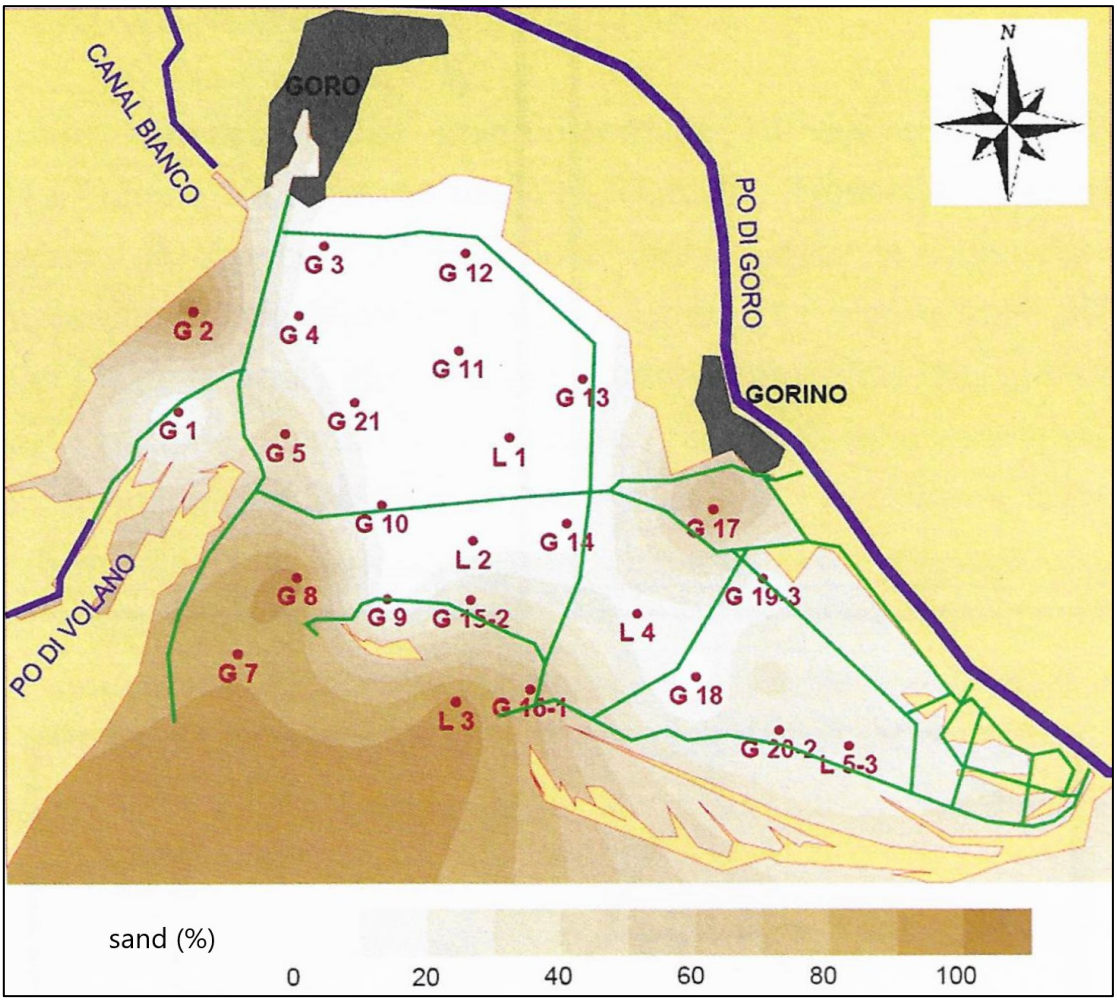

Figure 53: Distribution of sand in the Sacca di Goro (Bertelli and Vaccaro, 2007).

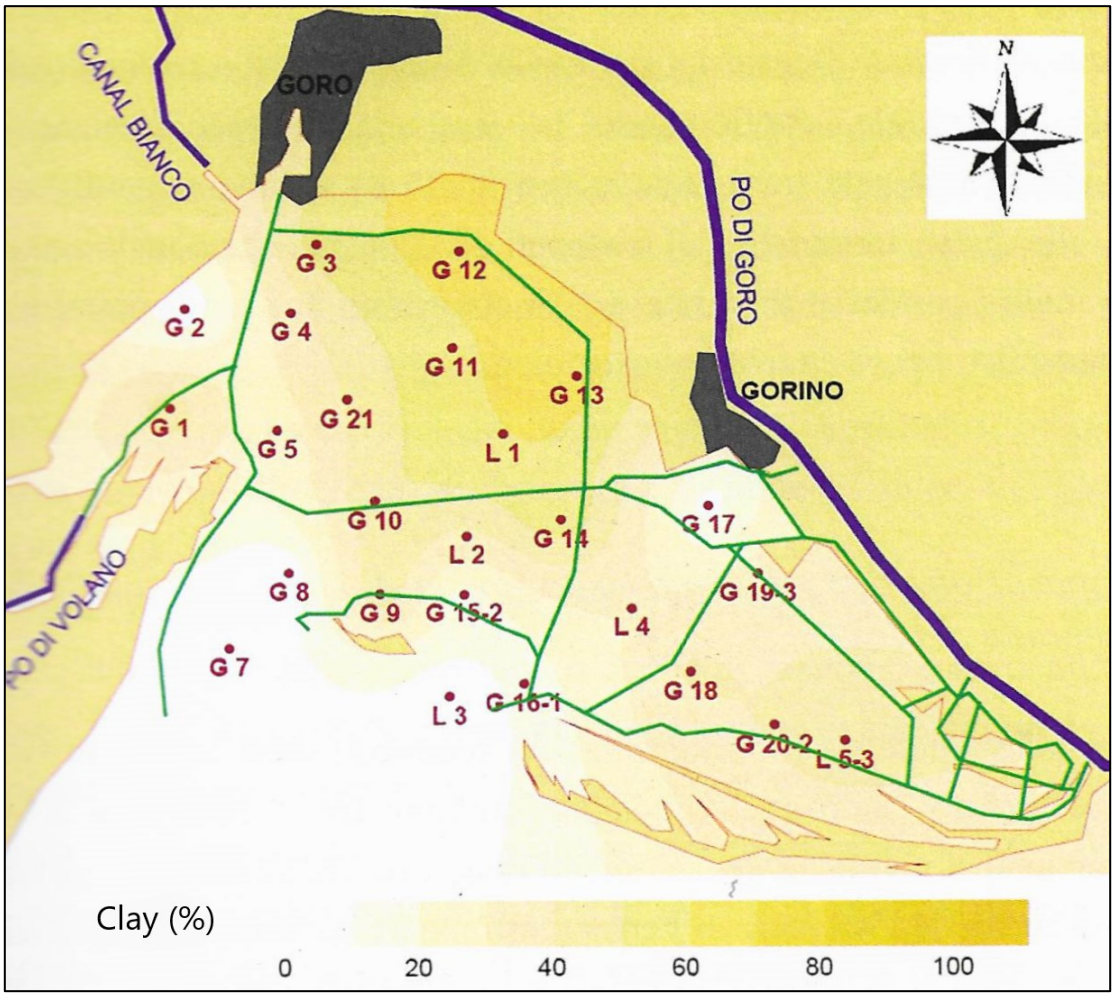

Figure 54: Distribution of clay in the Sacca di Goro (Bertelli and Vaccaro, 2007).

From a compositional point of view, the sediments of this area have two main distributions of silica and aluminium (Figure 54):
a distribution is characterized by high levels of silica (55 <% SiO_2 <65) and low levels of aluminium (10 <% Al_2O_3> 15), for the samples that are located near the coastal arrow and the openings to the sea where it is bound in the presence of sandy granulometry of the sand spit, and where the clayey sediments are washed away and subtracted due to storm surges.

The second distribution, whose range of variation is between 15 < % Al_2O_3 <20 and 50 < % SiO_2 <56. In this case, those environments more marginal to the coast and the central areas of the Sacca di Goro are characterized, in which higher aluminium values reflect the greater abundance of the finer granulometric phases (Bertelli and Vaccaro, 2007).

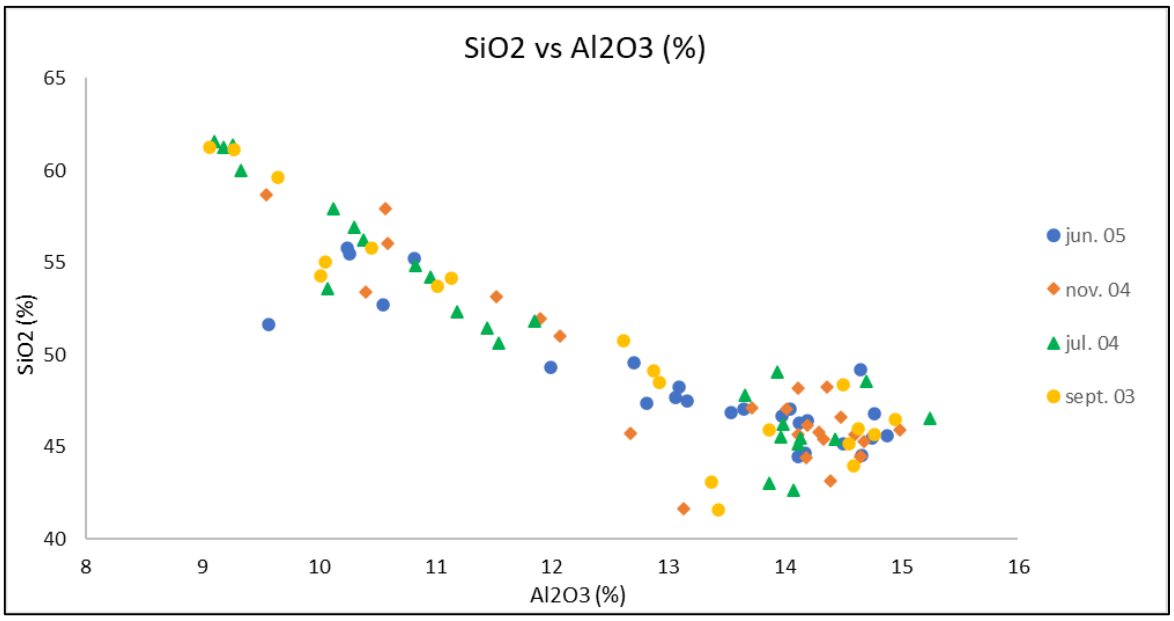

Figure 55: Scatter graph showing the silica and aluminium values in the samples taken in the various sampling activities. Data from Bertelli, 2005.

Calcium in the sediments of this area seems to be mainly linked to the presence of small shells or fragments of shells, which by natural processes are reduced to the size of the sediment granules and then transported together with them, acquiring the same sedimentological significance.

As regards the concentration of chromium and nickel, it emerged that many samples exceeded the legal limits of the legislative decree 152/06 for sites for public, private and residential green use. It should be emphasized, however, that in this context the samples remained within the average concentration range of the sediments of the province of Ferrara (100 < ppm Cr < 230; 65 < ppm Ni < 150). Two samples, in particular (in September 2003, July 2004, and June 2005), however, had a chromium concentration of about 300 ppm. These accumulations were in the

south-eastern part of the lagoon and near the mouth of the Po di Volano. The cause of this phenomenon could be attributed to the modest leaching of the sediments (Bertelli and Vaccaro, 2007). In general, however, the high concentrations of these two elements are attributable to natural invoices (Amorosi et al., 2002; Bianchini et al., 2002) and only partially to an anthropic impact on the territory (Vaccaro and Bertelli, 2007).
Similar considerations can be made regarding the concentrations of Cobalt and Vanadium. Also, in this case, there were numerous exceedances of the concentration limits, but in this case, the concentrations were still lower than the background of the province of Ferrara. Therefore, the high concentrations of these elements are attributable to the natural background characteristic of the sediments of the Po drainage basin (Vaccaro and Bertelli, 2007).

Experimental study

Authors: Carmela Vaccaro, Marzia Rizzo

During the meeting held in Bibione on 24th January 2020 between PP6 (Bibione Mare spa), PP8 (University of Ferrara) and PP9 (Consotium Future in Research), it was decided to install structures for the study on the various types of plastics degradation, in different coastal contexts and in relation to environment features, at the Bibione test site in March 2020. This would have provided useful information for plastic waste management based on its degradability. In February 2020, the Italian Government declared a state of emergency due to the Covid-19 emergency. Since that date, a series of increasingly restrictive decrees has gradually brought Italy to a state of closure, preventing all people from traveling, if not those strictly necessary. Due to these prohibitions, it was not possible to proceed with the installation in Bibione site of the above-mentioned structures and start the monitoring activities as scheduled and for this reason Partner 8 (University of Ferrara) requested the authorization for the installation of the structures in Goro (Ferrara) and to include it as test site. This request was approved and finalized during the Major Change procedure of the ECOMAP project.
The experimental study was carried out during the PhD Thesis of Dr. Marzia Rizzo, under the supervision of Prof. Carmela Vaccaro.
This study has analyzed and quantified the degradation of six types of commonly used plastics, polystyrene (PS), polypropylene (PP), high-density polyethylene (HDPE), low-density polyethylene (LDPE), polyethylene terephthalate (PET) and polyvinyl chloride (PVC).
Testing racks were built to allow the exposure of all types of plastics, in the form of strips.
Two testing racks were installed ne was deployed in the intertidal zone (Lagoon-IT) (44°50'26.0"N 12°17'37.0"E) so that it was inundated for approximately 12 hours per day. The other was

secured in the subtidal zone (Lagoon-ST) (44°50'25.6"N 12°17'37.7"E) at a depth of 30 cm in low tide conditions (Figure 56). Light intensity (150 to 1200 nm) and temperature were measured in each rack, using factory calibrated HOBO sensors (HOBO Pendant, UA-002-64), logging every 30 min and cleaned during each sampling.

Figure 56: Testing rack deployed in the Goro Lagoon in intertidal condition

At each sampling time point, total mass change and mass change after washing with hydrochloric acid were measured; from week 4 to week 28 samples chlorophyll *a* accumulation were measured. These plastic strips were kept in the dark and frozen (-20°C) until analysis. *Chl a* attached to plastic strips was extracted in a 90% acetone solution in the dark at -20°C for 24 h. The pigment concentration was measured by spectrophotometry (Agilent Cary 3500 UV-Vis double-beam spectrophotometer).
The 12- and 28-week exposure samples were also observed using a scanning electron microscope (SEM - model ZEISS EVO MA 15, coupled with an Energy Dispersive X-Ray Spectroscopy (EDS) system (Aztec Oxford apparatus, SDD detector, WD 8.5 mm, EHT 20 kV) provided with a LaB6 filament as electron source) for microstructural characterization and for determining element compositions.
For the geochemical characterization and monitoring of the waters, measurements of the chemical-physical parameters and analysis of the ions present in solution were carried out (pH, electrical conductivity (EC), total dissolved solids (TDS) and salinity values and the concentration of anions and cations) (Figure 57; Figure 58).

Lagoon					
pH	8.05	8.16	7.78	8.22	0.19
EC (ms/cm)	32.52	27.09	23.07	44.44	8.82
TDS (ppt)	16.69	16.23	11.83	22.22	4.19
Sal (psu)	20.45	16.69	14.49	28.67	5.96

Figure 57: Descriptive statistic of the chemical-physical parameters of the water measured by the HI98195 probe

Lagoon					
(ppm)	Mean	Median	Minimum	Maximum	Std.Dev.
F^-	0.85	0.81	0.38	1.46	0.36
Cl^-	14764.85	13777.90	9258.12	22008.58	4538.53
NO_2^-	n.d.				
Br^-	33.48	29.52	22.09	53.05	10.37
NO_3^-	2.76	2.76	2.34	3.17	0.58
PO_4^{3-}	n.d.				
SO_4^{2-}	1870.32	1797.25	1292.93	2743.89	534.99
Li	0.09	0.08	0.06	0.13	0.03
Be	0.00	0.00	0.00	0.00	0.00
B	2.40	2.28	1.53	3.44	0.77
Na	2293.05	2342.89	1948.08	2553.35	204.08
Mg	387.61	390.56	244.35	540.37	108.22
Al	0.04	0.00	0.00	0.15	0.06
P	0.06	0.08	0.00	0.15	0.06
K	184.47	176.48	118.42	268.03	58.64
Ca	204.25	192.94	136.28	293.00	59.68
Sc	0.00	0.00	0.00	0.00	0.00
Ti	0.11	0.11	0.06	0.16	0.04
V	0.00	0.00	0.00	0.00	0.00
Cr	0.00	0.00	0.00	0.00	0.00
Mn	0.01	0.01	0.00	0.04	0.01
Fe	0.07	0.05	0.00	0.22	0.08
Co	0.00	0.00	0.00	0.00	0.00
Ni	0.00	0.00	0.00	0.00	0.00
Cu	0.00	0.00	0.00	0.01	0.00
Zn	0.01	0.00	0.00	0.02	0.01
Ga	0.00	0.00	0.00	0.00	0.00
As	0.00	0.00	0.00	0.00	0.00
Se	0.00	0.00	0.00	0.00	0.00
Rb	0.05	0.05	0.03	0.07	0.02
Sr	3.81	3.80	2.26	5.32	1.22
Mo	0.00	0.00	0.00	0.00	0.00
Ag	0.00	0.00	0.00	0.00	0.00
Cd	0.00	0.00	0.00	0.00	0.00
Sn	0.00	0.00	0.00	0.00	0.00
Sb	0.00	0.00	0.00	0.00	0.00
Te	0.00	0.00	0.00	0.00	0.00
Ba	0.03	0.02	0.02	0.04	0.01
Hg	0.00	0.00	0.00	0.03	0.01
Tl	0.00	0.00	0.00	0.00	0.00
Pb	0.00	0.00	0.00	0.00	0.00
Bi	0.00	0.00	0.00	0.00	0.00
U	0.00	0.00	0.00	0.00	0.00

Figure 58: Descriptive statistic of the concentration of ions present in the lagoon water in which the plastic strips have been immersed

In the lagoon, the temperature varied according to the seasonal trend. In the subtidal zone it had more restricted ranges of variations as the sensor, and therefore the plastics, had always been immersed: during the hottest months it varied between 25°C and 30°C, while in the colder months between 5°C and 10°C. In the intertidal zone, on the other hand, a more marked oscillation was observed due to the cyclic emergence and immersion of the structure, with temperatures ranging between 20°C and 35°C in the warmer months and between 0°C and 10°C in the cold months (Figure 59; Figure 60).

Lagoon - ST			Lagoon - IT		
	Temperature (°C)	Intensity (Lux)		Temperature (°C)	Intensity (Lux)
2020			**2020**		
July	28.1	3049	July	27.9	21577
August	28.8	286	August	28.1	2915
September	24.5	448	September	23.5	3521
October	17.4	209	October	17.1	1238
November	14.0	702	November	13.0	3238
December	9.3	198	December	8.9	817
2021			**2021**		
January	7.5	254	January	6.5	1733
February	9.4	227	February	9.3	14783
March	13.1	118	March	12.5	34377

Figure 59: Monthly average values of temperature and light intensity recorded during exposure in the lagoon environment.

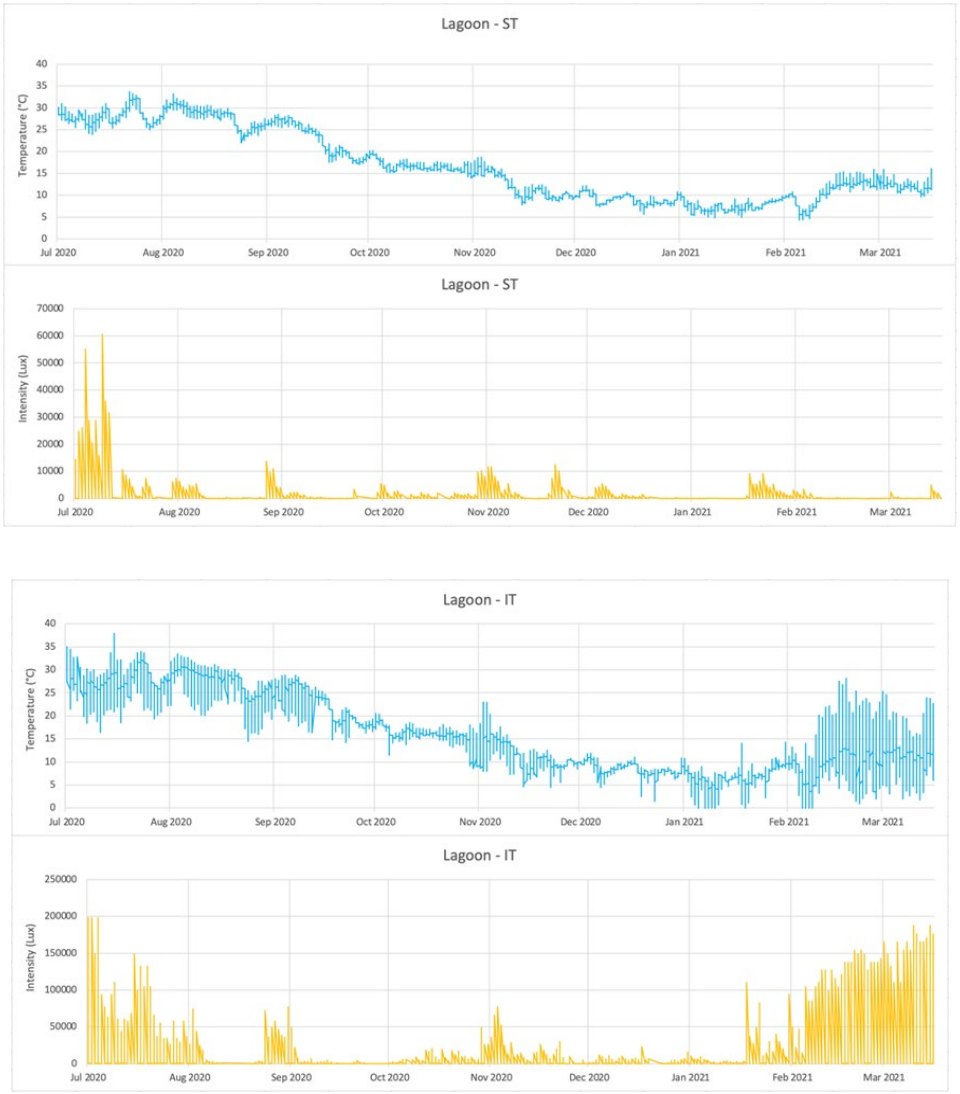

Figure 60: Trends of the temperature (top) and light intensity (bottom) parameters recorded by the HOBO sensor in the subtidal (ST) and intertidal (IT) zone of the lagoon

References

ABDULLA, A., & LINDEN, O. (EDS.). (2008). MARITIME TRAFFIC EFFECTS ON BIODIVERSITY IN THE MEDITERRANEAN SEA: REVIEW OF IMPACTS, PRIORITY AREAS AND MITIGATION MEASURES.

AMOROSI A., CENTINEO M.C., DINELLI E., LUCCHINI F., TATEO F. (2002). GEOCHEMICAL AND MINERALOGICAL VARIATIONS AS INDICATORS OF PROVENANCE CHANGES IN LATE QUATERNARY DEPOSITS OF SE PO PLAIN. SEDIMENTARY GEOLOGY, VOL. 151, PP. 273-292.

BALLY, A. W., BURBI, L., COOPER, C., GHELARDONI, R. (1986). BALANCED SECTIONS AND SEISMIC REFLECTION PROFILES ACROSS THE CENTRAL APENNINES. MEMORIE DELLA SOCIETÀ GEOLOGICA ITALIANA, 35: 237-310.

BERTELLI L. & VACCARO C. (2007). CARATTERIZZAZIONE GEOCHIMICA E GRANULOMETRICA DEI SEDIMENTI DELLA SACCA DI GORO (DELTA DEL PO). IN CARATTERIZZAZIONE GRANULOMETRICA, GEOCHIMICA E MICROBIOLOGICA DEI SEDIMENTI DELLA SACCA DI GORO. PROVINCIA DI FERRARA – SERVIZIO RISORSE IDRICHE E TUTELA AMBIENTALE. PP. 11-38.

BERTELLI L. (2005). STATO AMBIENTALE DELLA SACCA DI GORO (DELTA DEL PO) ATTRAVERSO LO STUDIO DELLE CARATTERISTICHE GEOCHIMICHE DEI SEDIMENTI. DOCTORAL THESIS.

BIANCHINI G., LAVIANO R., LOVO S., VACCARO C. (2002). CHEMICAL-MINERALOGICAL CHARACTERISATION OF CLAY SEDIMENTS AROUND FERRARA (ITALY): A TOOL FOR AN ENVIRONMENTAL ANALYSIS. APPLIED CLAY SCIENCE, VOL. 2, PP. 155-165.

BONDESAN M. (1985). QUADRO SCHEMATICO DELL'EVOLUZIONE GEOMORFOLOGICA OLOCENICA NEL TERRITORIO COMPRESO TRA ADRIA E RAVENNA. ATTI TAV. ROT. "IL DELTA DEL PO", ACC. SC. DELL'IST. DI BOLOGNA, PP. 23-36.

BONDESAN A., & MENEGHEL M. (2004). NOTE ILLUSTRATIVE DELLA CARTA GEOMORFOLOGICA DELLA PROVINCIA DI VENEZIA. ESEDRA EDITRICE.

BRAMBATI, A. (1987) STUDIO SEDIMENTOLOGICO E MARITTIMO-COSTIERO DEI LITORALI DEL FRIULI-VENEZIA GIULIA. REGIONE AUTONOMA FRIULI-VENEZIA GIULIA, DIR. REG. DEI LAV. PUBBL., SERVIZIO DELL'IDRAULICA, TRIESTE. 67 PP.

CARMINATI, E., DOGLIONI, C., & SCROCCA, D. (2003). APENNINES SUBDUCTION-RELATED SUBSIDENCE OF VENICE (ITALY). GEOPH. RESEARCH LETT., 30(13):50, 1-4.

CASTELLARIN, A., CANTELLI, L., FESCE, A., MERCIER, J., PICOTTI, V., PINI, G., . . . SELLI, L. (1992). ALPINE COMPRESSIONAL TECTONICS IN THE SOUTHERN ALPS. RELATIONSHIPS WITH THE N-APENNINES. ANNALES TECTONICAE 6, 62-94.

CASTELLARIN, A., & CANTELLI, L. (2000). NEO-ALPINE EVOLUTION OF THE SOUTHERN EASTERN ALPS. J. GEODYNAMICS,30, 251-274.

Cello, G. & Coppola, L. (1989). Modalità e stili deformativi nell'area Anconetana. Studi Geologici Camerti, 11: 37-47.

Cello, G., Deiana, G., Gazzani, D., Marchegiani, L., Mazzoli, S. (1996). Riconoscimento ed analisi di alcune associazioni di strutture sinsedimentarie pre-orogeniche in Appennino centrale. In: Cello, G., Deiana G., Pierantoni P. (Eds.), "Geodinamica e tettonica attiva del sistema Tirreno-Appennino", Studi Geologici Camerti, Vol. Spec 1995/1: 291-303.

Cello, G. & Tondi, E. (2011). Note illustrative della carta geologica d'Italia alla scala 1:50000 – foglio 282 – Ancona.

Centamore, E., Chiocchini, M., Deiana, G., Micarelli, A., & Pieruccini, U. (1971). Contributo alla conoscenza del Giurassico dell'Appennino umbro-marchigiano. Studi Geologici Camerti, 1: 7-90.

Ciavola P., Gatti M., Tessari U., Zamariolo A., Del Grande C. (2000). Caratterizzazione della morfologia di spiaggia lungo lo Scanno di Goro. Studi Costieri (2): 175-188.

Ciavola P., Gonella M., Tessari U., Zamariolo A. (2000). Contributo alla conoscenza del clima meteomarino della Sacca di Goro: misure correntometriche e mareografiche. In: studi costieri, dinamica e difesa dei litorali – gestione integrata della fascia costiera, n°2. A cura di Simeoni U., pp. 199-215.

Civeira, M. S., Ramos, C. G., Oliveira, M. L., Kautzmann, R. M., Taffarel, S. R., Teixeira, E. C., & Silva, L. F. (2016). Nano-mineralogy of suspended sediment during the beginning of coal rejects spill. Chemosphere, 145, 142-147.

Colacicchi R., Passeri L. & Pialli G. (1970). Nuovi dati sul Giurese umbro-marchigiano ed ipotesi per un inquadramento regionale. Memorie della Società Geologica Italiana, 9: 839-974.

Coltorti, M., Consoli, M., Dramis, F., Gentili, B., & Pambianchi, G. (1991). Evoluzione geomorfologica delle piane alluvionali delle Marche centro-meridionali. Geografia Fisica e Dinamica Quaternaria, 14(1), 87-100.

Cotecchia, V. (2006). The second Hans Cloos lecture. Experience drawn from the great Ancona landslide of 1982. Bulletin of engineering geology and the environment, 65(1), 1-41.

Crescenti U., Curzi P.V., Gallignani P., Gasperini M, Rainone M., Stefanon A. (1983). La frana di Ancona del 13 dicembre 1982; indagini a mare. Memorie della Società Geologica Italiana, 27: 545-553.

Davies, C., Tomlinson, K., & Stephenson, T. (1991). Heavy metals in River Tees estuary sediments. Environ Technol. 12, 961-972.

De Luca, G., Furesi, A., Micera, G., Panzanelli, A., Piu, P.C., Pilo, S.N. & Sanna G., (2005). Nature, distribution, and origin of polycyclic aromatic hydrocarbons (PAHs) in the sediments of Olbia harbour (northern Sardinia, Italy) - Mar. Pollut. Bull., 50, pp. 1223-1232.

Di Giulio, A., Fantoni, R., Zanferrari, A., Mancin, N., Toscani, G., Picotti, V., . . . Marchesini, A. (2005). Cenozoic architecture of the Venetian-Friulan Basin (NE Italy). Boll. Soc. Geol. It.

Doney, S., Fabry, V., Feely, R., & Kleypas, J. (2009). Ocean Acidification: The Other CO2 Problem. Annual Review of Marine Science, 1, 169-192.

Doglioni, C., & Bosellini, A. (1987). Eoalpine and mesoalpine tectonics in the Southern Alps. Geol. Rundsch 76(4), 745-754.

Doglioni, C. (1993). Some remarks on the origin of foredeeps. Tectonophysics, 228, 152-164.

Dramis F., Pambianchi G., Nesci O. & Consoli M. (1992). Il ruolo degli elementi strutturali trasversali nell'evoluzione tettonico-sedimentaria e geomorfologica della regione marchigiana. In: Tozzi, M., Cavinato G.P. & Parotto M. (Eds.), "Studi preliminari sull'acquisizione di dati del profilo CROP 11 Civitavecchia-Vasto", Studi Geologici Camerti, Vol. Spec. 1991/2: 287-293.

Fabbri, P., Zangheri, P., Bassan, V., Fagarazzi, E., Mazzuccato, A., Primon, S., Zogno, C. (2013). Sistemi idrogeologici della Provincia di Venezia – Acquiferi superficiali. Provincia di Venezia – Università degli Studi di Padova.

Fantoni, R., Catellani, D., Merlini, S., Rogledi, S., & Venturini, S. (2002). La registrazione degli eventi deformativi cenozoici nell'avampaese veneto-friulano. Mem. Sci. Geol., 57, 301-313.

Farabollini P., Gentili B., Materazzi M., & Pambianchi G., (2000). Analisi del rischio geo-ambientale: il bacino del Potenza nelle Marche centrali. Atti del Convengo CNG "Il territorio fragile", Roma, december 2000.

Fodor, L., Jelen, B., Martor, E., Skaberne, D., Car, J., & Vrabec, M. (1998). Miocene- Pliocene tectonic evolution of the Slovenian Periadriatic fault: implication for Alpine - Carpathian extrusion model. Tectonics 17/5, 690-709.

Folk, R. L. (1959): Practical petrographic classification of limestones. Bull. Am. Ass. Petrol. Geol. 43 (1): 1-38.

Fontana, A. (2004). Tra Tagliamento e Livenza. In A. Bondesan, & M. Meneghel, Note illustrative della carta geomorfologica della provincia di Venezia (p. 195-217). Padova: Ed. Esedra.

FONTANA, A., MOZZI, P., & BONDESAN, A. (2008). ALLUVIAL MEGAFANS IN THE VENETO-FRIULI PLAIN: EVIDENCE OF AGGRADING AND EROSIVE PHASES DURING LATE PLEISTOCENE AND HOLOCENE. IN P. PIERUCCINI, FLUVIAL ARCHITECTURE AND SEDIMENTARY SEQUENCES. ELSIEVER.

FONTANA, A. (2006). EVOLUZIONE GEOMORFOLOGICA DELLA BASSA PIANURA FRIULANA E SUE RELAZIONI CON LE DINAMICHE INSEDIATIVE ANTICHE. MONOGRAFIE MUSEO FRIULANO ST. NAT. UDINE.

FONTOLAN, G., BEZZI, A., & PILLON, S. (2011). RISCHIO DA MAREGGIATA. IN P. D. VENEZIA, ATLANTE GEOLOGICO DELLA PROVINCIA DI VENEZIA. CARTOGRAFIE E NOTE ILLUSTRATIVE. ANDREA VITTURI.

FONTOLAN G., COVELLI S, BEZZI A., TESOLIN V, SIMEONI U. (2000). STRATIGRAFIA DEI DEPOSITI RECENTI DELLA SACCA DI GORO. IN: STUDI COSTIERI, DINAMICA E DIFESA DEI LITORALI – GESTIONE INTEGRATA DELLA FASCIA COSTIERA, N°2. A CURA DI SIMEONI U., PP. 65-79.

GABBIANELLI G., DEL GRANDE C, SIMEONI U., ZAMARIOLO A., CALDERONI G. (2000). EVOLUZIONE DELL'AREA DI FOCE DEL PO DI GORO (DELTA DEL PO). IN: STUDI COSTIERI, DINAMICA E DIFESA DEI LITORALI – GESTIONE INTEGRATA DELLA FASCIA COSTIERA, N°2. A CURA DI SIMEONI U., PP. 45-63.

GAZZI, P., ZUFFA, G., GANDOLFI, G., & PAGANELLI, L. (1973). PROVENIENZA E DISPERSIONE LITORANEA DELLE SABBIE DELLE SPIAGGE ADRIATICHE FRA LE FOCI DELL'ISONZO E DEL FOGLIA: INQUADRAMENTO REGIONALE. MEM. SOC. GEOL. IT. 12, 37.

GORDINI, E., MAROCCO, R., & RAMELLA, R. (2006). DINAMICA MORFOLOGICA DEL LITORALE DEL DELTA DEL FIUME TAGLIAMENTO (ADRIATICO SETTENTRIONALE) IN RELAZIONE AI POSSIBILI INTERVENTI DI RIPASCIMENTO. IL QUATERNARIO - ITALIAN JOURNAL OF QUATERNARY SCIENCES, 19(1), 45-65

KAKLAMANOS, G., APREA, G., & THEODORISIS, G. (2020). MASS SPECTROMETRY: PRINCIPLE AND INSTRUMENTATION. CHEMICAL ANALYSIS OF FOOD (SECOND EDITION), ACADEMIC PRESS, 525-552.

LEE, K.T., TANABE, S., KOH C.H., (2001) DISTRIBUTION OF ORGANOCHLORINE PESTICIDES IN SEDIMENTS FROM KYEONGGI BAY AND NEARBY AREAS, KOREA ENVIRON. POLLUT., 114, PP. 207-213.

MARCHEGIANI, L., BERTOTTI, G., CELLO, G., DEIANA, G., MAZZOLI, S., & TONDI, E. (1999). PRE-OROGENIC TECTONICS IN THE UMBRIA–MARCHE SECTOR OF THE AFRO-ADRIATIC CONTINENTAL MARGIN. TECTONOPHYSICS, 315(1-4), 123-143.

MARCHEGIANI, L., DEIANA G., TONDI E., (1996). TETTONICA PRE-OROGENICA IN APPENNINO CENTRALE. STUDI GEOLOGICI CAMERTI, 14: 211-228.

MALI, M., DELL'ANNA, M. M., MASTRORILLI, P., DAMIANI, L., UNGARO, N., BELVISO, C., & FIORE, S. (2015). ARE CONVENTIONAL STATISTICAL TECHNIQUES EXHAUSTIVE FOR DEFINING METAL BACKGROUND CONCENTRATIONS IN HARBOUR SEDIMENTS? A CASE STUDY: THE COASTAL AREA OF BARI (SOUTHEAST ITALY). CHEMOSPHERE, 138, 708-717.

Mali, M., De Serio, F., Dell'Anna, M.M., Mastrorilli, P., Damiani, L., Mossa M., (2017). Enhancing the performance of hazard indexes in assessing hot spots of harbour areas by considering hydrodynamic parameters Ecol. Indic, 73, pp. 38-45.

Marocco, R. (1988). Conslderazioni sedimentologiche sui sondaggi S19 e S20 (Delta del Fiume Tagliamento). Gortania, Atti Mus. Friul. Sc. Nat., 10, 101-120.

Marocco, R. (1989). Evoluzione quaternana della laguna di Marano (Fn'uli- Venezia Giulla). Il Quaternario, 2, 125-137.

Massari, F. (1990). The foredeep of the northern Adriatic margin: evidence of diachronicity in deformation of Southern Alps. Riv. It. Paleont. Strat., 350-380.

Monai, M. (ed.) 2009. Gli eventi meteorologici estremi nella regione veneto. ARPAV - Verona, (VR).

Nanni, T. (1980). Note illustrative sulla geologia dell'anconetano. Ed. a cura della Regione Marche, Provincia di Ancona e Comune di Ancona, 47 pp.

Natali C., Fogli R., Bianchini G., Tassinari R., Tessari U. (2016). Heavy metals backgrounds in sediments from the Sacca di Goro (NE, Italy). Environmental quality 20, 15-26.

Natali, C., Bianchini, G., Vittori, L., Natale, M., & Tessari, U. (2018). Carbon and nitrogen pools in Padanian soils (Italy): Origin and dynamics of soil organic matter. Geochemistry, Volume 78, Issue 4, 490-499.

Naviaux, J., Subhas, A., Rollins, N., Berelson, W., Dong, S., & Adkins, J. (2019). Temperature dependence of calcite dissolution kinetics in seawater. Geochimica et Cosmochimica, 1, 363-384.

Newbury, D., & Ritchie, N. (2013). Is Scanning Electron Microscopy/Energy Dispersive X-ray Spectrometry (SEM/EDS) Quantitative? Scanning, 35(3), 141-168

Oliveira, M. L., Ward, C. R., French, D., Hower, J. C., Querol, X., & Silva, L. F. (2012). Mineralogy and leaching characteristics of beneficiated coal products from Santa Catarina, Brazil. International Journal of Coal Geology, 94, 314-325.

Pialli, G. (1971). Facies di piana cotidale nel Calcare Massiccio dell'Appennino umbro-marchigiano. Boll. Soc. Geol. It., 90: 481-507.

Ratschbacher, L., Frisch, W., & Linzer, H. (1991). Lateral extrusion in the eastern Alps, part 2: Tectonics 10/2, 257-271.

Ribeiro, J., Taffarel, S. R., Sampaio, C. H., Flores, D., & Silva, L. F. (2013). Mineral speciation and fate of some hazardous contaminants in coal waste pile from anthracite mining in Portugal. International Journal of Coal Geology, 109, 15-23.

Sakai, H., Kojima, Y., & Saito, K. (1986). Distribution of heavy metals in water and sieved sediments in the Toyohira River. Water Res 20, 559-567.

Sciarra, N., Pasculli, A., & Calista, M. (2006). The large Ancona landslide studies were revisited including stochastical spatial variability of mechanical parameters. In Proceedings of the 10th IAEG congress. Geol. soc. of London Paper (No. 807).

Scisciani, V., Agostini, S., Calamita, F., Pace, P., Cilli, A., Giori, I., & Paltrinieri, W. (2014). Positive inversion tectonics in foreland fold-and-thrust belts: a reappraisal of the Umbria–Marche Northern Apennines (Central Italy) by integrating geological and geophysical data. Tectonophysics, 637, 218-237.

Shepard, F. P. (1954). Nomenclature based on sand-silt-clay ratios. Journal of Sedimentary Research, 24(3), 151-158.

Simeoni U., Fontolan G.., Ciavola P. (2000) Morfodinamica delle bocche lagunari della Sacca di Goro. Studi Costieri,2: 123–138.TRAIL R.J.,

Simeoni, U., Fontolan, G., Dal Cin, R., Calderoni, G., & Zamariolo, A. (2000). Dinamica sedimentaria dell'area di Goro (Delta del Po). Studi costieri, 2, 139-151.

Thorne, L., & Nickless, G. (1981). The relation between heavy metals and particle size fractions within the Severn estuary (UK) inter-tidal sediments. Sci Total Environ 19, 207-213.

Tsapakis, M., Apostolaki, M., Eisenreich, S., Stephanou E.G., (2006). Atmospheric deposition and marine sedimentation fluxes of polycyclic aromatic hydrocarbons in the eastern Mediterranean Basin Environ. Sci. Technol., 40, pp. 4922-4927.

Turley, C. (2013). Chapter 2- Ocean Acidification. Managing Ocean Environments in a Changing Climate, 15-44.

Wakida, F., Lara-Ruiz, D., Temores-Pen˜a, J., Rodriguez-Ventura, J., Diaz, C., & Garcia-Flores, E. (2007). Heavy metals in sediments of the Tecate River, Mexico. Environ Geol (2008) 54, 637-642.

Zakaria, M.P., Takada, H., Tsutsumi, S., Ohno, K., Yamada, J., Kound, E., Kumata, H., (2002). Distribution of polycyclic aromatic hydrocarbons (PAHs) in rivers and estuaries in Malaysia: a widespread input of petrogenic PAHs Environ. Sci. Technol., 36, pp. 1907-1918.

ZANFERRARI, A., FONTANA, A., AVIGLIANO, R., & PAIERO, G. (2008). FOGLIO GEOLOGICO 086 "SAN VITO AL TAGLIAMENTO" E NOTE ILLUSTRATIVE. CARTA GEOLOGICA D'ITALIA ALLA SCALA 1:50,000.

ZUNICA, M. (1971) LE SPIAGGE DEL VENETO. RICERCHE SULLE VARIAZIONI DELLE SPIAGGE ITALIANE. CONSIGLIO NAZIONALE DELLE RICERCHE, TIPOGRAFIA ANTONIANA, PADOVA, 145 PP.